AD-A102 337 HELIONETICS INC SAN DIEGO CA LASER DIV F/G 20/5
SCALING AND DESIGN OF DISCHARGE-EXCITED RARE-GAS HALIDE LASERS.(U)
JAN 81 D E ROTHE, J I LEVATTER, R L SANDSTROM N00014-81-C-0044
UNCLASSIFIED HLD-81-1R NL

1 OF 2
AD A
102337

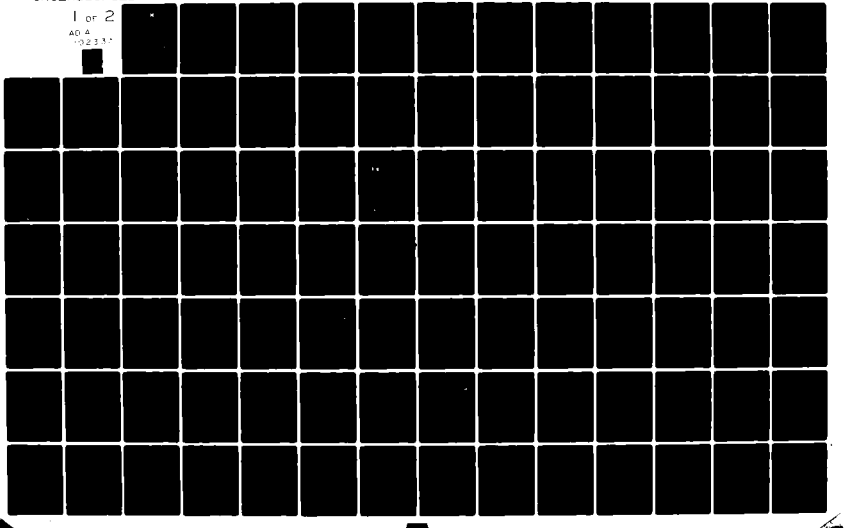

REPORT HLD-81-1R

HELIONETICS, INC.
LASER DIVISION

FINAL TECHNICAL REPORT

SCALING AND DESIGN OF DISCHARGE-EXCITED RARE-GAS HALIDE LASERS

CONTRACT N00014-81-C-0044

JANUARY 1981

By

D. E. Rothe, J. I. Levatter, R. L. Sandstrom, and P. B. Scott

HELIONETICS, INC.
Laser Division
3878 Ruffin Road
San Diego, CA 92123

Prepared for

OFFICE OF NAVAL RESEARCH
800 North Quincy Street
Arlington, Virginia 22217

REPORT HLD-81-1R

FINAL TECHNICAL REPORT

SCALING AND DESIGN OF DISCHARGE-EXCITED RARE-GAS HALIDE LASERS

CONTRACT N00014-81-C-0044

JANUARY 1981

By

D. E. Rothe, J. I. Levatter, R. L. Sandstrom, and P. B. Scott

HELIONETICS, INC.
Laser Division
3878 Ruffin Road
San Diego, CA 92123

Prepared for

OFFICE OF NAVAL RESEARCH
800 North Quincy Street
Arlington, Virginia 22217

UNCLASSIFIED

SECURITY CLASSIFICATION OF THIS PAGE (When Data Entered)

REPORT DOCUMENTATION PAGE	READ INSTRUCTIONS BEFORE COMPLETING FORM
1. REPORT NUMBER: HLD-81-1R	2. GOVT ACCESSION NO.: AD-A102337	3. RECIPIENT'S CATALOG NUMBER
4. TITLE (and Subtitle): Scaling and Design of High-Power Discharge-Excited Rare-Gas Halide Lasers	5. TYPE OF REPORT & PERIOD COVERED: Final Technical Report, 22 Sep 80 — 31 Dec 1980
	6. PERFORMING ORG. REPORT NUMBER
7. AUTHOR(s): D. E. Rothe, J. I./Levatter, R. L./Sandstrom and P. B./Scott	8. CONTRACT OR GRANT NUMBER(s): N00014-81-C-0044
9. PERFORMING ORGANIZATION NAME AND ADDRESS: Helionetics, Inc. 17312 Eastman St. Irvine, California 92714	10. PROGRAM ELEMENT, PROJECT, TASK AREA & WORK UNIT NUMBERS: RF62-581
11. CONTROLLING OFFICE NAME AND ADDRESS: Office of Naval Research 800 North Quincy Street Arlington, VA 22217	12. REPORT DATE: January 1981
	13. NUMBER OF PAGES: 109
14. MONITORING AGENCY NAME & ADDRESS (if different from Controlling Office): Defense Contract Administrative Services 34 Civic Center Plaza P. O. Box C-12700 Santa Ana, California 92712	15. SECURITY CLASS. (of this report): Unclassified
	15a. DECLASSIFICATION/DOWNGRADING SCHEDULE

16. DISTRIBUTION STATEMENT (of this Report)

Approved for Public Release; Distribution unlimited.

17. DISTRIBUTION STATEMENT (of the abstract entered in Block 20, if different from Report)

None

18. SUPPLEMENTARY NOTES

None

19. KEY WORDS (Continue on reverse side if necessary and identify by block number)

Electric-Discharge Excited Rare-Gas Halide Lasers, Energy and Pulse-Repetition-Frequency Scaling, UV versus X-ray Preionization, PFN Scaling and Limitations

20. ABSTRACT (Continue on reverse side if necessary and identify by block number)

The results of this study establish the feasibility of developing efficient high-average-power discharge-pumped rare-gas halide (RGH) lasers. An analysis of the scaling and limitations of PFN (pulse-forming network)-driven, electric discharge-pumped RGH lasers has been performed. The design of a 100 W XeCl laser is described in detail. The relative merits of uv and X-ray preionization and their applicability to RGH lasers have been investigated, and the scaling limits of output pulse energy and pulse-repetition frequencies (PRF) have been explored. The design concepts presented permit pulse energy scaling to the kilojoule range, where limitations exist only because of increasing dielectric stress in the PFN. Gas dynamic flow considerations predict that kilojoule lasers can be developed with PRFs in the kilohertz range. Practical limits appear to be reached at a pulse frequency of 3kHz (3 MW average power).

DD FORM 1 JAN 73 1473 EDITION OF 1 NOV 65 IS OBSOLETE

UNCLASSIFIED

SECURITY CLASSIFICATION OF THIS PAGE (When Data Entered)

TABLE OF CONTENTS

	SUMMARY	i
	List of Illustrations	iv
1.0	INTRODUCTION	1
2.0	EXCIMER LASER DESIGN CONSIDERATIONS	3
	2.1 Rare-Gas Halide Laser Characteristics	3
	2.2 Requirements for Uniform Stable Discharges	4
	2.3 Previous Discharge Work	8
	2.3.1 Performance of a Discrete-Component LC-Network	8
	2.3.2 Performance of a Distributed-Impedance Water-Line Driven RGH Laser	11
	2.4 Outline for 1 J-100 Hz Laser Development	14
	2.4.1 Laser Configuration	18
	2.4.2 Laser Discharge Chamber	20
	2.4.3 Pulse Forming Network	22
	2.4.4 Preionization	29
	2.4.5 Triggered Multichannel Rail Gap	31
	2.4.6 Gas Flow, Turbulence and Acoustic Damping	34
	2.4.7 Optical Cavity Design	37
3.0	PULSE ENERGY SCALING	42
	3.1 Switching Considerations	43
	3.2 Electric Stress in Water Line	46
	3.3 Design Parameters for 20 J, 100 J and 1 kJ Lasers	48
4.0	PREIONIZATION TECHNIQUES	54
	4.1 Ultraviolet vs. X-ray Preionization	54
	4.2 Flux Uniformity for Discrete Spark UV Preionizers	55
5.0	HIGH-AVERAGE POWER LASERS	63
	5.1 Effects of Acoustic Waves and Turbulence on Optical Beam Quality	
	5.1.1 Random Disturbances	63
	5.1.2 Ordered Disturbances	64
	5.1.3 Flow Turbulence	65
	5.1.4 Shock Waves	65
	5.2 Gas Flow as a Function of Average Power	67
	5.3 Practical Scaling Limits	69
6.0	CONCLUSIONS	71
7.0	REFERENCES	73
	APPENDIX A--Description of Calculation of Preionization Distribution	A1
	APPENDIX B--PERSONNEL	B1
	APPENDIX C--Distribution List	C1

SUMMARY

Rare-gas halide (RGH) excimer lasers are the most efficient high-power lasers known which emit in the near-ultraviolet (uv) part of the electromagnetic spectrum. Their short wavelength makes them ideally suited for a number of applications important to present DOD and DOE programs*. Some of the advantages, which short-wave lasers have over the presently more developed high-power infrared (IR) lasers (CO_2, CO, HF/DF, Nd-Glass, YAG), are:

1. Low diffraction losses resulting in high beam collimation and high energy density projected onto a distant target ($\sim 1/\lambda^2$). This leads to applications in strategic communications networks and in long-range tactical weapons systems.
2. Strong interaction with the atoms and molecules of most substances (electronic excitation, ionization and dissociation as opposed to the simple heating effects of IR-lasers interacting with the vibrational and rotational modes of molecules, and better coupling to dense plasmas. This is important for photochemistry (isotope separation), interaction with plasmas (inertial confinement fusion), and possibly direct laser weapons applications.
3. Strong absorption in semiconductors and low reflectivity from metal surfaces. This leads to efficient surface annealing of semiconductors and to strong interactions of laser beams with metallic targets.

Whereas high pulse energies and high intrinsic efficiencies have been demonstrated with e-beam pumped RGH lasers, such devices employ a mechanically fragile e-beam window foil which limits these lasers to low pulse-repetition frequencies (PRF). Self-sustained discharge-pumped lasers, on the other hand, have no such limitations and are suitable for high-PRF operation. The present study was undertaken to explore whether the discharge-pumped RGH laser can be further developed to meet projected requirements for future DOD applications in terms of pulse energy, efficiency and average power. Specifically, this work has established the feasibility of scaling discharge-pumped RGH laser systems to high pulse energies and to high average power, and has defined the limits imposed by electric discharge instabilities and by gasdynamic flow problems associated with high pulse-repetition frequencies. A unique laser configuration

*The importance of laser applications to DOD and DOE programs has recently been reviewed by the U.S. Senate Subcommittee on Science, Technology and Space. The hearings have been summarized in: "Laser Research and Applications", U.S. Senate Report prepared for Committee on Commerce, Science and Transportation, U.S. Gov. Print. Office, Washington, D.C. (Nov. 1980).

which contains all the elements necessary for high discharge stability and for scalability, has been developed by Helionetics. It is based on a thorough understanding of the physical factors necessary for creating stable large-volume electric discharges in high-pressure electronegative gas mixtures, as well as on new technological developments involving efficient preionization techniques and the design of a scalable impedance-matched constant-voltage pulse-forming network (PFN) switched by a new (proprietary) low-impedance, triggered rail-type spark gap.

Electrical, mechanical and optical design parameters have been established for a moderately-high-average-power RGH laser emitting 1 to 2 joule pulses at a PRF of 100 pulses per second (>100 W average power). It has been demonstrated that the successful development of this laser in a 20 month period is possible with present "in-house" technolgoy. Although future large RGH laser systems will employ X-ray preionization techniques, this laser will be preionized by hard uv radiation from spark sources located behind one of the discharge electrodes. UV spark preionization is chosen here because it is sufficient for the relatively small discharge volume, and because uv spark sources are more easily implemented than an X-ray generator. The most efficient spark source arrangement for providing uniform illumination has been calculated and is presented in this report. Operational lifetime for such a 100 XeCl laser system is predicted to be well in excess of 10^{10} pulses. The combination of high pulse energy (1-2 J), moderately high average power (100-200 W), excellent beam uniformity ($\pm$5% variation or less) and long life will take this Helionetics RGH laser far beyond any uv laser system presently available and will, for the first time, provide a viable high-average-power uv laser source for a multitude of applications.

Pulse energy scaling has been investigated for X-ray preionized discharge lasers driven by a double water Blumlein PFN. It is concluded that the range of preionizing X-rays and the problems associated with fast high-voltage switching technology do not impose any severe scaling limitations. The design concepts presented permit pulse energy scaling into the kilojoule range. Further scaling is limited only because of increasingly high dielectric stress in the water PFN. This dielectric stress limitation represents a real barrier, preventing pulse energy scaling beyond several kilojoules, unless the duration of the pump pulse

and optical pulse can be stretched into the microsecond range. Design parameters for a 20 J, a 100 J and a possible 1 kJ XeCl laser are given. Only the development of the kilojoule system requires advanced R and D to establish discharge stability data not presently available.

For the development of high-average-power lasers (multikilowatt to megawatt) operating at PRFs in the kilohertz regime, a carefully designed gas flow system is required, which provides efficient gas exchange and incorporates means for controlling flow turbulence and suppressing acoustic disturbances. Gasdynamic flow considerations, based on supersonic windtunnel design practices, predict that efficient high-power RGH lasers can be constructed with pulse energies of several kilojoules and with PRFs of several kilohertz. Such systems would be capable of average powers in the megawatt range and would make a significant impact on strategic (ground-based blue-green communication system) and tactical warfare (air-to-air combat and optical countermeasures) and on large-scale industrial chemical and materials processing.

LIST OF ILLUSTRATIONS

Figure 2-1	Discharge Characteristics for 1ℓ Transverse Discharge Laser	10
Figure 2-2	Discharge Voltage and XeCl Laser Output Power for a 100 and 200 ns PFN	12
Figure 2-3	Schematic of Electrical System for 1 J/Pulse XeCl Laser	19
Figure 2-4	Operational Relationship of the Major Components of the UV-Preionized Laser System	21
Figure 2-5	Parallel-Plate Blumlein Drive	25
Figure 2-6	Sequence of Determining Design Variables for Blumlein-Driven Laser	28
Figure 2-7	Design Condition and Operating Range of Proposed Laser System	30
Figure 2-8	Interrelationship of the Various Laser Subsystems for an X-Ray Preionized Laser	32
Figure 2-9	Schematic of Gas Recirculation System	36
Figure 2-10	Low-Magnification Continuously-Coupled Unstable Resonator	38
Figure 2-11	High-Magnification Unstable Cavity with Cylindrical Mirrors and One-Sided Output	39
Figure 3-1	Method of Matching a Large Low-Inductance Rail Gap to a Doubly-Tapered Constant-Impedance Blumlein-Type PFN	45
Figure 3-2	Schematic of Overall Electrical System for a 20 J XeCl Laser	50
Figure 3-3	Approximate Size of a Typical 20 Joule XeCl Laser	51
Figure 4-1	Geometry for UV Spark Preionization	56
Figures 4-2 to 4-6	Calculated Preionization Density Profiles	57-62
Figure 5-1	Gas Flow Requirements for 1 kJ/Pulse High-PRF Laser	68
Figure A-1	Symbols Used in Calculation of Preionization Distribution	A2

Table 2-1	Specifications of Helionetics' High-Power RGH Laser System for Semiconductor Processing	15
Table 2-2	Available Wavelengths and Potential Applications	16
Table 3-1	Scaled-Up X-Ray Preionized XeCl Discharge Lasers	52

1.0 INTRODUCTION

Efficient, compact and reliable high-average-power pulsed gas lasers emitting in the near-uv and visible portions of the spectrum are of considerable interest for both commercial and military applications.* Potential DoD applications of such devices lie in the areas of optical detection and ranging, laser communications systems (which cannot be interfered with, which can penetrate sea water, and which are not affected by the electromagnetic disturbances caused by solar flares or nuclear weapons blasts), airborne laser weapons and optical countermeasures. Commercial applications exist in the fields of photochemistry (laser catalyzed reactions and isotope separation), space technology (communications, remote sensing, ranging and power transmission), solar cell annealing, semiconductor processing, and machining of materials (surface etching, cutting and drilling of very hard, very tough or very soft materials, dynamic balancing, etc.)

High-power RGH excimer lasers, [1] operating at high pulse repetition frequencies (PRF), are directly applicable to several Navy programs, including strategic space-to-submarine communication and laser processing of high-bandwidth semiconductor devices [2] in support of technical goals of the VHSIC program. This report is the result of a study which has addressed technology critical to the feasibility of developing such a laser. In particular, the problems related to the generation of large-volume uniform electric discharges in high-pressure electronegative gas mixtures has been critically reviewed.

Practical laser systems for such applications require high average and peak powers, good beam quality, high overall efficiencies, high reliability and low maintenance. The recently discovered rare-gas-halide (RHG) excimer lasers [3-9] are the most powerful and efficient ultraviolet laser sources known to date and have the potential for being developed into advanced laser systems of practical interest and national importance. Present e-beam pumped [3,4] and e-beam sustained [5] RGH lasers have demonstrated

---

*The importance of laser applications to DOD and DOE programs has recently been reviewed by the U.S. Senate Subcommittee on Science, Technology and Space. The hearings have been summarized in: "Laser Research and Applications" U.S. Senate Report prepared for Committee on Commerce, Science and Transportation, U.S. Gov. Print. Office, Washington, D.C. (Nov. 1980)

high pulse energy, high efficiency and the potential for scaling to large sizes. Electron-beam pumped devices, however, are highly complex and would require costly maintenance schedules, if scaled to high pulse rates and high average powers. These lasers require the use of a mechanically fragile and thermally heavily loaded window foil between the high-vacuum electron gun chamber and the high-pressure laser plenum. This foil is subject to the combined action of thermal heating, shock-wave pressure pulses, radiation damage and chemical attack by corrosive halogen compounds. As a consequence, the lifetime of such foils is very short (between 10^2 to 10^5 pulses) even with advanced design practices and under ideal conditions. The resulting downtime is unacceptable for a practical high-average-power laser device. Lasers excited by self-sustained uniform electric discharges[6-9] have no such limitations.

Pulse energies of several joules have already been demonstrated[9] with discharge-excited RGH lasers at low PRF, but the potential exists for extending the output of such lasers to much higher pulse energies and higher average powers. Helionetics is presently developing with internal funding a 1 joule/pulse, 100 watt average-power XeCl laser with high reliability, excellent beam uniformity and long life (see Appendix A).

Herein we propose the development and evaluation of a 20 joule pulse avalanche discharge pumped XeCl laser over a two year period. The evaluation is to include parameter studies adequate for verifying or modifying the laser scaling laws discussed herein.

Section 2 deals specifically with the necessary conditions[10] for generating stable uniform avalanche discharges in high-pressure gases. The problems associated with scaling of avalanche discharge lasers to high optical pulse energies are discussed in Section 3. Section 4 specifically discusses the proposed 20 joule laser. In Section 5 the proposed evaluation and optimization program is described.

2.0 EXCIMER LASER DESIGN CONSIDERATIONS

Avalanche discharge excited RGH lasers are a convenient source of intense ultraviolet radiation. Herein we discuss the design of these lasers to produce many joules of diffraction-limited output energy[9] at PRFs from a few hundred to several thousand pulses per second,[11,12] yielding average powers at kilowatt levels. Unfortunately, however, most discharge pumped excimer lasers today are limited to repetition rates of only a few hertz, and to pulse energies of a fraction of a joule. In this section, the present status of discharge pumped excimer lasers, and the physics and engineering requirements that limit the energy output of such systems are discussed.

2.1 Rare-Gas Halide Laser Characteristics

In principle, the operation of an avalanche discharge laser is straightforward. Upon application of a fast-rising high-voltage pulse (substantially above the DC breakdown voltage), the initially low-level electron density within the discharge volume exponentially increases until limited by the discharge circuit. The circuit impedance, in turn, must be chosen such that an adequate discharge pumping rate is achieved during the excitation pulse.

In order to understand the fundamental constraints involved in scaling discharge pumped RGH lasers, one must examine the engineering problems that limit the pulse repetition rate and pulse energy of these lasers. The maximum PRF is generally determined by the speed at which the laser gases can be moved through the electrode region, since the gases must be replaced between pulses to remove residual ionization and waste heat. At very high PRFs above approximately 1 kilohertz, care must also be taken to minimize the discharge-inhomogenizing effects of acoustic and thermal disturbances caused by the impulsive energy loading of the gas. Research addressing the various problems associated with high repetition rate, fast-flow lasers[11,12] has now progressed to the point where scaling the pulse repetition frequency beyond 1 kilohertz is possible. Scaling the pulse energy to levels much greater than 1 joule, however, has not met with as much success until very recently.[9,10]

The laser output energy of discharge pumped excimers has generally been limited to a fraction of a joule and the optical pulse duration to a few tens of nanoseconds because of discharge instabilities. The latter are encountered when the discharge volume, the discharge duration, or the discharge power density is increased. The phenomenon responsible for the discharge instability, and hence the energy limit, is the tendency for a high-pressure electronegative gas discharge to degenerate from its initial volumetric avalanche state into that of an arc discharge.

An arc is an electric discharge of extremely high current density which occupies a very limited volume. Laser action in the presence of arcing is of course impossible, not only because of the inadequate excitation in regions of low current density, but also because of the too rapid thermal equilibration in high-current regions. Both of the effects tend to discourage the formation of a laser population inversion. Another detrimental feature associated with arcing is the very low plasma resistivity of the arc channel itself. Once an arc occurs, the resistance of the discharge will fall to a value substantially below the impedance of the driving circuit, making it extremely difficult to deposit energy into the discharge efficiently. The problem of arc channel formation has therefore been a fundamental limitation in the design of avalanche discharge lasers. Under appropriate conditions however, it is possible to avoid this transition and produce an arbitrarily large, homogeneous, avalanche discharge suitable for excimer laser excitation.

2.2 Requirements for Uniform Stable Discharges

The necessary conditions for the homogeneous formation of pulsed avalanche discharges at high gas pressures have recently been examined by Levatter and Lin.[10] Their analysis qualitatively and quantitatively defines the criteria necessary to create a homogeneous volume avalanche discharge under high E/n (electric field/gas density) conditions. This analysis also

clarifies the distinction between temporal and spatial discharge instabilities, a point that has previously been confused in the literature. A preionized self-sustained avalanche discharge undergoes exponential current multiplication during the early phases of the discharge development. Such a process is by definition non-steady or "unstable" in the temporal sense. However, if spatial homogeneity of the discharge current distribution can be maintained as time progresses, the current growth must eventually cease as the resistive impedance of the discharge begins to drop below the output impedance of the driving circuit. An avalanche discharge can thus be spatially stable while not being temporally stable. The key lies in maintaining spatial discharge homogeneity. It has been shown that atmospheric-pressure, spatially non-uniform avalanche discharges will quickly (within 10 to 20 nsec) coalesce into an arc.[13] Therefore, it is imperative that the initial formative stage of the discharge be extremely uniform.

According to Levatter and Lin,[10] provided certain criteria are met simultaneously, a homogeneous formative discharge phase can be achieved even in electronegative gas mixtures commonly used in rare-gas halide laser systems. The requirements are: (1) the electric field within the discharge volume must be uniform; (2) the discharge preionization must be sufficiently uniform; (3) the preionization density must be greater than a certain minimum value, $n_e(\text{min})$, that is dependent on the gas mixture, gas pressure, and discharge voltage risetime; and (4) the time rate of change of the ratio of the discharge electric field to the gas number density, $d(E/n)/dt$ must be large enough to avoid the formation of a non-preionized region near the cathode surface. For a given discharge electrode spacing and gas pressure, $d(E/n)/dt$ is equivalent to specifying a voltage risetime, τ_r. The exact value of τ_r required for criterion (4) to be satisfied is dependent on the gas pressure and particular gas composition.

In addition to the above four criteria, in order to achieve efficient power transfer to the discharge plasma, it is necessary that a suitable low-impedance PFN be employed which is matched to the discharge impedance at the discharge sustaining voltage. Furthermore, the PFN must be capable

of acting as a constant current source to inhibit two-step ionization processes, which can lead to a bulk plasma ionization runaway and a corresponding discharge impedance collapse.

The constraints placed on a self-sustained discharge-pumped excimer laser by the previous criteria are moderately severe, particularly those constraints resulting from the preionization and voltage risetime requirements (criteria (2), (3), and (4)). It is instructive here to consider the magnitude of $n_e(\text{min})$ and the maximum allowable voltage risetime, τ_r, necessary for the successful operation of a one-atmosphere XeF(He:Xe:F_2 = 200:8:1) laser. Such a system requires a minimum calculated preionization density of $n_e(\text{min}) \gtrsim 2 \times 10^5$ cm^{-3}, and a maximum voltage risetime of $\tau_r \lesssim 16$ ns. The same laser at six atmospheres requires $n_e(\text{min}) \gtrsim 3 \times 10^6$ cm^{-3} and $\tau_r \lesssim 6$ ns.

Producing such a fast voltage risetime and an adequate preionization density that is volumetrically uniform is not trivial. Because most discharge-excited excimer lasers are pumped with low-impedance ($Z \lesssim 1\ \Omega$) pulse-forming networks (PFNs), the voltage risetime requirement (4) is usually the most difficult to fulfill. In order to produce the required voltage risetime, it is necessary to employ a fast-acting, high-current, high-voltage switch. The switch must be capable of a di/dt approaching 10^{13} A/s, a dv/dt $\simeq 10^{13}$ V/s, and a peak current of approximately 10^5 amperes. Although hydrogen thyratrons capable of meeting these switching levels are under development*, no such thyratron exists today. At present, multichannel rail gaps provide the only practical alternative.

Conventional single-arc-channel spark gaps can handle very high peak voltages and currents, but they are not capable of producing a sufficiently large di/dt and dv/dt from a low-impedance source. This limitation is primarily due to the finite resistive formative phase of the spark channel.[15] In addition, single-arc-channel switching of low-impedance PFNs is a high-loss process. That is, a large fraction of the switched PFN energy is deposited in the spark-gap arc channel and not in the discharge load. This causes severe electrode erosion, which results in switch lifetimes being

*E.G.& G. is presently developing a low-inductance, high-di/dt tube under contract with DOE/LASL.

relatively short ($<10^6$ shots). However, by utilizing multiple parallel spark channels, the switching speed can be greatly increased, so that rise-times of only a few nanoseconds are possible, and the total energy deposited in the switch can be reduced to only a few percent of the total energy transferred through the gap. Under these conditions, switch lifetimes in excess of 10^{10} shots should be obtainable.

The criterion related to achieving uniform electron preionization presents the second major challenge involved in creating a volumetric avalanche discharge. Uniform preionization is essential to the homogenous formation of an avalanche discharge at high gas pressures where strong electronic and ionic diffusion effects are not significant. Corona[18], uv-arc [6-8,11,17], and X-ray sources[9,19,20] have been employed for excimer laser preionization, but only the uv-arc and X-ray techniques are capable of providing a sufficiently uniform volumetric preionization level, at least for large systems. Both the uv-arc and X-ray preionization methods rely on simple photoionization processes. Ultraviolet preionization has been used very successfully with the rare-gas halide excimers, but it is most likely limited to discharge volumes less than 10 liters because of the relatively large absorption coefficient of uv photons in high-pressure RGH mixtures. X-rays, although more difficult to implement, allow scaling to very large discharge volumes (>100 liters) because of their intrinsically large mass penetration power.[21] The relatively small absorption coefficient of X-rays also leads to very uniform ion densities. Thus, multiple uv-arcs for small and medium size systems, and X-rays for larger, high-energy lasers appear to be the most suitable preionization techniques.

Having reviewed the major physical parameters necessary to create spatially uniform avalanche discharges in high pressure electronegative excimer laser gas mixtures, it appears that at least two preionization techniques are satisfactory, and that sufficiently fast voltage risetimes can readily be achieved using multiple-arc switching techniques.

2.3 Previous Discharge Work

In this section the characteristics of a typical discrete-LC pulse-forming network are compared with the superior performance of a rail-gap-switched, distributed-impedance PFN.

2.3.1 Performance of a Discrete-Component LC-Network

The following data summarize some results obtained by Rothe[22] (now with Helionetics, formerly with Northrop RTC) in recent experiments performed with a 1 liter uv-preionized RGH laser, using a discrete-component LC network. These results are representative of the best performance that can be achieved with such a pulse generator. Even though discharge stability and impedance matching were achieved only during a transient phase of the discharge, the data demonstrate that high intrinsic laser efficiencies (2-7%) are possible.

This laser was operated with KrF and XeCl with output energies in the 0.5 J range. Characteristic E/p values were 3 kV/cm-atm, and the electric energy loading was approximately 35 J/l-atm. Operating pressure was 2.6 atm with gas mixtures consisting of F_2/Kr/He = 3/40/2000 torr and HCl/Xe/He = 4/20/2000 torr partial pressures. Optical pulse duration was typically 35 ns, and the overall efficiency was 0.5%.

Analysis of the voltage and current input pulses and of the optical output pulse as a function of time showed that the single most important factor affecting the laser performance was the efficiency with which electrical power was transferred from the circuit to the discharge. Because of impedance mismatch between circuit and rapidly varying load, most of the stored energy was dissipated elsewhere in the circuit or was added to the gas at a rate well below lasing threshold. This condition caused the overall laser efficiency to be less than one percent, even though the intrinsic efficiency, based on electric energy actually added to the gas during the laser pulse, was much larger.

The important portions of the measured voltage and current pulses are reproduced in Figure 2-1. A set of barium titanate peaking capacitors (totaling 4 nF) inside the discharge chamber was used to steepen the current rate-of-rise of the discharge pulse. Charging voltage was 55 kV.

The time of discharge initiation is well marked by the sudden drop in voltage and the simultaneous increase in current. The voltage drops to zero as the current reaches its maximum value. The current going through the discharge (I_D) was derived by adding the peaking circuit current (I_{Pk}) and the current I_1 fed into the system by the external circuit. The power (P_D) deposited in the gas was then found by multiplying the voltage pulse (V) with the discharge current (I_D). Note that the power dissipated (P_D) displays a pulse shape similar to that of the laser pulse. The first peak is almost entirely due to the energy temporarily stored in the peaking capacitors. The second peak is due to additional energy pumped in by the external capacitors and barely reaches lasing threshold, so that the corresponding extracted optical pulse is relatively weak. The discharge impedance (R_D), obtained by dividing the V-curve by the I_D- characteristic, exhibits somewhat of a plateau at the one-ohm level for approximately 30 ns.

By comparing the energy in the laser pulse with the amounts of electric energy stored in various parts of the circuit, or dissipated in the discharge, values for the overall efficiency and for the intrinsic laser efficiency can be calculated. These are:

(a) Efficiency based on total energy stored in capacitors (wall-plug efficiency): 0.5%

(b) Efficiency based on total energy deposited in gas, as measured by V- and I-probes: 2.2%

(c) Efficiency of first laser spike based on energy stored in peaking capacitors: 7%

The last figure shows that the intrinsic efficiencies of self-sustained discharge-excited rare-gas halide lasers are not too different from those of e-beam pumped systems. Evidently the prime reason for the low overall efficiency (≈1%) of most self-sustained devices lies in their inability to

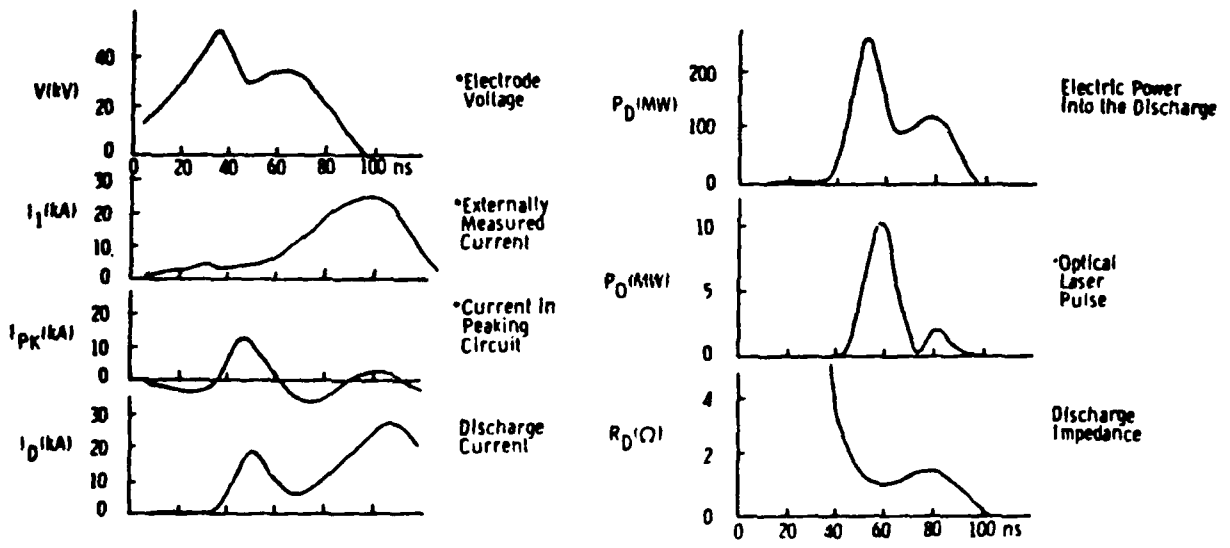

Figure 2-1. Discharge Characteristics for 1ℓ Transverse Discharge Laser (KrF) from Ref. 22. (*Quantities measured directly; I_D, P_D and R_D curves were derived from the measured parameters.)

transfer all of the stored energy to the gas at a rate which is consistent with good laser energy extraction. The development of a discharge-pumped KrF or XeCl laser with 3 percent overall efficiency thus appears to be feasible, provided that a stable discharge can be maintained and that the impedance-matching problem can be solved. The recent work of Lin and Levatter,[9,10] as implemented in the Helionetics excimer laser development program, provides the technology for achieving this.

2.3.2 Performance of a Distributed-Impedance Water-Line Driven RGH Laser

Taking proper account of the electric field, preionization and voltage-risetime factors, a large-volume (~2.5 liter), low-inductance, X-ray preionized discharge-pumped excimer laser was constructed by Levatter[23]. This laser was built in order to investigate the temporal and spatial scaling limits of self-sustained discharge excimers. The laser consisted of a low-inductance (≈4 nH) discharge chamber made of 304 stainless steel, Teflon, aluminum, and Kynar (polyvinylidene fluoride) in order to make the system halogen-compatible. The discharge electrodes were connected to a double-parallel-plate water transmission line driven by a multi-arc-channel rail gap. The maximum pressure capability of the laser was 6 atmospheres, and the electrode spacing could be varied between 1 to 6 cm, giving a maximum usable discharge volume of approximately 2.5 liters. The laser PFN had a nominal line impedance of 0.5Ω and had a stepwise variable electrical length (two-way transit time). To date, electrical pulse durations of 100 and 200 ns have been employed. The line was switched by a self-triggered rail gap that operated in approximately 100 simultaneous arc channels, producing a voltage risetime on the discharge electrodes of approximately 10 ns [see Figure 2-2(a) and (c)].

Using typical rare-gas halide laser gas mixtures, very homogeneous avalanche discharges were obtained with energy loadings as high as 400 J/liter-atm with no sign of arcing. With XeCl, a laser output of 2.5 joules was obtained from a one liter volume, and nearly 5 joules were obtained from a 2.5 liter volume using the 100 ns length PFN. The best laser efficiency (laser energy/stored PFN energy) achieved under these conditions was 1.4%.

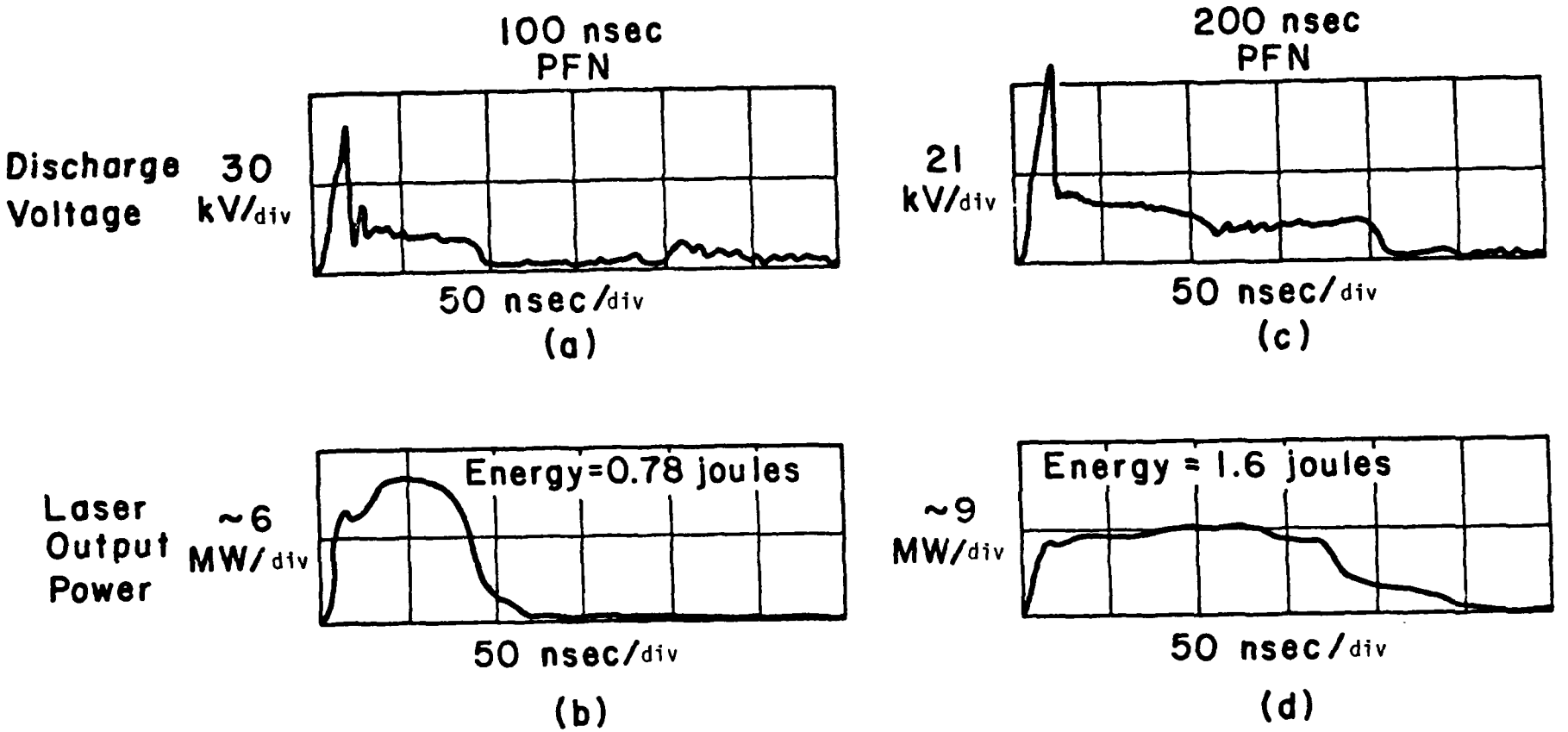

Figure 2-2. Discharge Voltage and XeCl Laser Output Power for a 100 and 200 ns PFN. The discharge volume was 1 liter and the gas mixture was He:Ar:Xe:HCl = 74.8:20:5:0.2 at a total gas pressure of 1 atm. (from Ref. 23).

More recent experiments with XeCl and 200 ns PFN have produced stable, uniform discharges with a corresponding 200 ns long laser output pulse [Figure 2-2(c) and (d)]. Note in the discharge voltage waveforms of Figures 2-2(a) and (c), that after the initial voltage collapse, the voltage trace exhibits a quasi-steady plateau, indicating that the discharge was running in a spatially homogeneous, stable, self-sustained mode for the remainder of the electrical pulse. As a result, the laser output beam, in both the 100 and 200 ns experiments, was extremely uniform over a 3 cm x 3 cm area.

Figures 2-2(b) and (d) show typical XeCl laser output power observed in 100 ns and 200 ns discharges under otherwise identical experimental conditions. The gas mixture used was He/Ar/Xe/HCl 74.8/20/5/0.2 at a total gas pressure of 1 atmosphere. The discharge volume was approximately 1 liter (3x3x110 cm^3), and the PFN charging voltage was 50kV. It can be seen that the optical pulse width from the 200 ns discharge was about twice as long as from the 100 ns discharge, while the peak power remained approximately the same (≈9 MW). Thus, the laser output energy from the 200 ns discharge was also approximately twice the energy obtained from the 100 ns discharge. This demonstrates that temporal scaling of the laser output with discharge duration applies over this range.

Tests in which the gas pressure in the discharge was increased from 1 atm to 2 atm showed that the voltage waveforms were quite independent of gas pressure. At all pressures, a stable voltage plateau was observed over the entire 200 ns period.

The XeCl laser output, on the other hand, showed a much stronger pressure dependence. As the total gas pressure increased, the peak laser output power first increased and then decreased. The width of the optical pulse, however, appeared to decrease monotonically with increasing gas pressure. The reason for such premature termination of the optical pulse at the high gas pressures is not clear at this time. It may be due to quenching processes interfering with the formation kinetics of excited XeCl, or it may be caused by an increased rate of formation of tri-atomic absorbing species at higher gas pressures. In addition to this simple pressure dependence, the optical pulse width also appeared to be mixture dependent. When neon was substituted for helium as the dilutent gas under otherwise similar conditions, the laser

output duration was found to vary with the dilution ratio in such a way that the higher thedilution ratio, the longer the laser output pulse. In fact, with a highly dilute mixture of Ne/Xe/HCl = 99.2/0.8/0.06, it was possible to maintain a full 200 ns laser output at gas pressures up to 2.7 atm.

It is evident that, because of the complicated nature of the kinetics and discharge physics, further work is required before these observed phenomena can be fully understood. However, the principles underlying the basic kinetics and discharge processes are now sufficiently in hand to permit high confidence design and construction of relatively high-energy, high-average-power uv lasers.

2.4 Outline for 1J - 100 Hz Laser Development

Levatter and Lin, acting as consultants to Helionetics, in conjunction with other Helionetics personnel, such as Drs. Rothe and Sandstrom, have developed a number of new and innovative techniques which implement the results of the previously described discharge formation analysis. These techniques have led to a rare-gas halide excimer laser design which has uniform discharge characteristics with a one to two joule output.

Helionetics, Inc. is presently committed to a 22 month program for developing a 100 W discharge-pumped excimer laser for commercial applications. Current plans involve substantial internal funding in addition to anticipated Navy support. The Helionetics laser is being built to meet the following specifications, which are not too different from those required for the XeCl pump laser of a space-based strategic laser communication system.

TABLE 2-1

SPECIFICATIONS OF HELIONETICS' HIGH-POWER RGH LASER SYSTEM FOR SEMICONDUCTOR PROCESSING

Wavelength	3080 Å, 2490 Å, and others
Energy per pulse	1 joule @ 1% efficiency
Pulse repetition rate	100 Hz
Average power	100 W
Optical pulse duration	80 ns
Spatial distribution of optical output	Uniform across a 2.5x2.5 cm^2 area±5%
Estimated system life	$\sim 10^{10}$ pulses
Component life before servicing	$>10^8$ pulses (300 h)

Of the above specifications, the most significant are the laser pulse energy, repetition rate (and hence average power), optical beam uniformity, and component lifetime. The achievement of this combination of features will take the Helionetics uv-laser system far beyond any laser now in existence, and will provide for the first time a viable high-energy, high-average-power, ultraviolet laser with a multitude of applications.

The same basic laser system will be able to provide many different output wavelengths, depending on the gas mixture introduced into the discharge chamber. Some of the molecular species, which have demonstrated efficient laser action in the uv and visible, are listed below together with their laser wavelengths and potential applications.

TABLE 2-2

AVAILABLE WAVELENGTHS AND POTENTIAL APPLICATIONS

Lasing Molecule	Wavelength (nm)	Potential Applications
ArF	194	Silicon Purification, Chemical Kinetics Studies
KrF	249	Semiconductor Processing, Inertial Confinement Fusion (ICF), Uranium Enrichment, Ablation of Metal Surfaces
XeCl	308	Solar Cell Annealing, VLSI and VHSIC Processing, Blue-Green Strategic Communications, Uranium Enrichment
XeF	350	Solar Cell Annealing, Deuterium Enrichment

With some modifications, the laser can also be made to work on the interhalogens such as IF, extending the available wavelength range to the visible, e.g.

IF	491	Strategic Underwater Communications

Almost all of these wavelengths may be used for semiconductor processing and photochemical applications. The best wavelength for a specific application has to be determined by experiment. The available wavelength range can be extended into the visible and into the vacuum ultraviolet (vuv) by employing the RGH laser as a pump laser for nonlinear frequency conversion schemes. Frequency down-conversion by stimulated Raman scattering in metallic vapors[24,25] and molecular gases[26] has recently been demonstrated with high efficiency. Short uv wavelengths below 100 nm may be produced by frequency tripling[27] in suitable gases and vapors.

For certain photochemical processes requiring high selectivity and for strategic communications[28] requiring high signal-to-background discrimination (attainable by use of a narrow-band resonance filter, e.g., at the receiver end), it is necessary that the laser source have a narrow bandwidth and be continuously tunable to a precise center wavelength. The bandwidth of the gain profile of typical RGH lasers ranges from a few nanometers to several tens of nanometers, providing at least a limited amount of continuous tunability[29]. The broad frequency bandwidth of these lasers also makes them ideally suited for the amplification of extremely short (picosecond) laser pulses[30], useful for the study of processes requiring extremely high peak powers (e.g., coherent X-ray generation).

For strategic communications with submerged submarines one of the actively pursued concepts within the Navy's blue-green laser program involves one or more space-based lasers with average power output between 200 to 1000 W at 480 nm and with overall systems efficiencies greater than 1%. Presently active research and development efforts are directed towards a 2 joule/pulse laser operating at 100 pulses per second. The 200 W output characteristic was chosen solely because of power availability on the proposed satellite station. A 10 joule/pulse laser would be preferable, because it may successfully communicate with submarines at greater depth, over wider areas and in regions of the ocean covered by heavy cloud layers.

At present, only two laser concepts are sufficiently advanced for serious consideration by the Navy for the space-based system. One approach is the

in-band $HgBr_2$ laser, the other is a Raman-shifted XeCl laser. Energy conversion efficiencies in the Raman process are not much greater than 50%, so that the single-pulse XeCl laser efficiency has to be between 2.5 and 3% to meet the overall system efficiency goal of one percent.

The Lin-Levatter laser[9,23] has already demonstrated an efficiency of 1.4% despite an approximately 2:1 line-to-load mismatch. We expect that by correctly matching the PFN to the discharge load, an efficiency of over 2% can be achieved. Should this efficiency be realized, the Helionetics laser system will be able to produce blue-green pulse energies in excess of a joule.

The design of the proposed laser incorporates all the criteria established by Levatter and Lin[10] which have been shown to be essential to achieving controlled, uniform discharges resulting in high laser efficiency and good beam quality. Several novel concepts have been included in the new laser design. A short discussion of these features and techniques follows.

2.4.1 Laser Configuration

The lasing gas mixture is excited by a fast-rising high-voltage constant-current pulse generated by a folded parallel-plate water Blumlein drive (Figure 2-3). The pumping pulse is applied to two carefully contoured parallel nickel electrodes arranged in a typical TE-laser geometry. The electrodes are spaced 3 cm apart and are 75 cm long, resulting in a discharge volume of 0.68 liters. A uniform preionization level is established in the discharge gap by hard uv-radiation generated by firing a spark array just prior to the pumping pulse. This spark array is located behind the screen cathode, which has an approximately 66% open surface area.

The discharge chamber is part of a closed-cycle gas recirculation flow loop, capable of providing a uniform gas flow transversely through the discharge gap at a velocity of more than 10 m/s. This is sufficient for a pulse repetition frequency of up to 200 Hz with a gas clearing ratio (flush factor) of 2 between pulses.

Figure 2-3

SCHEMATIC OF ELECTRICAL SYSTEM FOR 1J/PULSE XeCl LASER

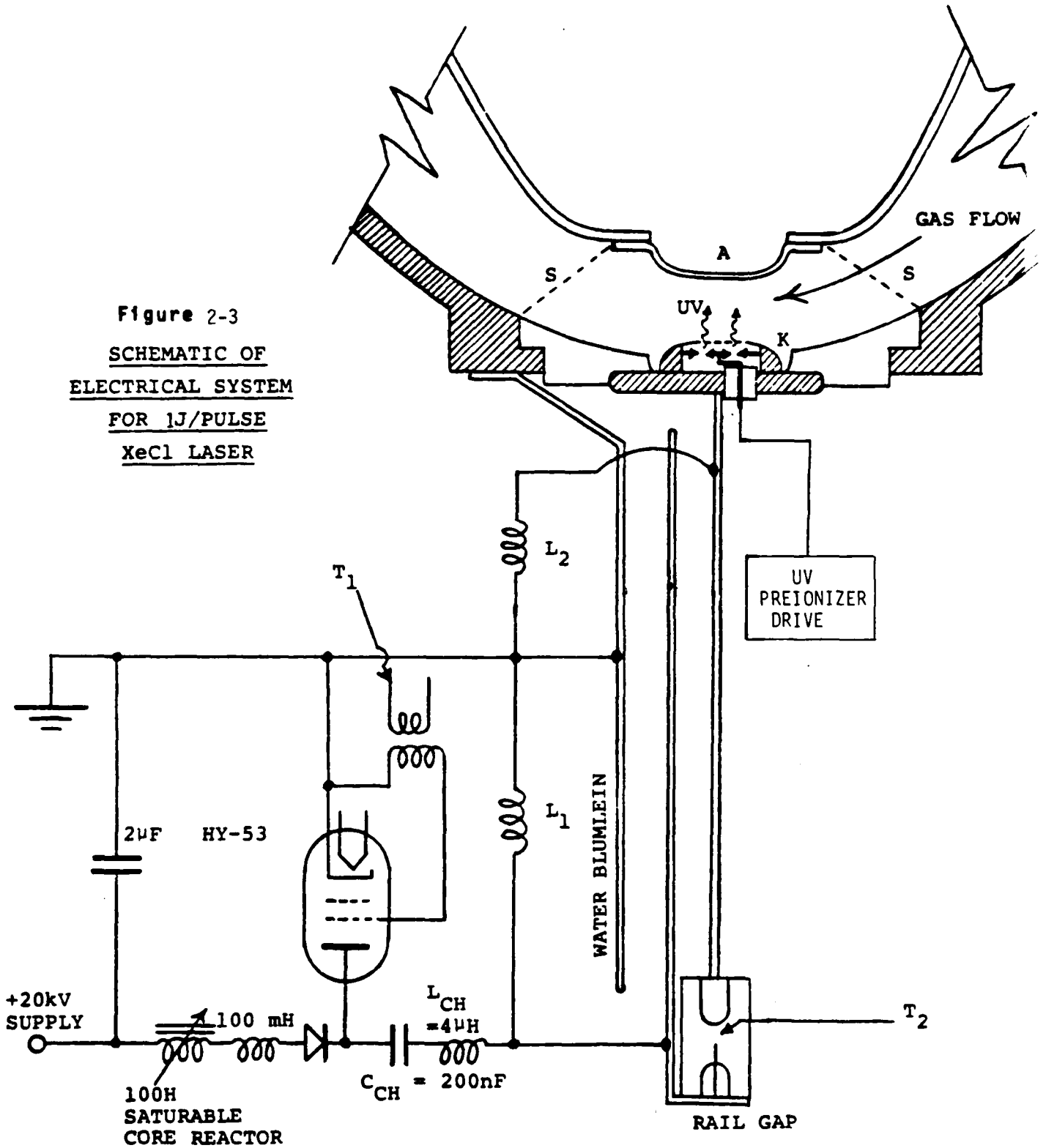

The water Blumlein acts as a temporary energy storage only, and is slowly ($\sim$2 μs) pulse-charged just prior to discharging this energy into the laser head. The water lines are pulse-charged from a primary capacitor by means of a hydrogen-filled double-grid EG&G HY-53 ceramic thyratron, operated well below the manufacturer's quoted specifications for long switch life. The primary capacitor is resonantly charged via a saturable-core reactor from a DC high-voltage power supply (see Schematic 2-3). A triggerable multichannel rail gap of novel design is used to discharge the Blumlein circuit into the laser gas. When this rail gap is fired, two electric waves are launched along the Blumlein plates. A fast-travelling electric pulse, containing a relatively small amount of energy travels along a solid-dieletric transmission line (small ε, high wave speed) and arrives at the preionization spark assembly approximately 30 ns before the main pulse arrives at the electrodes via the water line (high ε, low wave speed). Hence, the preionization pulse automatically precedes the discharge pulse by a predetermined time interval without the use of active time delay circuits and associated trigger pulse generators. This technique greatly simplifies the operation of the laser and therefore significantly increases the reliability of the system. The operational relationship between the various sub-systems of this laser is illustrated in Figure 2-4.

2.4.2 Laser Discharge Chamber

The laser discharge chamber must simultaneously be capable of withstanding a high voltage impulse and also have a very low electrical inductance. The effect of additional inductance would be to increase the discharge current risetime. If the current rise time is a substantial fraction of the total electrical pulse duration, only a relatively small fraction of the PFN energy can be delivered to the discharge efficiently. Therefore, ultra-low inductance connections will be employed by attaching the Blumlein plates along their entire width to metal structures which support the discharge electrodes (Figure 2-3). High-voltage tracking and flashover will be eliminated by using an appropriate insulator surface geometry inside the laser chamber, and by using water as a high-voltage insulator at the PFN-laser chamber interface. The particular geometry of the laser-PFN interface is such that

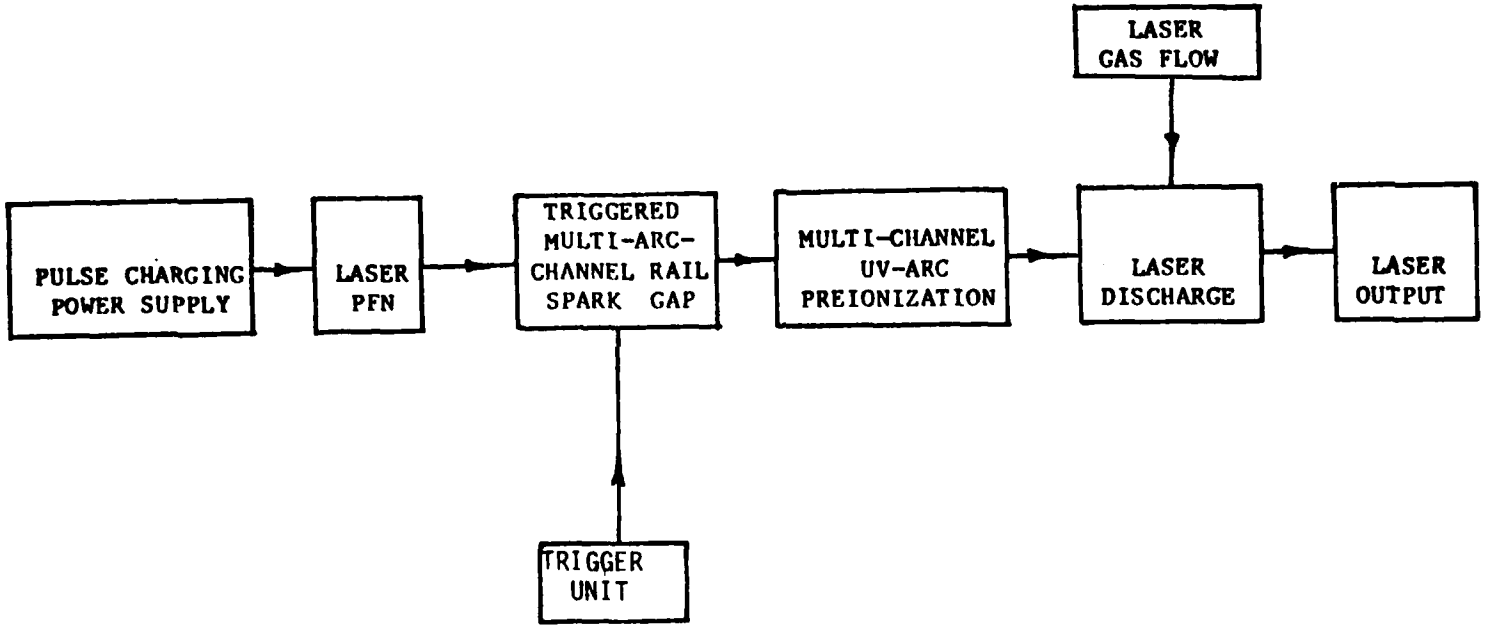

Figure 2-4. Operational Relationship of the Major Components of the UV-Preionized Laser System.

the transmission-line characteristic impedance is essentially maintained all the way up to the discharge electrodes. The only unmatched circuit inductance is that due to the discharge volume itself, and is estimated to be approximately 4 nanohenries. Therefore, the discharge current risetime(10 to 90%) is calculated to be 2.2 L/R = 11 ns, which is less than 1/7 of the total electrical pulse duration. This value is acceptable. (The discharge impedance, R, has been taken to be approximately 0.8 ohm).

Material selection for the laser chamber, electrodes, flow ducts, heat exchanger and all other parts in contact with the corrosive laser gas mixture, is of critical importance for the useful life of a laser gas fill. Metallic surfaces will be nickel-200, electroless nickel coatings on aluminum, or possibly Hastelloy-C276. The use of stainless steel alloys will be avoided, because of their poor chemical resistance to HCl. When choosing solid nickel (or other ferromagnetic materials) for parts located within the discharge current loop, care must be exercised so as not to increase the electrical inductance of the discharge circuit. Only Teflon or Kynar will be used for electrical insulators to make the laser chamber completely halogen compatible.

2.4.3 Pulse-Forming Network

The high-voltage laser pulse-forming network (PFN) is the principal discharge energy delivery system. As such, its characteristics are essential in determining the operation of the entire laser. The PFN must simultaneously have a low characteristic impedance to match the estimated discharge load, a large stored energy to allow an energy deposition of 100 to 300 J/liter in the laser gases, the ability to withstand a high charging potential and the capability of producing a square voltage pulse (risetime≈10 nsec) with a 50-100 ns duration.

The design requirements of a low output impedance and a fast voltage risetime preclude the possibility of using a discrete LC network for the laser PFN, since it is generally not possible to reduce the connection inductance of each capacitor section in a discrete network to a sufficiently low value. The alternative is a distributed PFN, i.e., a transmission line. This type

of PFN is capable of producing a low-impedance, fast-rising voltage pulse with a frequency response limited only by the skin effect of the conducting surfaces and by the intrinsic losses of the dielectric.

There are two general categories of dielectric materials suitable for high-voltage applications: (1) solids (e.g., Mylar polyester, Kapton, mica, etc.), and (2) liquids (e.g., water, alcohol, oil, etc.). Solid dielectrics, however, have a fundamental limitation; the storage of high energy densities requires a very high electrical stress, which can lead to dielectric fatigue and eventual component failure.

Although liquid dielectrics are not without limitations, they have several important advantages. Water, alcohol, and oil are the most commonly used liquid dielectrics, but only water has both a high dielectric constant and a low dielectric loss tangent. For short-duration, high-voltage impulses of less than 10^{-5} seconds, pure water behaves as a high-quality insulator. Since H_2O is a polar molecule, it also possesses an exceptionally high dielectric constant ($\approx$80) throughout a broad frequency range. This makes it easy to store relatively large amounts of energy per unit volume without putting a high electric stress on tne dielectric. Typically, high-quality, low-loss solid dielectrics have dielectric constants of only 3 or 4. The energy stored in a polarizable medium is proportional to the dielectric constant and to the square of the electric field. Hence, the required stress in a water dielectric is approximately 1/5 the stress in a solid dielectric medium of comparable energy density.

A further advantage of the high dielectric constant of water is the slow propagation velocity of an electromagnetic wave in such a highly polarizable medium. The electrical pulse length (two-way transit time), τ_p, produced by a parallel plate transmission line is simply

$$\tau_p = 2 \times \varepsilon^{\frac{1}{2}}/c \quad , \qquad (2\text{-}1)$$

where x is the physical length of the line, c is the speed of light in vacuo, and ε is the dielectric constant. Since $\varepsilon = 80$ for water, the physical length of a water transmission line is roughly 1/6 that of a solid dielectric transmission line of equivalent pulse length. Water was chosen as the most suitable

dielectric material for the present laser PFN, because it results in an energy storage system that is compact, self-healing, stressed well below breakdown, is easily capable of storing the required energy and will, therefore, be reliable.

The specific form of water transmission line chosen is a folded parallel-plate Blumlein configuration as shown in Figure 2-5. In operation the center plate is pulse-charged (see circuit in Figure 2-3) to a potential V_o in a period of approximately 2 μs. When fully charged, the energy stored in the water Blumlein is discharged into the laser cavity by triggering a low-inductance rail gap, located between the center plate and one of the grounded plates at the opposite end of the laser discharge section. The resulting electric pulse travels down one part of the line and is reflected from the open-circuit end of the discharge section. At that time the voltage across the discharge electrodes reaches $2V_o$, well above the breakdown voltage of the gas mixture in the discharge gap. As the avalanche discharge develops, its impedance, R, drops from infinity to a value of less than 1 ohm in a few nanoseconds. The discharge voltage, V_L, drops accordingly from $2V_o$ to a sustaining value near V_o, if the PFN source impedance is well matched to the discharge load impedance, R. The latter depends on the discharge gap and the power loading of the gas. The impedances are matched, if the impedance, Z, of each Blumlein section, i.e.

$$Z = \left(\frac{\mu_o}{\varepsilon_o}\right)^{\frac{1}{2}} \frac{b}{a}\, \varepsilon^{-\frac{1}{2}} \qquad (2\text{-}2)$$

is equal to R/2. Symbols b and a represent the Blumlein plate separation and the line width, respectively (see Figure 2-5).

A logical design sequence for specifying the Blumlein drive, discharge dimensions and electrical parameters for such a laser is given by steps (A) through (F), starting with a specified optical pulse energy (U_o) and a known laser efficiency (η_L):

(A) Specified parameters: 1. Optical Pulse Energy = U_o

2. Laser Efficiency (Elec.) = η_L

These determine electrical energy stored

$U = U_o/\eta_L = P\tau_p$, where (2-3)

P = Electrical power into discharge (rectangular pulse of duration τ_p assumed)

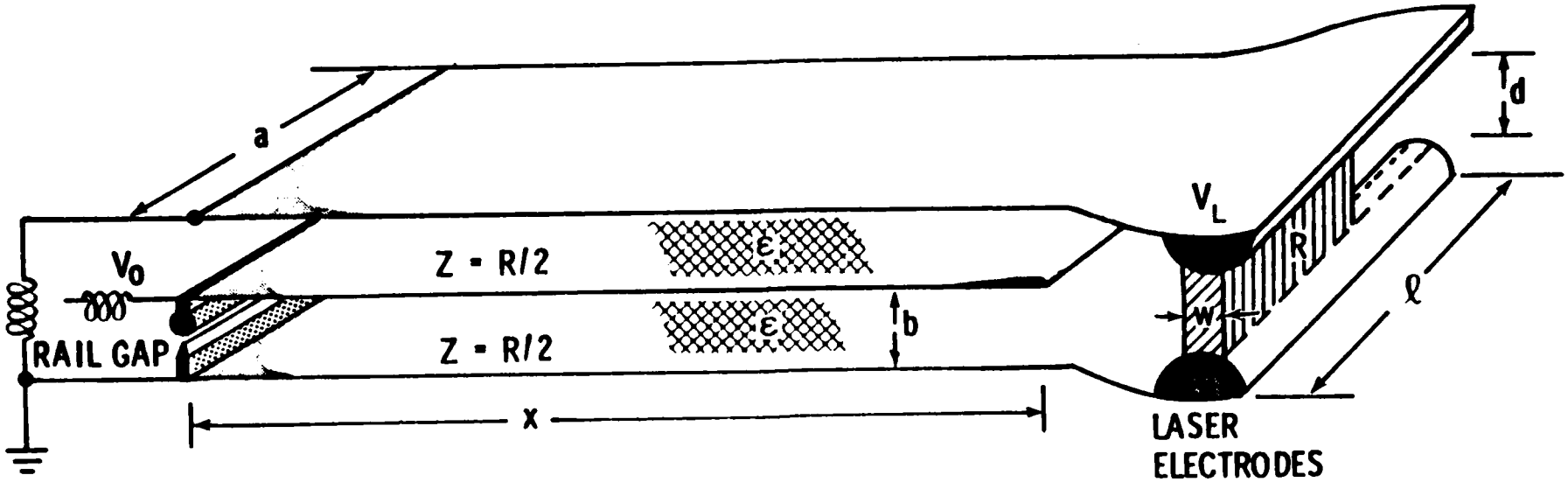

R = DISCHARGE (LOAD) IMPEDANCE (MOSTLY RESISTIVE)

LINE IMPEDANCE: $Z = Z_0 \frac{b}{a} \varepsilon^{-1/2}$, where $Z_0 = (\mu_0/\varepsilon_0)^{1/2} = 377\,\Omega$ = IMPEDANCE OF FREE SPACE

and ε = RELATIVE DIELECTRIC CONSTANT OF LINE INSULATION

FOR MATCHED LOAD: $Z = R/2$, $V_L = V_0$

ENERGY STORED: $U = CV_0^2/2$

PULSE LENGTH: $\tau_p = 2x\varepsilon^{1/2}/c$, where $c = 2.99 \times 10^8$ m/s = SPEED OF LIGHT IN VACUO $= 1/\sqrt{\varepsilon_0 \mu_0}$

TOTAL CAPACITANCE: $C = 2\varepsilon_0 \varepsilon x \cdot \frac{a}{b} = 2U/V_0^2 = \tau_p/Z$

Figure 2-5. Parallel-plate Blumlein Drive

(B) Choose best gas mixture ratio and gas density, ρ, on the basis of optimum laser chemical kinetics.

(C) Determine equilibrium E/n from discharge kinetics calculations. Electron production (ionization) = Electron losses (recombination + attachment)

(D) Choose a set of values for

P/υ = Electric power density in discharge

U/υ = Electric energy density in discharge

$\tau_p = U/P$ = Pulse duration

- - - - - -

P/υ Should be well above pumping requirements for achieving lasing threshold.

U/υ Should be below the energy densities which empirically lead to arc instabilities.

τ_p Should be consistent with efficient laser energy extraction (i.e., significantly longer than transient rise and fall-times of the voltage and current pulses and significantly longer than the optical build-up time).

- - - - - -

This determines the discharge volume, $\upsilon = U/(U/\upsilon)$, the pumping power, $P = (P/\upsilon)\upsilon$ and line length.

$$x = \tau_p \, c\varepsilon^{-\frac{1}{2}}/2 \qquad (2\text{-}4)$$

(E) Choose discharge geometry, $\upsilon = dw\ell$, and dielectric (ε)

ℓ = Discharge length, generally chosen to be less than 1m for limiting total optical gain to a controllable value and for ease of matching to a transverse gas flow channel.

w = Discharge width; w≫d for good optical mode properties.

d = Electrode separation; should be consistent with voltage levels than can easily be switched.

Choice of d determines charging voltage

$$V_o = \frac{E}{n} \cdot \frac{\rho}{\rho_o} \cdot n_o \cdot d \qquad (2\text{-}5)$$

and the discharge and line impedances

$$R = 2Z = V_o^2/P = 2\tau_p/C \qquad (2\text{-}6)$$

ε should be large for high-density of energy storage and compact design (ε = 80 for water). The transmission-line aspect ratio is then also determined.

$$\frac{b}{a} = \varepsilon^{\frac{1}{2}} Z/Z_0 \quad , \tag{2-7}$$

where $Z_0 = (\mu_0/\varepsilon_0)^{\frac{1}{2}} = 377\Omega$ = impedance of free space.

(F) Choose suitable dimensions for b and a

$$b = V_0/\alpha\phi \quad , \tag{2-8}$$

where ϕ = electric breakdown strength of the dielectric and $\alpha < 1$. For $\alpha > 0.5$, the dwell time of the charge on the transmission line (time between charging and discharging of line) should be less than 1 μs.

Make a $\approx \ell$, the laser length, to facilitate easy matching of the line to the laser discharge section.

The described sequence of determining the design variables for a Blumlein-driven RGH laser is illustrated graphically in Figure 2-6.

Discharge characteristics and design parameters for the present PFN are:

Optical pulse energy:	U_0 = 1 to 2 J
Laser efficiency:	$\eta_L > 1\%$
Electrical energy stored:	U = 100 J
Electric field in discharge:	$E/n = 1.5 \times 10^{-16}$ V-cm^2 = 4.0 kV/cm - atm
Gas pressure:	p = 2.7 atm
Energy density in discharge:	$U/p\upsilon$ = 55 J/l - atm
Electric power density:	P/υ = 1.85 MW/cm^3
Pulse duration:	τ_p = 80 ns
Line length (Blumlein):	x = 1.34 m
Discharge volume:	υ = d x w x ℓ = 3 x 3 x 75 cm^3 = 0.68 l
Charging voltage:	V_0 = 32 kV
Discharge impedance:	R = 0.8 ohm
Line impedance:	Z = R/2 = 0.4 ohm
Line width:	a = 85 cm
Plate separation (Blumlein):	b = 8 mm
Electric stress in water:	ϕ_w = 39 kV/cm
Blumlein capacitance:	C = 200 nF

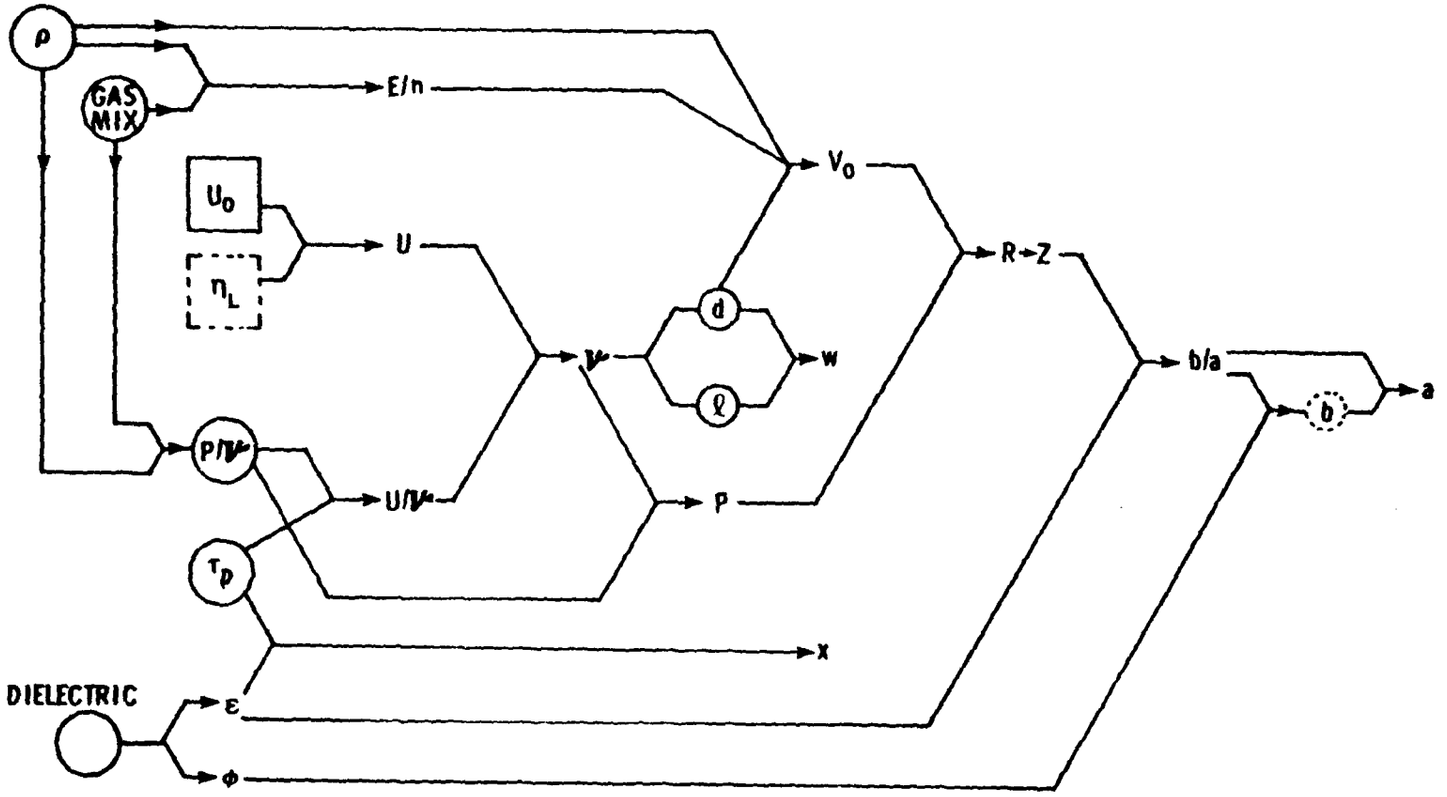

Figure 2-6. Sequence of Determining Design Variables for Blumlein-driven Laser.

The above electrical parameters are based on discharge kinetics considerations for a He/Ar/Xe/HCl mixture of 75/20/5/0.2 percentage ratio at 2050 torr total pressure. This gas mixture was chosen, because it has demonstrated high energy output per unit volume (2.5 J/liter)[10] at a relatively low total gas pressure of 2.5 atm.

The design parameters were chosen such that, for a gas pressure of 2.67 atm and a charging voltage of 32 kV, the Blumlein drive impedance is perfectly matched to the discharge impedance for optimum power transfer. In practice, the E/n for stable discharge operation may be somewhat different from the predicted value, so that the voltage across the discharge may be higher or lower than the charging voltage of the Blumlein (higher or lower than half the initial line-doubled voltage, indicative of an impedance mismatch). By adjusting the charging voltage or the gas pressure, the applied V/p can be matched to the discharge E/n value. The present laser system will permit large variation of pressure (2 to 4 atm) and charging voltage (22 kV to 40 kV) to achieve this. The available operating range is indicated by the cross-hatched area in Figure 2-7. Alternatively, the E/n of the discharge can be changed by changing the gas mixture ratios, thereby adjusting the discharge impedance to the drive circuit. However, it is best to optimize the gas mixture independently, so as to realize the most favorable chemical reaction kinetics for the laser process.

2.4.4 Preionization

For the sake of simplicity and reliability, the present design makes use of uv-spark preionization, rather than X-ray preionization as employed by Levatter. As will be shown in Section 4, sufficiently uniform and intense preionizing radiation can be produced by a properly designed spark array, provided that the dimensions of the discharge volume are sufficiently small, so that the ionizing uv-flux is not strongly attenuated by absorption within the interelectrode gap.

X-rays have the advantage that they can preionize large gas volumes very uniformly. This feature is of paramount importance for scaling the pulse energy of discharge-excited excimer lasers to values beyond 10 joules (Section 3).

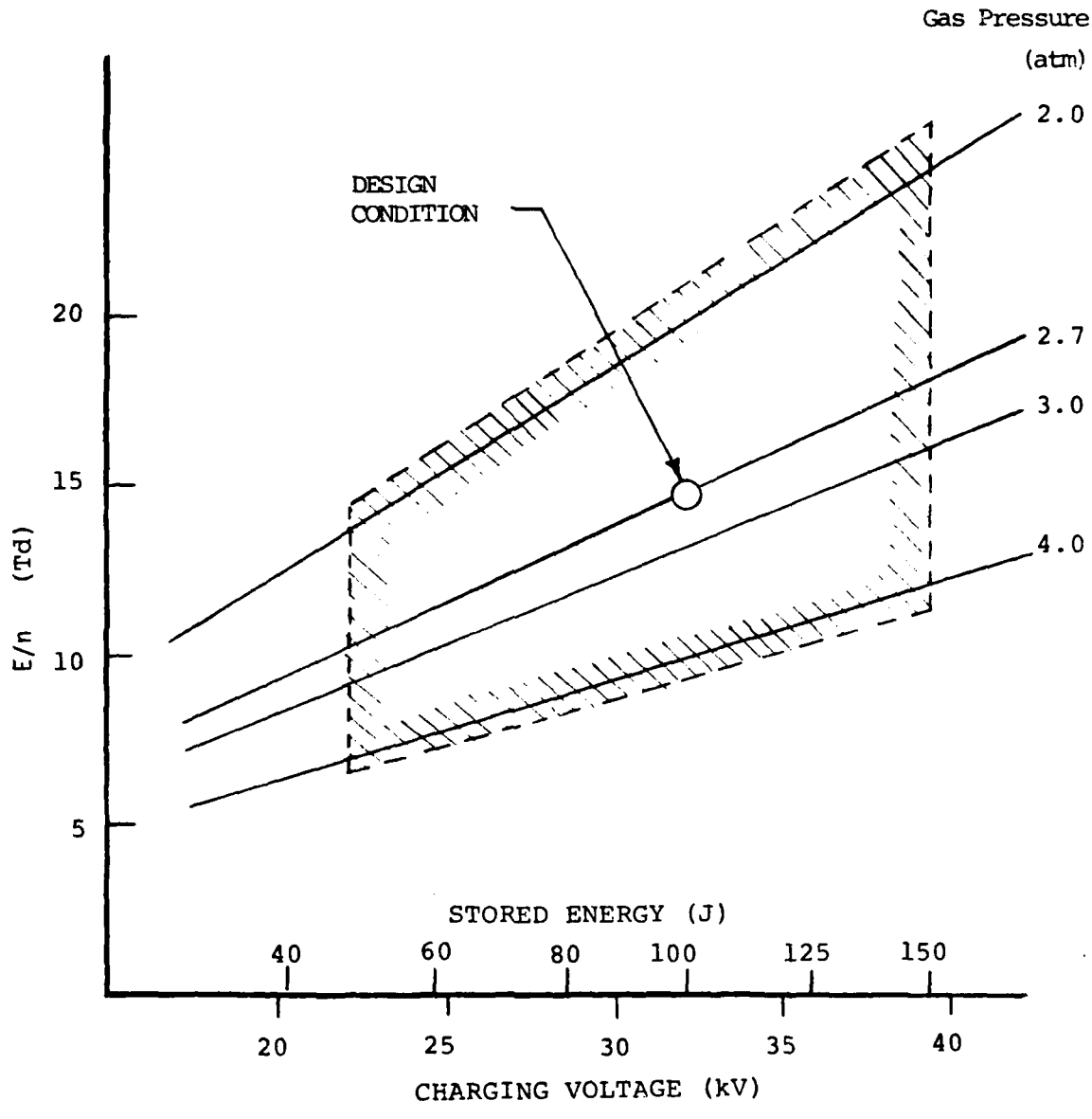

Figure 2-7. Design Condition and Operating Range as determined by Gas Pressure and Voltage Capability of Proposed Laser System.

Provisions have been made in the present laser design to substitute an X-ray preionizer for the uv-spark array, should the uv-spark preionization lack the required uniformity for producing long-duration stable discharge pulses, although this substitution is not expected to be necessary. The X-ray generator, which could be either a WIP gun[31] or a cold-cathode e-beam unit, would be mounted behind a thin (<3mm thick) nickel-coated aluminum anode, as shown in Figure 2-3.

Although additional trigger and delay circuits are required for the implementation of an X-ray preionizer (Figure 2-8), the cathode design and Blumlein geometry becomes simpler. This would permit the use of a double Blumlein drive instead of the single Blumlein design shown in Figure 2-3. Such a geometry would cut the PFN impedance in half and make it possible to match the PFN to a laser discharge operating at a higher power loading. Recent calculations by Lin[32] have shown that this may be important for increasing the laser efficiency.

2.4.5. Triggered Multichannel Rail Gap

The risetime at the leading edge of the voltage pulse arriving at the discharge electrodes is determined by the closure time of the rail gap switch. In order to provide a sufficiently fast voltage risetime of less than 10 ns, the resistive and inductive breakdown phases of the switch must be reduced to a minimum by ensuring that the gap breaks down in many parallel arc channels. Multichannel arc operation[15,16,17] requires careful electrode design, uniform electrode spacing, a low-impedance drive network, a judicious choice of gas mixture, and a means of ensuring simultaneous breakdown at many points. Competition between parallel arc channels for carrying a major part of the total current requires that a large number of breakdown channels form simultaneously (i.e., within a few nanoseconds). For a self-triggered gap this means a fast-rising voltage pulse has to be applied to the rail electrodes. Hence, the Blumlein plates have to be charged relatively quickly (in a few hundred nanoseconds) with such a switch. With Helionetics' triggered rail gap design, however, the Blumlein plates can be charged more slowly, thereby reducing the current and di/dt requirements of the thyratron and other charging-circuit components. Multichannel breakdown is initiated here by triggering the gap simultaneously at many points along the length of the rail electrodes with a fast trigger pulse.

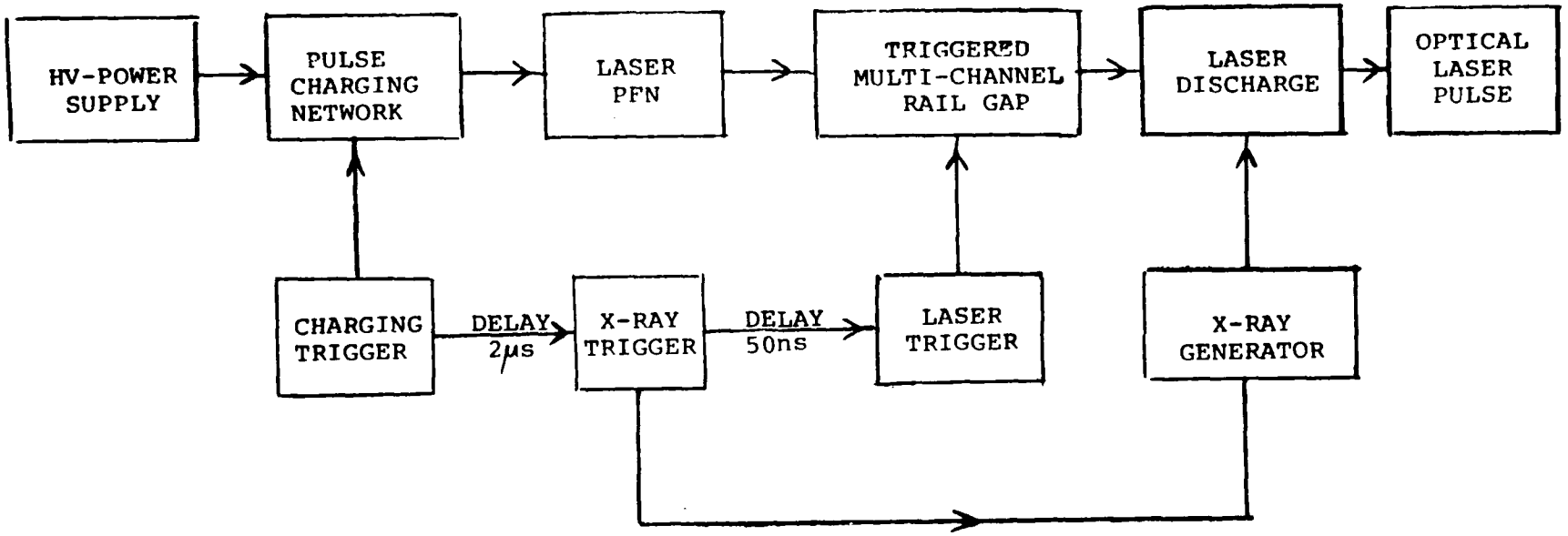

Figure 2-8. Interrelationship of the Various Laser Subsystems for an X-ray Preionized Laser.

Helionetics has developed a new type of triggered multichannel rail gap of proprietary design which breaks down in approximately 100 arc channels, yet is not susceptible to trigger erosion or transient electrical coupling which can limit the useful lifetime of ordinary triggered spark gaps.

The rail gap has to hold off the charging potential for only a few microseconds before it is triggered. After the electrical pulse it has a time period of approximately 10 ms for recovery (i.e., for deionization), so that the typical "hold-on" problems, generally experienced with high-PRF spark gaps, do not apply here. Nevertheless the hot gas has to be cleared out of the interelectrode gap between pulses, so that the rail gap breaks down consistently in a large number (>100) of spark channels. Since one electrode is essentially a knife edge, large clearing ratios can easily be achieved with a moderate gas flow of approximately 100 CFM (about 1/10 the gas flow required for clearing the laser cavity).

The spark gap gas will be dry air, nitrogen, or possibly an Ar-N_2 or Ar-O_2 mixture. The presence of oxygen in the gas is desirable, in order to inhibit the deposition of metal vapor eroded from the spark electrodes on nearby insulator surfaces. Insulating materials used in the construction of the rail gap are glass, Kynar and Teflon, materials which are highly resistant to degradation by ultraviolet light and to chemical attack by ozone or other reactive materials generated by the sparks.

The life of a spark gap is limited by spark erosion, which causes successive destruction of the switch electrodes and deposition of the eroded material on adjacent insulator surfaces. The erosion of metal from single-channel spark electrodes has been quantitatively studied for various electrode geometries and materials by Gruber et al.[33] The amount of electrode material removed was found to correlate quite accurately with the charge Q transferred per pulse. The dependence of the erosion on current and pulse length was found to be weak. Furthermore, it was found that the erosion per pulse was not a linear function of Q, but varied approximately as Q^2. This makes the total amount of electrode material removed per pulse inversely proportional to the number of spark channels. Also for a rail gap the erosion is distributed over the entire length of the rail electrodes. On the basis of these arguments, the estimated useful life of the Helionetics rail gap is in excess of 10^{10} pulses.

For a single-channel gap, employing tungsten-copper electrodes and switching a similar charge, only 5×10^6 shots are needed to remove 1 mm^3 of electrode material. Since this is essentially all removed from a small surface area, severe pitting can be expected, thereby restricting the life of a single-channel gap to a few million shots. It is of interest to note here, however, that with careful design even a single-channel spark gap can approach lifetimes of 10^8 pulses or more. For example, Keto et al.[34] have recently operated a high-PRF coaxial spark gap for more than 10^8 shots without cleaning.

2.4.6 Gas Flow, Turbulence and Acoustic Damping

In a high-PRF discharge-pumped excimer laser approximately 98% of the electric power fed into the discharge ends up as waste heat. It is therefore necessary to flow the gas mixture through the discharge gap to transport the heated gas to a cooling unit and to remove thermal inhomogeneities and acoustic disturbances left over from previous pulses. The most efficient way of exchanging the heated gas between pulses is to flow transverse to the TE-laser electrodes. In the present design a fraction of the mainflow (10-20%) is diverted into the cathode grid to flush out the spark assembly located behind the screen cathode.

Because of boundary layer effects on the electrodes and because of upstream disturbances created by shock waves from the discharge pulse, it is necessary for the flow to displace the discharge volume several times (clearing ratio or flush factor) between pulses. For the system under consideration, a modest flow velocity of 10 to 15 m/s provides a clearing ratio of more than 2 for pulse repetition rates up to 200 Hz. The volumetric gas flow requirements are less than 1000 CFM.

Apart from the cooling requirements of the laser, the gas recirculation has two prime objectives:

1. The gaseous medium between the electrodes has to be restored to a uniform baseline condition after each pulse, so that the discharge stability and uniformity of the succeeding pulse is not compromised.

2. The refractive index of the laser medium has to be kept sufficiently uniform throughout the optical cavity to maintain good optical beam characteristics. Care must therefore be taken to condition the gas flow, so as to remove objectionable density gradients due to pressure fluctuations and temperature non-uniformities.

The effects of random and ordered density disturbances, due to acoustic effects and free-stream turbulence, on the optical beam quality are discussed in Section 5.1.

The gas recirculation system will include heat exchangers, flow straighteners, acoustic damping devices and screens for generating small-scale turbulence, for dissipating shock wave energy and for transmitting the electrical pulse to the anode (see Figure 2-9). For long-life closed-cycle operation, some chemical cleanup will also be required. This can be performed at a slow rate in a secondary loop without significant power expenditure. For chemical reprocessing in a closed system, the necessary recycling rate has been shown[35] to be less than 10 cm^3/s for a similar size XeCl laser system. However, other processes such as particulate accumulation on optical surfaces may increase this number somewhat. This value also depends very much on the chemical inertness and cleanliness of all materials in contact with the gas and on the rate of contamination from electrode materials. The latter, in turn, is a strong function of the type of discharge (streamers or diffuse glow) and of the mode of preionization. A baseline number for the useful lifetime of a gas mixture without cleanup is given by the recent results of Miller et al.[12], who obtained more than 2.5×10^6 pulses from a 250Hz uv-preionized XeCl laser.

The second-largest power input into the laser system (after the electric power input to energize the laser discharge) goes into driving the gas compressor for recirculating the laser mixture. The overall efficiency of the laser system is therefore strongly influenced by the viscous pressure losses produced by the presence of heat exchangers, flow straighteners, acoustic damping sections, sharp turns and changes in the wall contours and other impedances in the gas flow loop. By keeping the cooling and acoustic damping requirements low, and by streamlining the flow duct, the pressure drop, Δp, in the flow loop can be minimized to reduce the compressor input

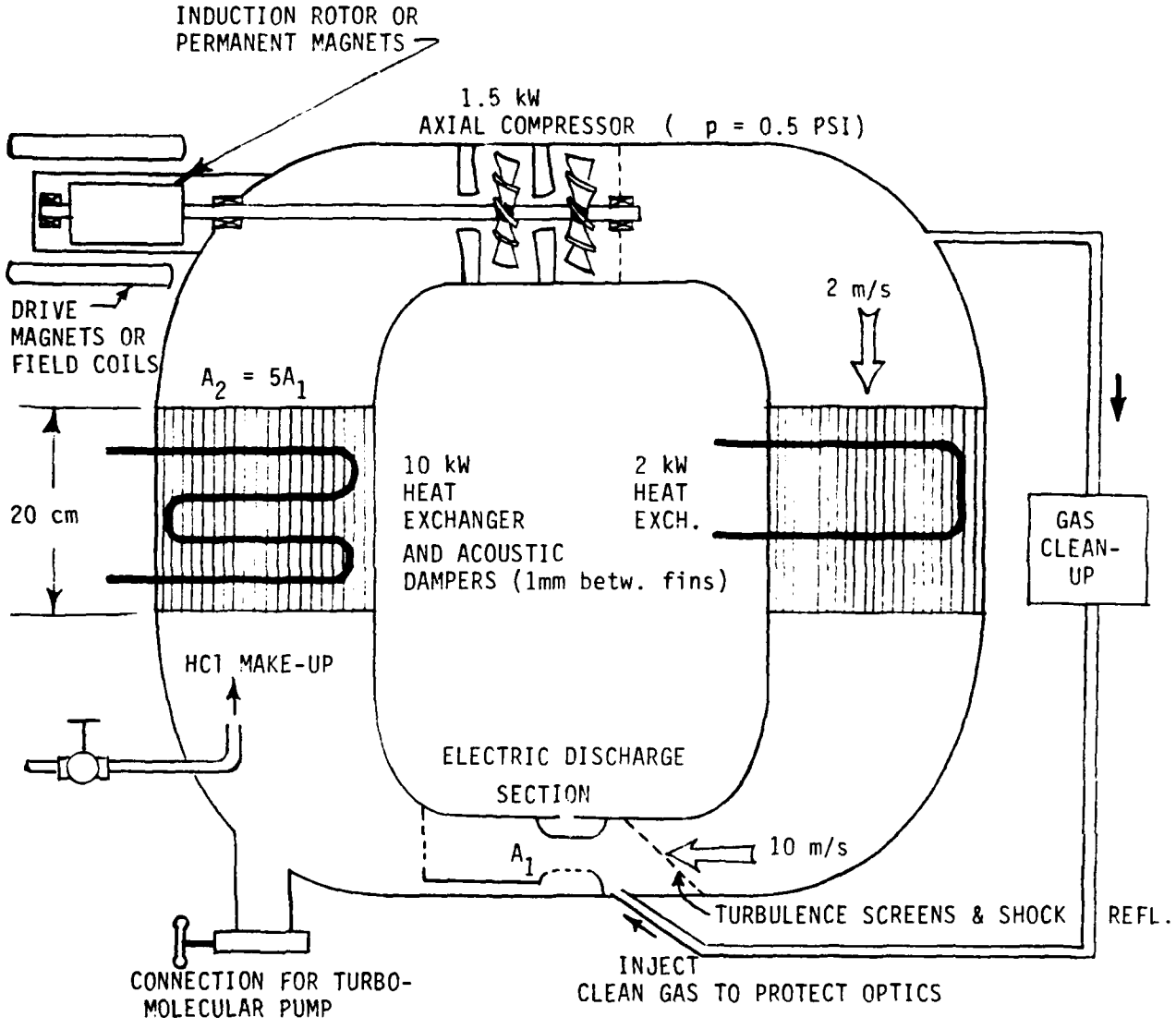

Figure 2-9. Schematic of Gas Recirculation System

power. For the present system Δp is estimated to be less than 0.5 PSI. The compressor power required (for incompressible flow) is given by:

$$P_c = \frac{d\upsilon}{dt}\Delta p = \upsilon\beta f\Delta p \ , \qquad (2\text{-}9)$$

where $d\upsilon/dt$ = volumetric gas flow rate, υ = discharge volume, β = flush factor, and f = pulse repetition frequency. This works out to approximately 1.5 kW here and compares with 10 to 20 kW going into the discharge.

The compressor will consist of a multistage vane-axial fan or a centrifugal blower. One problem area and a source of gas contamination is the shaft seal required between the motor and the compressor fan. Shaft seals can be avoided altogether, if the torque is transmitted through the duct wall to the fan rotor by means of a magnetic coupling (Figure 2-9). As a second choice, a multistage ferrofluidic shaft seal[36] could also be considered. The fluorocarbon-based sealing fluid would, however, most likely be a source of gas contamination. The use of non-lubricated fan bearings inside the laser system represents another challenge. Recently, Rothe[37] has operated a specially designed set of Rulon-J (Dixon Corp. T.M.) bearings in a heated mercury-halide laser for more than 50 hours. Rulon-J is a polyimide-reinforced Teflon and should also be compatible with gas mixtures used in the Helionetics system. For long-life closed-cycle operation all surfaces in the flow system exposed to the gas mixture will be made compatible for service with HCl, F_2, NF_3, etc. Questionable materials such as aluminum, copper, stainless steel, etc., will be nickel- or Teflon-coated.

2.4.7 Optical Cavity Design

In order to obtain near-diffraction-limited beam divergence and a sufficiently uniform intensity profile in the near field (flat top with steeply falling-off edges) a high-Fresnel-number, positive-branch, confocal unstable resonator[38] is considered. With the conventional unstable resonator design, the edge-coupled output beam (so-called "donut mode") has a hole in the center, where the beam is obscured by the totally reflective convex output mirror. This feature is undesirable for many applications. Figures 2-10 and 2-11 give two unstable resonator configurations which avoid having a centrally obscured area in the beam cross section.

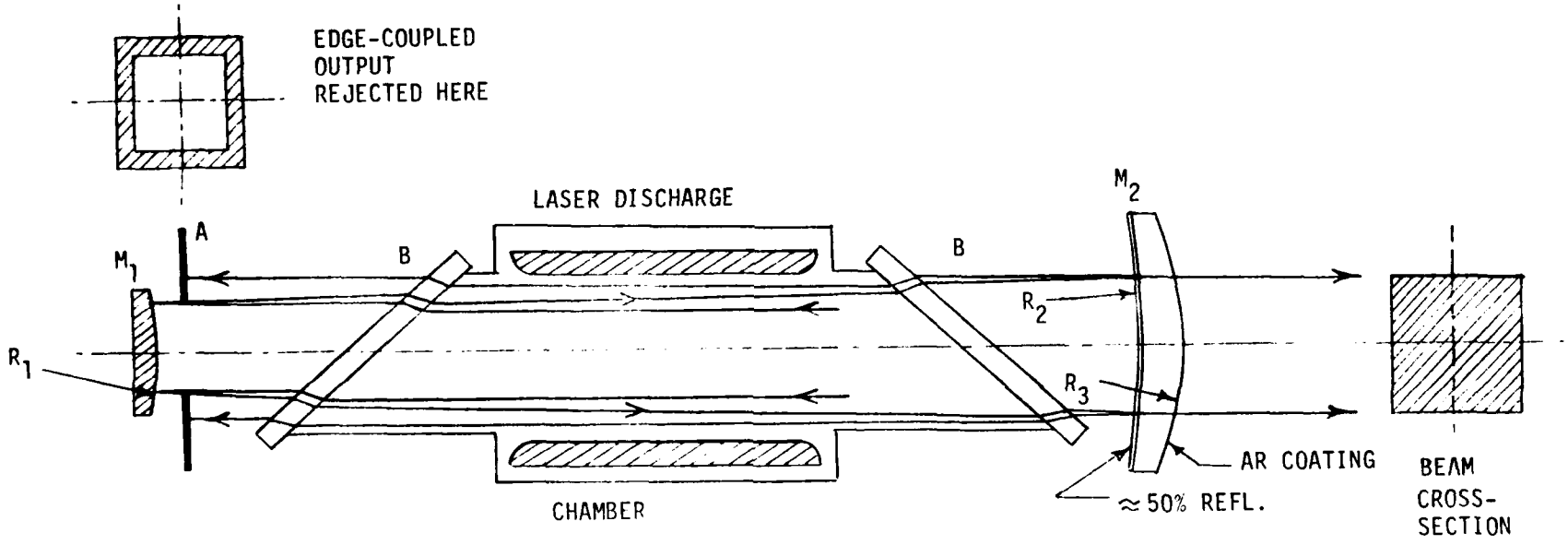

Figure 2-10. Low-Magnification Continuously-Coupled Unstable Resonator

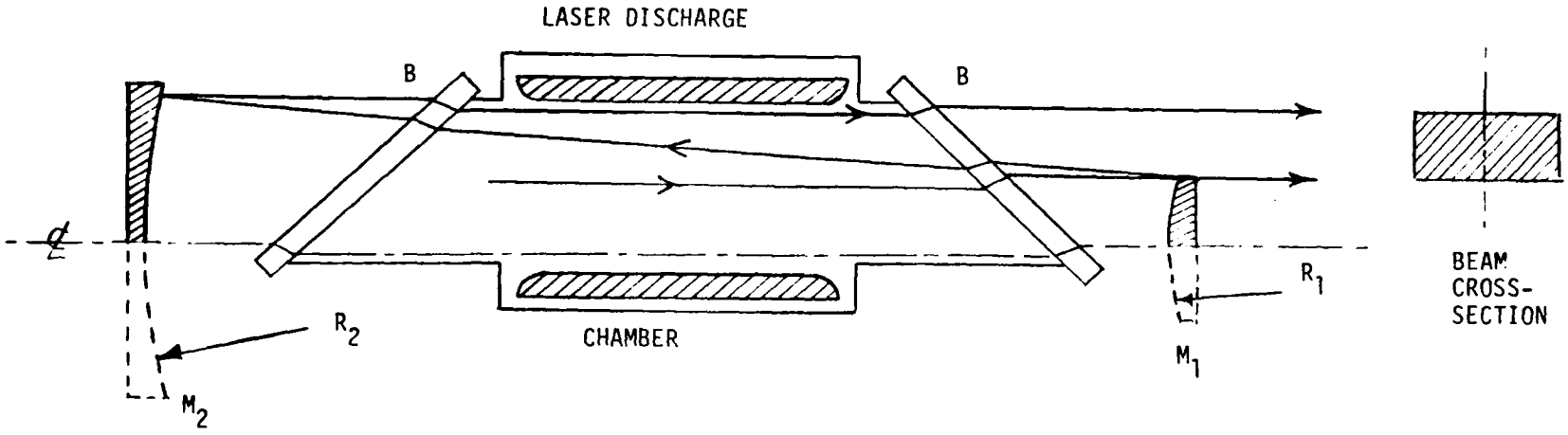

Figure 2-11. High-Magnification Unstable Cavity with Cylindrical Mirrors and One-Sided Output

In the first version (Figure 2-10), a confocal arrangement of spherical mirrors is employed. M_1 is a convex high-reflectivity mirror, whereas M_2 is a partially reflective concave quartz mirror. The useful output is coupled through this mirror in a spatially continuous mode. Since the discharge region is square, the beam cross-section is also square. The edge-coupled output is rejected at the aperture A. The round-trip magnification M is kept low in this design to minimize the beam energy rejected at the edge. The reflectivity of M_2 and the magnification M must be chosen so that the energy in the edge-coupled beam is small compared with the energy in the continuously-coupled output beam. On the other hand, M must be large enough to provide a large rejection ratio for high-order modes in order for the optical cavity to retain the mode-selective properties of an unstable resonator. Recent experiments[39,40] have shown that a low-order single-transverse-mode can be continuously coupled out with cavity magnifications as low as M = 1.15 to 1.20. This corresponds to an edge-coupled loss of approximately 10 to 20%. The radii of the two reflectors are related to the round-trip magnification by the well-known formulae[38,41] for a confocal system:

$$R_1 = -\frac{2L}{M-1} \qquad (2\text{-}10)$$

and

$$R_2 = \frac{2ML}{M-1}\ , \qquad (2\text{-}11)$$

where L is the cavity length. The geometric edge-coupled output is

$$\gamma = \frac{M^2-1}{M^2} \qquad (2\text{-}12)$$

Diffraction effects, however, reduce the output coupling to a smaller value[41] close to

$$\gamma = \left(\frac{M^2-1}{M^2}\right)^2 \qquad (2\text{-}13)$$

Total cavity loss for the resonator configuration in Figure 2-10 is, of course, the sum of the edge-coupled loss and the continuously-coupled output.

The second surface of output mirror M_2 should be anti-reflection coated to prevent parasitic modes. Its radius of curvature R_3 should be chosen so that M_2 acts as a converging lens to collimate the output beam.

The alternative resonator shown in Figure 2-11 makes use of cylindrical reflectors placed off-axis with respect to the centerline of the discharge. The output is taken over one edge of the convex reflector M_1. The geometric output coupling for this resonator is

$$\gamma = \frac{M-1}{M} \qquad (2\text{-}14)$$

It may be advantageous to add a small amount of curvature to one of the mirrors in the transverse direction (normal to the plane of Figure 2-11) to "stabilize" the mode structure in that direction also.

There are several advantages to this type of resonator:

1. Apart from the uncoated quartz Brewster windows B, which seal in the laser gases, there are no transmissive optical substrates and coatings which are subject to optical damage.
2. All-reflective metal mirrors can be used. This permits easy cooling and temperature stabilization for handling high average powers without undue distortion of the optical figure.
3. There is no "hole" in the output beam, and no support spiders are necessary to hold the convex output coupler.

For the system under construction the optimum output coupling will first be determined in a series of tests in which a set of stable resonator optics (e.g., with 20%, 30%, 50%, and 80% reflectivities) are used. The round trip magnification and radii of curvature of the reflectors for either unstable cavity can then be determined from Equations (2-10) to (2-14).

The uv pulse energy density incident on the optical surfaces is less than ¼ J/cm^2. This value is far below the established damage thresholds[42] of 5 to 10 J/cm^2 for multilayer dielectric coatings on molybdenum substrates. Pulse energy scaling, as discussed in the next section, does not significantly alter this situation. As the laser cavity is scaled up, the cross-sectional area of the optical beam increases proportionally to the output pulse energy as a consequence of the gain length being held approximately constant. The energy density on the optics is therefore independent of laser size.

At high PRF, however, the high average power density in the optical beam will necessitate cooling of the optical windows and reflectors. Totally reflective metal mirrors may easily be water cooled. Transmissive optics have to be made from high-grade uv-quartz (Suprasil) to minimize the absorption and heating in these windows.

3.0 PULSE ENERGY SCALING

Strict adherence to the discharge stability requirements (Section 2.2) and the use of X-ray preionization opens up the possibility for scaling the output pulse energy of discharge-excited RGH lasers to kilojoule levels. Since the laser gases have a low absorption coefficient for X-rays in the 50 keV to 100 keV range, these X-rays can easily penetrate superatmospheric laser mixtures for distances of several meters. X-rays are therefore ideally suited for providing a uniform preionization level in large discharge volumes.

There appear to exist no basic physical limitations[10] that would prevent the scaling of stable avalanche discharges to large volumes. Similarly, the water Blumlein and the rail gap can in principle be scaled to conform with the storage and switching of large amounts of electric energy. The discharge volume, however, cannot be scaled equally in all three dimensions. For example, scaling of the length l of the discharge (along the optical axis) beyond about 2 m would lead to superfluorescence and parasitic optical oscillations, unless the laser system is operated in a master oscillator-power amplifier configuration. This is particularly so, because the gain of most RGH lasers is quite high (0.05 to 0.15 cm^{-1}). This restriction limits the width of the water Blumlein plates, and hence increases the electric stress in the water as the energy storage is scaled up. For an impedance-matched PFN, the electric stress in the water Blumlein (Section 3.3) reaches critically high levels (>100 kV/cm) at laser pulse energies of several kilojoules. Also at similar optical pulse energies (one or two kilojoules) the PFN voltages to be switched become very high (>500 kV). Designing high-voltage equipment to handle such potentials is a difficult engineering task, but not impossible.

In this section some of the specific problem areas associated with the energy scaling of discharge-pumped RGH lasers are discussed, and some possible solutions are presented.

3.1 Switching Considerations

The discharge impedance R can be expressed in terms of the plasma conductivity σ and the discharge geometry by

$$R = d/\sigma w \ell \quad , \tag{3-1}$$

where w and ℓ are the discharge width and electrode length, and d is the elec rode separation. For a given set of optimum values for the power loading of the gas, E/n of the discharge and the gas density ρ, the plasma conductivity σ will be constant. For reasons of limiting the laser gain to a controllable value, ℓ should also not be increased beyond a certain maximum length. If, furthermore, d and w are increased proportionally as the laser is scaled up, then R remains approximately constant. Hence one can expect all efficient discharge-pumped RGH lasers to have discharge impedances around the 1 ohm level, independent of laser size. Similarly, the matched PFN line impedance will be around $Z \approx 0.5\Omega$, just as for the 1J laser described in Section 2.4. On the basis of these arguments, it is now appropriate to look at the scaling requirements for the discharge switch (i.e., the rail gap).

For a Blumlein configuration, the closing time of the switch (i.e., the current rate-of-rise at the rail gap) determines directly the voltage risetime at the discharge electrodes. The maximum permissible voltage risetime for initiating a uniform, stable discharge, however, has been shown by Levatter and Lin[10] to be on the order of 10 ns and to be almost independent of discharge volume (for fixed E/n and ρ). The closing time of the switch consists of a resistive phase and an inductive phase so that the current risetime at the switch can be expressed as the sum of the resistive and inductive risetimes:

$$\tau_{GAP} = \tau_R + \tau_L \tag{3-2}$$

An empirical relation[16] for the duration of the resistive phase of an air gap in ns is

$$\tau_R \approx 88\ Z^{-\frac{1}{3}} \left(\frac{E}{\rho}\right)^{-\frac{4}{3}} N^{-\frac{1}{3}} \rho^{-\frac{5}{6}} \quad , \tag{3-3}$$

where Z is the driving impedance of the PFN line in ohms, N is the number of parallel arc channels, ρ is the gas density in amagats, and the electric field E is measured in 10 kV/cm units. Since there is not much leeway in adjusting E/ρ or Z (see previous paragraph), τ_R can only be kept small by increasing the gas density or the number of breakdown channels N. Note that τ_R is

independent of the physical size of the gap.

The duration of the inductive phase may be expressed as

$$\tau_L = \frac{L_{LOOP}}{Z} + \frac{L_{SC}}{NZ} \quad , \tag{3-4}$$

where L_{LOOP} is the solenoidal loop inductance, introduced by the fact that the current sheet from the distributed PFN has to be wrapped around the physical volume of the rail gap electrodes and insulators; L_{SC} is the inductance of a single arc channel. In Martin's[16] analysis, the first term of Equation (3-4) was ignored. It is included here, however, because for physically large rail gaps this term may well dominate the switch closing time.

For a small RGH laser with 1 or 2 joule output (Section 2), switched by a well-designed multichannel rail gap (with N≈100), the resistive phase dominates over the inductive phase. τ_R is typically 5 ns, whereas τ_L is approximately 2 ns long for such a laser. As the laser system is scaled up, however, the voltages V_o to be switched increase. Up to perhaps V_o = 150 kv (50 joule RGH laser) such a rail gap may be operated without increasing its physical size, simply by increasing the gas pressure in the gap and/or by employing gas mixtures containing high concentrations of SF_6 or other electronegative gases. Beyond this voltage level the electrode gap and the physical size of the rail gap assembly have to be increased. If proper care is not exercised in scaling the dimensions of the rail gap in relation to the PFN, the L_{LOOP}/Z term can easily account for a 10 ns risetime by itself.

If the loop inductance of the rail gap is to be kept constant, then the length of the rail electrodes must be increased proportionally to the increase in area enclosed by the current loop. Matching a wide rail gap to a narrower Blumlein PFN (width limited by gain length of laser) requires that the Blumlein plates be tapered. For maintaining a constant-impedance line and for making L_{LOOP}/Z small, the Blumlein plate separation b must be tapered as well as the width a of the plates, as shown in Figure 3-1. According to Equation (2-2) a constant b/a ratio is required for a constant line impedance. With this method of maintaining a low switch inductance, there exists no limit to the successful scaling of the switching network.

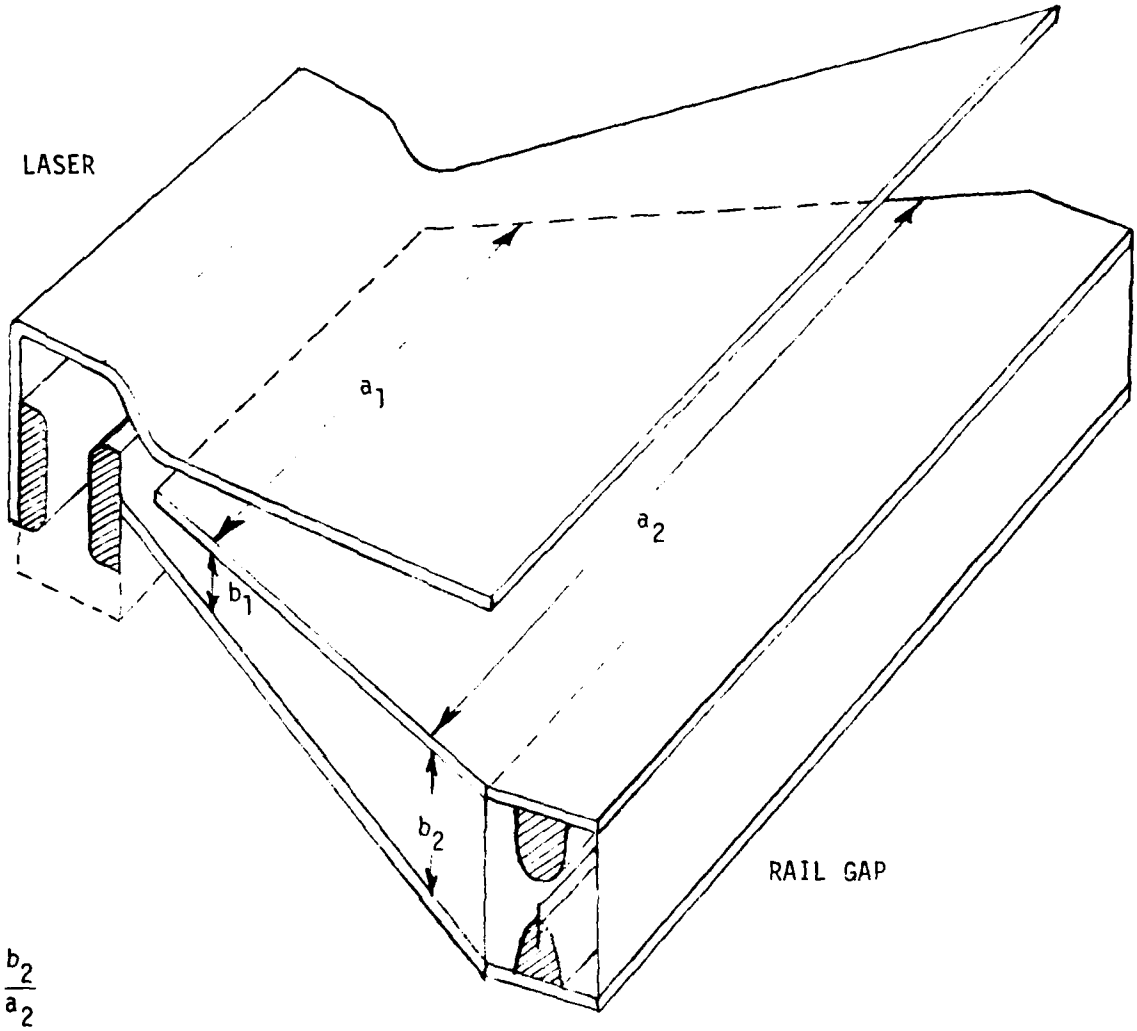

$$\frac{b_1}{a_1} = \frac{b_2}{a_2}$$

Figure 3-1. Method of Matching a Large Low-Inductance Rail Gap to a Doubly-Tapered Constant-Impedance Blumlein-Type PFN.

The method of pulse charging the Blumlein drive must also be investigated for its scalability. Since the charging pulse duration can be several microseconds long, the peak currents and di/dt values which the charging switch has to handle are only moderately severe. There presently exist reliable thyratron switches which can satisfy these requirements up to charging voltages of 120 kV (corresponding to a 40 J/pulse laser). For scaling to larger pulse energies and higher charging voltages, the switching may be performed with several "lower-voltage" (70 kV) thyratrons in parallel. The high-current, moderately-high-voltage pulse can then be boosted to the required charging potential by means of a pulse transformer. The relatively long pulse duration makes the pulse transformer design straightforward.

3.2 Electric Stress in Water Line

In the previous section we have shown that the high-voltage switch requirements do not pose a severe limitation to the scaling of discharge-pumped RGH lasers. As the pulse energy and the corresponding charging voltage are scaled up, however, the electric stress in the water Blumlein eventually reaches a value close to the ultimate breakdown stress of water. As will be shown in Section 3.3, this does not become a limiting factor for lasers with less than kilojoule output energies.

From the relations listed in Figure 2-5, the electric stress ϕ_w in the water line can be expressed as

$$\phi_w = \frac{V_o}{b} = \frac{Z_o}{\varepsilon^{\frac{1}{2}} n_o} \frac{U/\rho v}{(E/n)} \frac{(w/d)}{(a/\ell)} \frac{d}{\tau_p} , \qquad (3\text{-}5)$$

where the symbols are the same as defined previously (Z_o = 377 ohm, n_o = Loschmidt number, ρ = gas density in amagats). The discharge field E/n is constant for a particular type of RGH laser. Similarly, the electric energy density per amagat deposited by the discharge into the gas is limited to a certain value dictated by discharge stability and may be taken as a constant for scaling considerations. For a square discharge cross-section w/d = 1, and for a PFN matched in width to the discharge length a/ℓ = 1. It is therefore evident from Relation (3-5) that ϕ_w increases linearly with the discharge gap d and varies inversely with the pulse length τ_p.

Scaling in optical output energy U_o requires scaling of the mass of the gas medium ($\rho w a \ell$) in the discharge, i.e.,

$$U_o = \eta_L U = \eta_L (U/\rho\upsilon)\, \rho w d \ell \quad , \tag{3-6}$$

which shows a linear dependence of optical energy on mass in the discharge volume. If ρ, w/d, a/ℓ and τ_p are held constant and the discharge volume is scaled geometrically (i.e., $d \sim U_o^{\frac{1}{3}}$), then

$$\phi_w \sim U_o^{\frac{1}{3}} \tag{3-7}$$

If ℓ is also restricted to a maximum length to avoid parasitic oscillations in the laser cavity, ϕ_w goes up as the square root of the pulse energy:

$$\phi_w \sim U_o^{\frac{1}{2}} \tag{3-8}$$

The problem can be alleviated somewhat however by choosing w/d<1, by making a/ℓ>1 or by increasing the pulse length τ_p. Being able to stretch the stable, constant-voltage duration of the discharge pulse is therefore of extreme importance for achieving very high optical pulse energies. Levatter [23] has previously demonstrated stable discharge operation for pulse lengths up to 200 ns, and it appears quite feasible that 300 ns long laser pulses may be achieved in the near future.

3.3 Design Parameters for 20 J, 100 J and 1 kJ Lasers

This section gives the results of sample calculations for defining the characteristic design parameters of scaled-up XeCl lasers. The procedure for deriving these quantities followed closely the scheme outlined in Section 2.4.3. The design of a 20 J RGH laser can be realized with present technology, as the numbers below indicate, even if the laser efficiency is less than 2 per cent.

Design of a 20 J XeCl Laser

Optical Pulse Energy	U_o = 20 J
Laser Efficiency	η_L = 2%
Electrical Energy/Pulse	U = 1000 J
Electric Field in Discharge	E/n = 4 kV/cm-atm = 1.5×10^{-16} V-cm^2
Gas Pressure	p = 3 atm
Energy Loading	$U/p\upsilon$ = 60 J/l-atm
Pulse Duration	τ_p = 130 ns
Electrical Power	P = 7.7 GW
Pump Power Densities	P/υ = 1.4 MW/cm^3
Discharge Volume	υ = d x w x ℓ = 8 x 8 x 87 cm^3 = 5.6 l
Discharge Voltage (Charge Voltage)	V_o = 96 kV
Discharge Impedance	R = V_o^2/P = 1.2Ω
Line Impedance	Z = 0.6Ω
Length of Blumlein Plates	x = 1.75 m
Width of Blumlein Plates	a = 1.00 m
Plate Separation	b = 1.4 cm
Stress in Water Dielectric	ϕ = 68 kV/cm

For a single-pulse unit, the electric stress of 68 kV/cm is quite acceptable. For a high-PRF version a double-Blumlein configuration would reduce the electric stress in the water line to 34 kV/cm, increasing the laser system's reliability.

Uniform preionization of the discharge volume can be achieved for this laser with an X-ray generator having the following physical and electrical characteristics:

X-ray Window Area (electrode made from 2mm thick aluminum)	8 x 87 cm^2
E-beam Target Area	6 x 85 cm^2
E-beam Current Density	1.3 A/cm^2
Total Current	667 A
Pulse Length	200 ns
Electron Energy	75 kV
Electric Energy Switched	10 J/pulse

A schematic of such a 20 J XeCl laser is shown in Figure 3-2. Note that the charging voltages ($V_0 \simeq$ 100 kV) and currents (6 kA) can easily be switched with conventional thyratrons, such as an EEV-CX1192 tube. A charging period of 5 μs has been assumed here. The approximate physical size of a low-PRF version (no gas recirculation loop) of such a laser is given in Figure 3-3.

In Table 3-1 some typical electrical parameters and physical dimensions for X-ray preionized XeCl discharge lasers with 100 J and 1 kJ output energies are listed. The electrical laser efficiency has been assumed to be 2%, and a rather modest pulse energy loading of the gas of 60 J/ℓ-atm at 3 atm pressure has been postulated. The design for both lasers is based on the use of a double water Blumlein PFN, which is charged with the aid of a step-up pulse transformer. For the 1 kJ laser the very high PFN voltage requires that the low-inductance rail gap be relatively large. In order to physically and electrically match this gap to the PFN, a doubly-tapered Blumlein design, as shown in Figure 3-1, may have to be employed. All other parameters will remain unchanged, except that the electric stress in the water will be reduced below the calculated 60 kV/cm and will reach that value only near the laser discharge chamber.

Whereas the 100 J laser design is still relatively straightforward, insofar that only proven concepts have been assumed, the 1 kJ laser design requires some extrapolation of certain aspects of present-day technology.

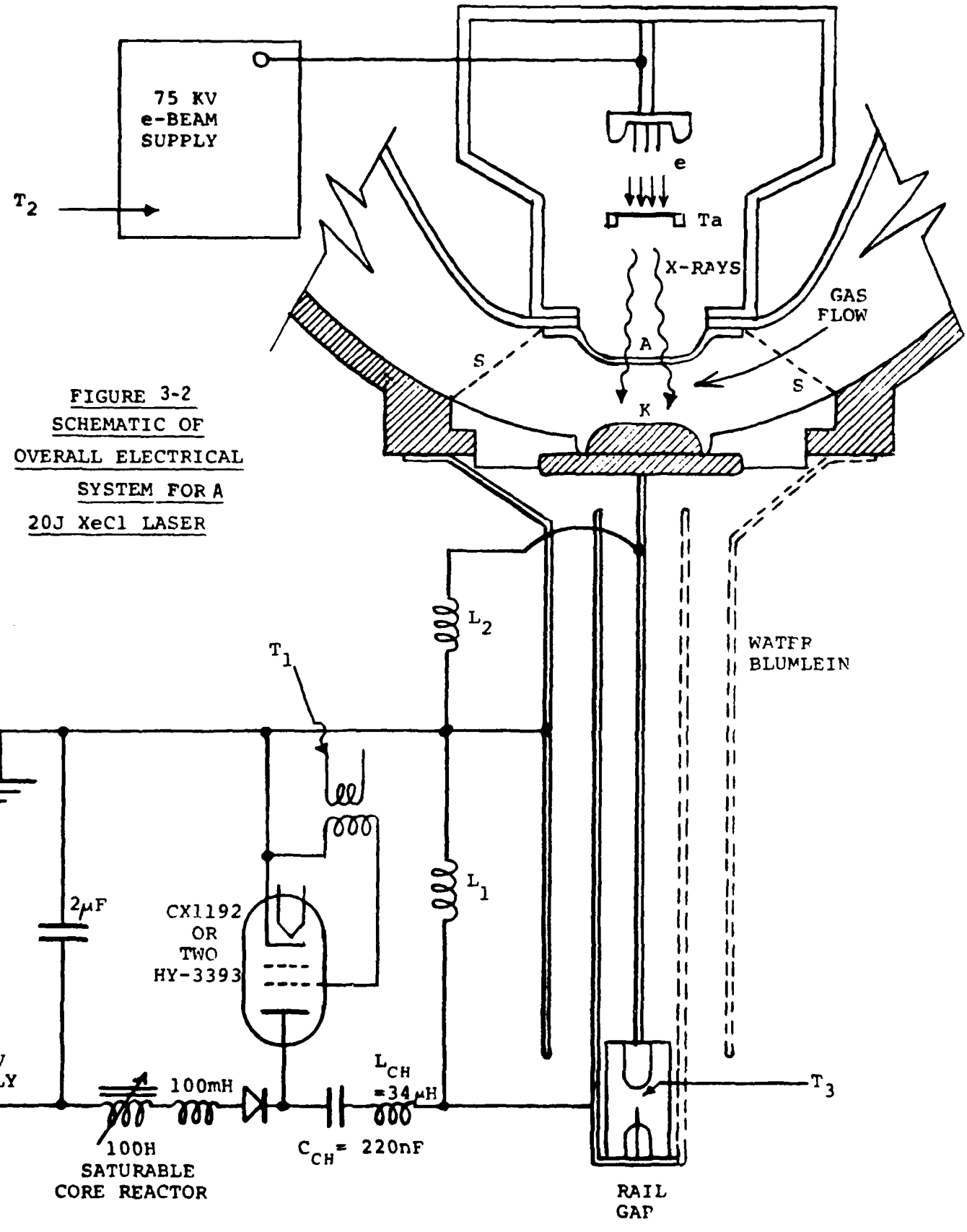

FIGURE 3-2
SCHEMATIC OF
OVERALL ELECTRICAL
SYSTEM FOR A
20J XeCl LASER

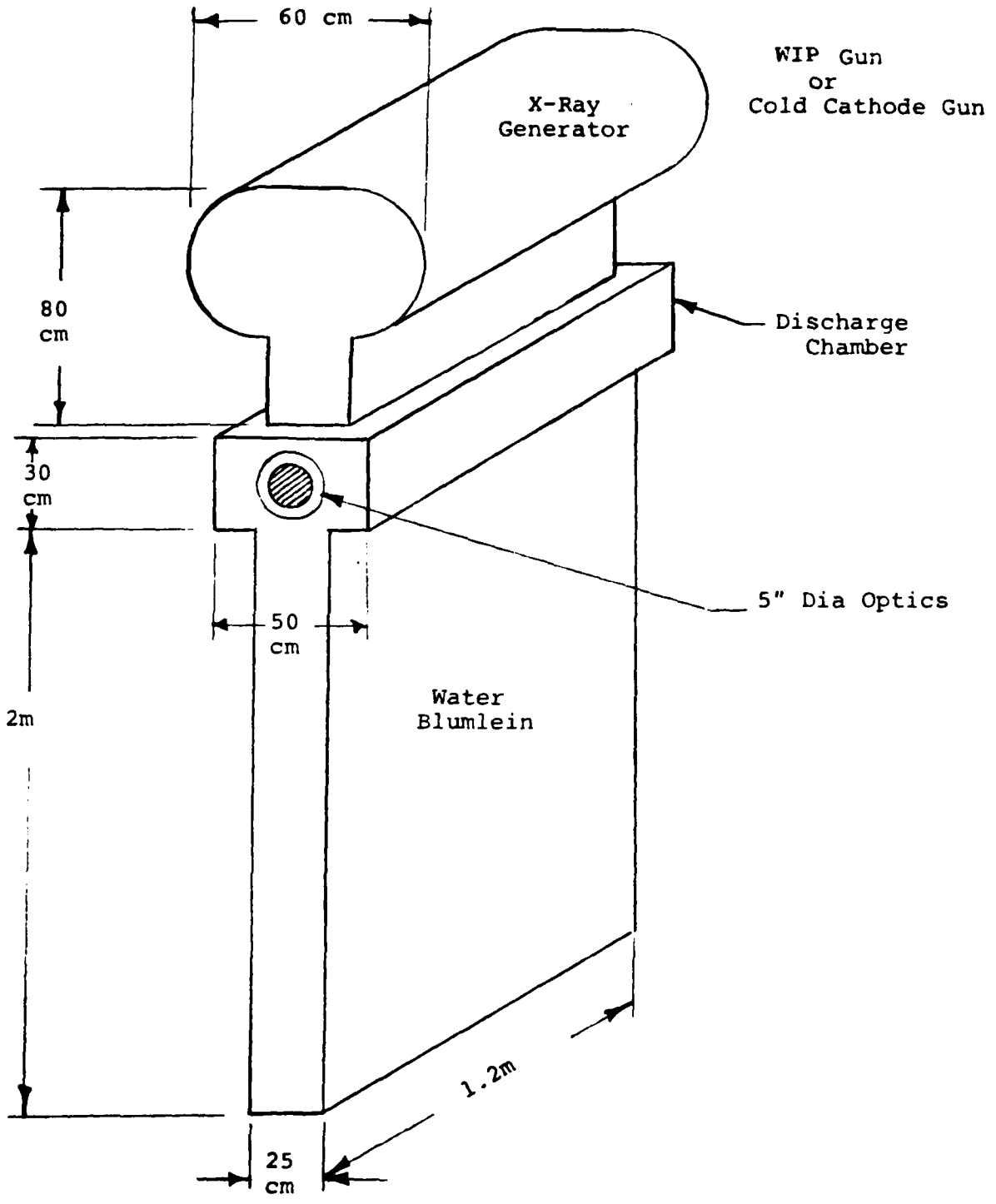

Figure 3-3 . Approximate Size of a Typical 20 Joule XeCl Laser

TABLE 3-1

SCALED-UP X-RAY PREIONIZED XeCl DISCHARGE LASERS

Based on: Laser Efficiency η_L = 2%

E/n = 4 kV/cm-atm

= 1.5×10^{-16} V-cm^2

El. Pulse Energy Loading U/pv = 60 J/l-atm

Gas Pressure p = 3 atm

	100 J/PULSE	1000 J/PULSE
Electric Pulse Energy (U)	5000 J	50 kJ
Pulse Length (τ)	200 ns	300 ns
Discharge Volume ($dxwx\ell$)	15 x 15 x 125 cm^3	33 x 33 x 250 cm^3
Pump Power Density (P/v)	0.9 MW/cm^3	0.6 MW/cm^3
Discharge Voltage (V_o)	180 kV	400 kV
Discharge Impedance (R)	1.3 Ω	0.96 Ω
Blumlein Plate Spacing (b)	4.6 cm	6.8 cm
Blumlein Plate Width (a)	1.5 m	3 m
El. Stress in Double Blumlein (ϕ_w)	40 kV/cm	60 kV/cm

HELIONETICS, INC.
LASER DIVISION

Before such a high-energy laser can be built, some development work will be necessary in the following areas:

1. It remains to be demonstrated that a stable avalanche-type high-pressure glow discharge can be produced in an electrode gap of 1/3 m, and that this large-volume (270 ℓ) discharge can be maintained at a constant impedance level for 300 ns.
2. The very high PFN voltages (400 kV) require careful application of sophisticated HV techniques for prevention of corona and electrical breakdown.
3. Because of the 2.5 m gain length, various forms of parasitic mode suppression will have to be employed. The relatively low pump power density of 0.6 MW/cm^3 helps in reducing the optical gain somewhat.

Aside from the above concerns, there exist no physical restrictions that would preclude the successful development of discharge-pumped RGH lasers with output pulses in the kilojoule range.

4.0 PREIONIZATION TECHNIQUES

The establishment of a stable, spatially homogeneous avalanche discharge in rare gas halide mixtures requires preionization of the gas prior to the application of the main discharge voltage. Two general preionization criteria have been established: First, the initial ionization density must be sufficiently large to smooth out any local gradients in the space-charge field and thereby inhibit streamer formation[10,43]. The minimum ionization density required is estimated to be about 10^6 cm^{-3}, depending on the gas mixture and voltage risetime across the electrodes. Second, the ionization density must be uniform in a plane normal to the discharge current. Ionization density gradients parallel to the current direction are unimportant as long as the density does not fall below the estimated minimum[44].

4.1 Ultraviolet vs. X-ray Preionization

Various preionization sources have been used, including electron beams[45], X-rays[9,10], uv spark arrays[6-8,17,46], and corona bars[47]. X-ray and uv photoionization sources offer the most promise for use in moderate-to-high-power, high-repetition-rate excimer lasers. X-rays are capable of producing the highest uniformity, and because of their large mass-penetration power are well suited to large-volume, high-pressure laser systems. However, the X-ray source requires additional weight and complexity in the form of:

- An additional high voltage supply (50 kv minimum).
- A vacuum system housing the field-emission or plasma electron source.
- An X-ray transmissive electrode, which must also support the laser gas at its operating pressure.
- A heavy-metal target foil (which may be combined with the X-ray transmissive electrode) suitable as an X-ray source upon electron bombardment.
- Additional time delay and trigger electronics for timing the X-ray pulse relative to the discharge pulse.

Because of these complexities, ultraviolet sources are preferred for preionization of small lasers (with electrode-electrode gaps on the order of 10 atm-cm or less). A properly designed spark source can provide sufficiently dense and uniform photoionization in such systems, as illustrated in the next section.

4.2 Flux Uniformity for Discrete Spark UV Preionizers

The relative simplicity of uv spark preionization recommends it for small to moderate size lasers. The preferred geometry (Figure 4-1a) locates the spark array behind a screen electrode. Locating spark arrays to the side of the electrodes (an arrangement commonly used with CO_2 TEA lasers) is not recommended for self-sustained discharge-excited excimer lasers, since this geometry results in large transverse ionization density gradients.

In the preferred arrangement with the sparks located behind a screen electrode, three effects produce notable non-uniformity of the preionization: the discrete nature of the sparks, attenuation by absorption in the laser gas, and shadowing effects produced by the screen electrode. For sufficiently close spacing of the sparks and sufficiently low absorption (small discharge volume and low pressure) any degree of uniformity can be obtained in principle. In practice, we attempt to maintain constant preionization to within 5% from side to side of the discharge. Along the current path the preionization falls by a factor of two from the cathode (screen) to the anode, but this variation does not affect the discharge.

Profiles of the uv intensity (and hence of the preionization) at various levels within a 3 cm square cross-section discharge have been calculated by the means of a computer program described in Appendix A. The simple two-row spark array of Figure 4-1b performs adequately when properly positioned. These calculations assume isotropically radiating point sources and include absorption by the laser gas as well as the effects of the screen electrode. The assumed screen is of 66% transparency with round holes of D=2t,where t is the thickness of the screen. Normalized intensity profiles in a direction transverse to the laser axis and electrodes are presented in Figure 4-2 for three different levels (0, 1.5, and 3 cm above the screen). Zero absorption and no screen effects are assumed for these first plots. With the spark array positioned 2.2 cm behind the screen electrode, the 2.2, 3.7, and 5.2 cm z-values correspond to positions at the screen,midway between the electrodes, and at the plane of the anode,respectively. As can be seen, the uniformity is barely acceptable, the intensity variation from center to side of the electrode being approximately 8%. We emphasize that this is a hypothetical case presented for reference only, as a physical screen has transmissivity less than one and a collimating effect due to its finite thickness.

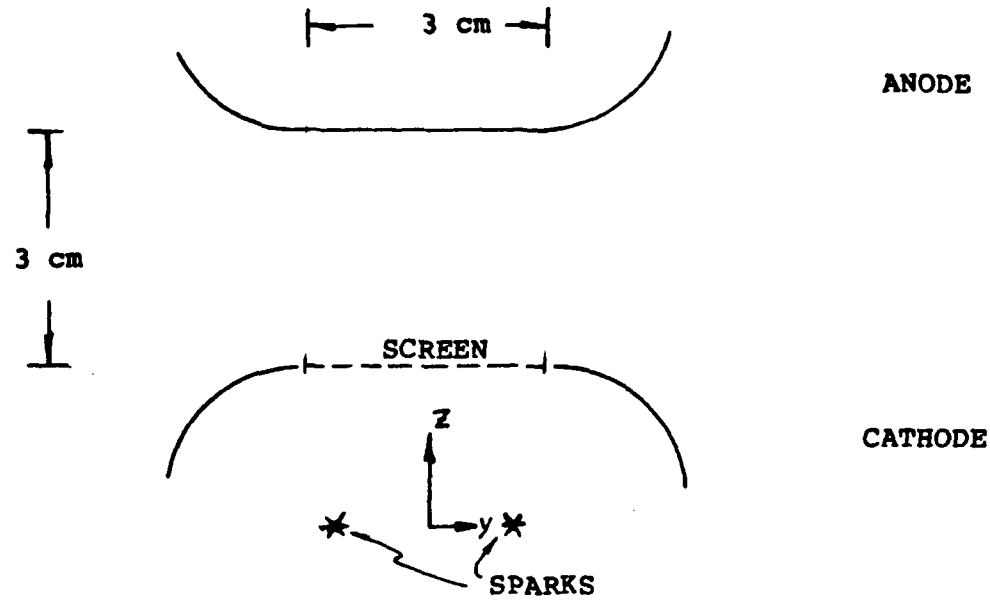

Figure 4-1a. Preferred geometry for UV spark preionization. Dimensions are for a typical discharge cavity, and are used in the preionization density profile calculations presented herein.

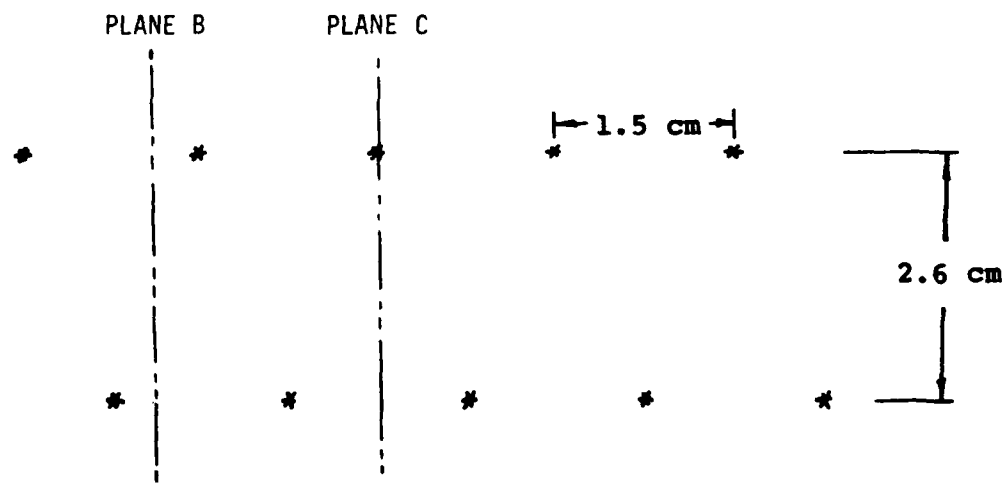

Figure 4-1b. This simple double row spark array is used for the preionization profile calculations.

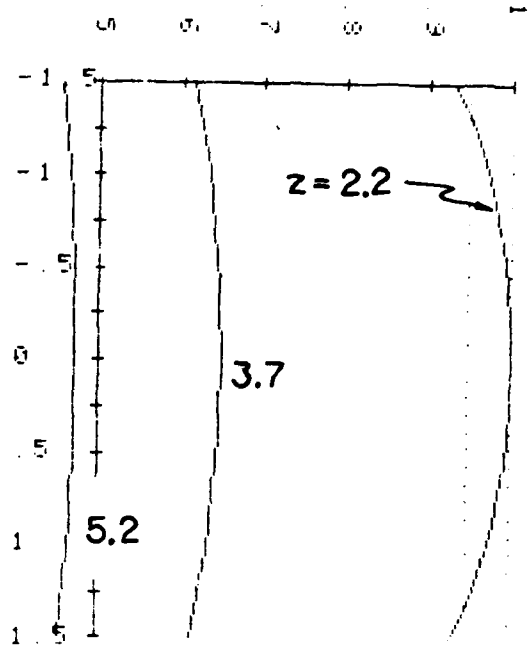


```
X =   0
Z =   2.2 , 3.7 , 5.2

ABS. COEFF.=   0
SCREEN TRANSMISSIVITY 1

T/D=  .1

CELL SIZE=   1.5 , 2.8

SPARK COORDS.

-.375 -1.3   0
 .375  1.3   0

_
```

Figure 4-2. Calculated preionization density tangential to the cathode (screen electrode), at the midsection of the discharge, and at the anode. The scale is arbitrary, by normalizing all densities to the peak of the curve representative of the plane of the screen electrode (z = 2.2). This calculation represents the hypothetical case of a fully transmissive screen (T=1) and no gas absorption.

One method of manufacturing screens for these purposes is by electrochemical etching. Etched screens can be obtained with transmissivities as high as two thirds. The hole size D can be made as small as the screen thickness t, but making D=2t provides a more evenly distributed ionization in the discharge gap. The smaller the hole the more directed is the radiation, as can be seen from Figure 4-3, which compares the effects of varying D/t. Note that in the case of D=t we observe two directed beams of ionizing light at lateral positions y=±1.3 cm. This effect is also evident for D=2t, causing the intensity profile to be mildly double-peaked.

The effects of uv absorption by the laser gas mix are shown in Figure 4-4. These three profiles were generated at 2.2 cm from the spark array (tangential to the screen electrode) using values of A = 0, 0.1, and 0.5 for the absorption coefficient. Serious non-uniformity is observed only for absorption coefficients of 0.2 and above. Based on the uv absorption data compiled by Denes et al.[48] using standard excimer laser gases, it appears that the absorption coefficient may be safely taken to be about 0.1 cm^{-1} or less throughout most of the 1000-2000 Angstrom wavelength range.

A series of profiles presented in Figure 4-5 incorporates both the effects of absorption and the electrode screen. The absorption coefficient is taken to be 0.1 cm^{-1}, and the screen transmissivity is 0.66 with t/D = 0.5. As in figure 4-2, these plots were generated at 2.2, 3.7, and 5.2 cm from the spark array, corresponding to the locations of the screen electrode, midsection and the anode.

The transverse intensity profiles reproduced in Figures 4-2 to 4-5 were calculated in a vertical plane midway between sparks (Plane B in Figure 4-1b). Intensity profiles taken in other planes, however, do not look significantly different. A worst case profile is presented as Figure 4-6, taken at the screen electrode directly over a spark (Plane C in Figure 4-1b). Note that even in this case the preionization density is uniform to within 10 per cent over the discharge region. Similarly, the calculated intensity variations in the longitudinal direction (along the rows of sparks) are less than a few percent. An array of discrete spark sources can thus be arranged to provide adquately uniform illumination throughout the entire discharge volume.

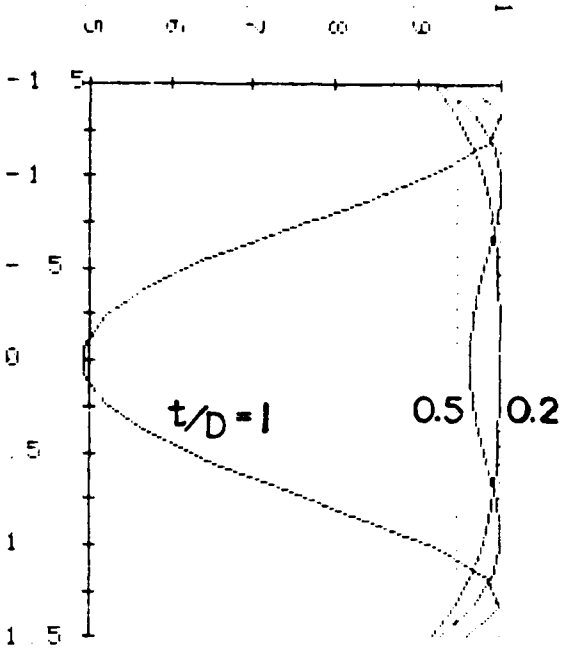


```
X =  0 , 0 , 0
Z =  2 2
ABS. COEFF.=  0

SCREEN TRANSMISSIVITY .66

T/D= .5 T/D= .2 T/D= 1
CELL SIZE:  1 5 , 2.8

SPARK COORDS:

-.375 -1.3  0
 .375  1 3  0
```

Figure 4-3. Calculated preionization density tangential to the cathode as a function of t/D, the ratio of the screen thickness to the hole diameter. Each of these curves is normalized to its peak value. The relative peak values are 1, 0.51, and 0.25 respectively for t/D = 0.2, 0.5, and 1.0.

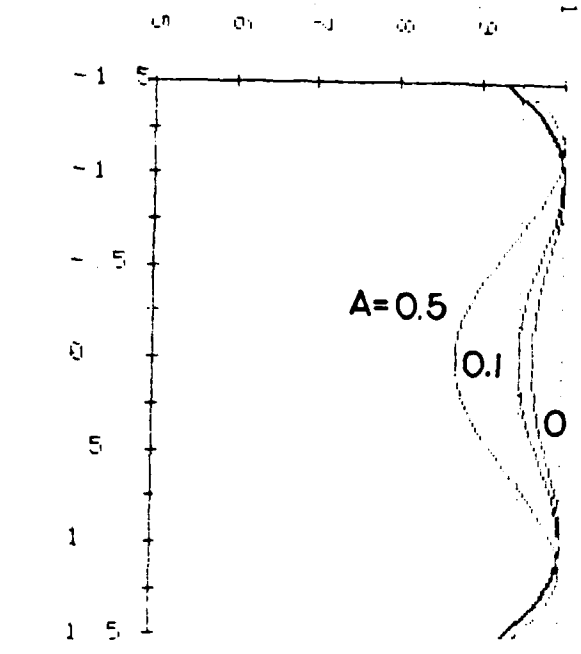

Z = 2.2
ABS COEFF = 0 . 1
, 5

SCREEN TRANSMISSIVITY .66

T/D= 5

CELL SIZE 1.5 , 2.5

SPARK COORDS

-.375 -1.3 0
.375 1.3 0

Figure 4-4. Preionization density as a function of the absorption coefficient of the laser gas calculated tangential to the screen electrode. These curves are normalized to their respective peak values; 1, 0.76, and 0.27 for A=0, 0.1, and 0.5.

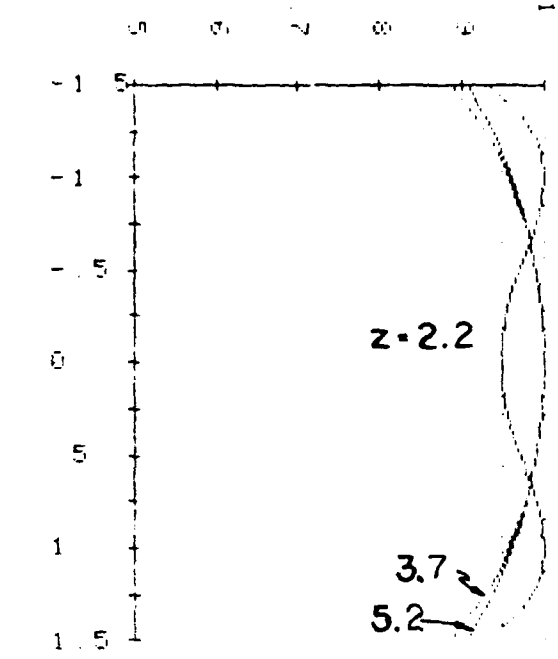


```
N =  0
Z =  2.2 , 3.7 , 5.2

ABS. COEFF. =  .1
SCREEN TRANSMISSIVITY .66

T/D=  .5

CELL SIZE=  1.5 , 2.8

SPARK COORDS

-.375 -1.3  0
 .375  1.3  0
```

Figure 4-5. Profiles representative of the design of the Helionetics one-joule laser. The absorption is taken as 0.1 cm^{-1} and the transmissivity is 0.66 with t/D = 0.5. The curves are normalized to the peak of the z = 2.2 cm (screen electrode) case with relative peak values of 1, 0.67, and 0.45 respectively for z = 2.2, 3.7, and 5.2 cm.

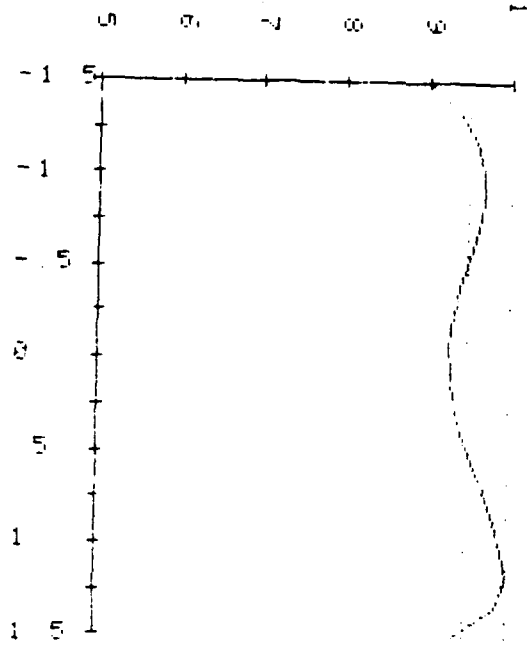


```
Y =    .375
Z =    2.2
ABS. COEFF. =    1
SCREEN TRANSMISSIVITY  .66

T/D=  .5

CELL SIZE:   1.5  .2  .8

SPARK COORDS:

-  .375  -1.3   0
   .375   1.3   0

_
```

Figure 4-6. The "worst case" profile taken over the spark at z = 2.2 cm.

5.0 HIGH-AVERAGE POWER LASERS

High average powers can be achieved by pulsing the discharge-pumped RGH laser at PRFs in the kilohertz range. Removal of heat and medium inhomogeneities from the optical cavity requires a fast gas exchange rate with a flush factor of approximately 2. Medium inhomogeneities may be caused by pressure waves generated by the pump pulse (acoustic disturbances), by free-stream flow turbulence and by non-uniform energy deposition in the discharge. The amount of flow conditioning and acoustic damping required depends on the desired optical beam quality. Acoustic damping and gas flow considerations for high-PRF RGH lasers are discussed in this section.

5.1 Effects of Acoustic Waves and Turbulence on Optical Beam Quality

5.1.1 Random Disturbances

The effects of random disturbances in the optical medium of a laser on the beam divergence and far-field extinction have been analysed by Sutton[49]. Propagation of a laser beam through a non-homogeneous gain medium of length L causes an attenuation of the beam intensity in the center of the far field, given by

$$\frac{I}{I_o} = e^{-\alpha L} \quad , \tag{5-1}$$

where the attenuation coefficient α can be expressed in terms of random fluctuations in the refractive index n by

$$\alpha = 2(2\pi/\lambda)^2 \langle \Delta n^2 \rangle s \tag{5-2}$$

The symbol s refers to the characteristic scale length of the random inhomogeneities. Combining Equations (5-1) and (5-2) and solving for Δn gives

$$\Delta n \simeq \frac{\lambda}{2\pi} \sqrt{\frac{\ell n(I_o/I)}{2sL}} \tag{5-3}$$

But the refractive index of a gas is simply related to the gas density ρ by

$$n = 1 + \frac{\beta}{\rho_o} \rho \quad , \tag{5-4}$$

where β/ρ_o is the Gladstone-Dale constant. Hence

$$\frac{\Delta n}{n-1} = \frac{\Delta \rho}{\rho} \tag{5-5}$$

The permissible density fluctuation for a given far-field attenuation is thus given by

$$\frac{\Delta\rho}{\rho} = \frac{\lambda}{2\pi}\frac{1}{(n-1)}\sqrt{\frac{\ell n(I_o/I)}{2sL}} \quad . \tag{5-6}$$

The corresponding pressure fluctuations are

$$\frac{\Delta p}{p} = \gamma\frac{\Delta\rho}{\rho} \quad . \tag{5-7}$$

For a typical XeCl laser mixture of He/Xe/HCl = 97.8/2/0.2 at 2 atmospheres, the refractive index is $n = 1 + 9.8 \times 10^{-5}$. Assume a typical random scale length s of 3mm (e.g., small-scale turbulence) and a 1m optical cavity length. Then the maximum allowable density fluctuation for a near-diffraction-limited beam ($I/I_o = 0.8$) is

$$\left(\frac{\Delta\rho}{\rho}\right)_{RAND} \leq 3 \times 10^{-3} \tag{5-8}$$

For a gas mixture containing mostly neon instead of helium, (n-1) is approximately twice as large, and the maximum random density disturbance is

$$\left(\frac{\Delta\rho}{\rho}\right)_{RAND} \leq 1 \times 10^{-3} \tag{5-9}$$

5.1.2 Ordered Disturbances

For an ordered disturbance, such as a shock moving at right angles to the optical axis, the phase distortion is integrated along the entire cavity length. The phase discontinuity across a shock of strength $\Delta\rho$ is

$$\Delta\phi = \frac{2\pi L}{\lambda}\Delta n = \frac{2\pi L}{\lambda}(n-1)\frac{\Delta\rho}{\rho} \tag{5-10}$$

The effects of such a step discontinuity in the output phase on the far-field beam consist of both a beam steering and a beam spreading effect. A detailed analysis[50] of the far-field intensity patterns shows that for $I/I_o > 0.8$ the maximum permissible phase discontinuity at the output aperture is $\pi/2$. Hence, from Equation (5-10)

$$\left(\frac{\Delta\rho}{\rho}\right)_{ORD} \leq \frac{\lambda}{4L(n-1)} \tag{5-11}$$

For the helium-rich laser mixture this value is

$$\left(\frac{\Delta\rho}{\rho}\right)_{ORD} \leq 7\times10^{-4} \tag{5-12}$$

and $$\left(\frac{\Delta\rho}{\rho}\right)_{ORD} \leq 3 \times 10^{-4} \qquad (5\text{-}13)$$

for the neon mixture.

5.1.3 Flow Turbulence

The density variations due to turbulent velocity fluctuations Δu can be shown to be

$$\left(\frac{\Delta\rho}{\rho}\right)_{TURB} = (\lambda-1)M^2 \frac{\Delta u}{u} \qquad (5\text{-}14)$$

for an adiabatic irreversible process. M here is the free-stream Mach number.

For the 1 J, 100 Hz Helionetics laser, the required flow Mach number is only 0.015. Turbulent density fluctuations are estimated from Equation (5-14) to be approximately 10^{-5}. This is well below the permissible random fluctuation specified by Equations (5-8) or (5-9). The effect of turbulence on the optical beam quality is therefore negligible for medium-average-power laser systems.

For high-average-power lasers, operating with kilohertz pulse frequencies, the necessary gas flow Mach numbers can easily be near unity. It is therefore evident from Equation (5-14) that such large, high-power lasers require careful control of the cavity turbulence by suitable upstream screens. The drag introduced by placing such flow-conditioning devices in a high-speed flow, however, may drastically increase the power input requirements for the gas recirculation compressor.

5.1.4 Shock Waves

The sudden heating of the gas by the discharge pulse results in shock waves, which propagate throughout the flow system, and which can affect the optical medium homogeneity of subsequent pulses, if the shock energy is not sufficiently randomized and dissipated during the interpulse period. Because of the high power density dissipated in the cathode sheath, a strong shock wave is produced at the cathode surface and travels towards the anode. A somewhat weaker shock results from the heating of the positive column and expands at right angles to the current pulse.

In order to illustrate the severity of the shock disturbances, we will calculate the initial pressure rise across these shocks for pulse energy loadings and discharge current densities which are representative for all RGH lasers considered here.

Consider the shock wave produced by the bulk heating of the discharge volume first. The heat content of a monatomic gas ($\frac{3}{2}nkT$) at 2 atm and 300°K is 0.304 J/cm^3. For a pumping pulse of 1 MW/cm^3 lasting 100 ns the internal energy of the gas is increased by 20% over this value, if it is assumed that 2/3 of the electronic pulse energy goes directly into gas heating (1/3 goes into electronic excitation and ionization). This causes an immediate temperature and pressure rise corresponding to

$$T_4/T_1 = p_4/p_1 = 1.2 \quad , \tag{5-15}$$

whereas the density remains essentially constant, due to the inertia of the gas and the short duration of the pump pulse. After the discharge pulse, shock waves propagate outward from the discharge region, while rarefaction waves travel inward.

The strength M_s of the shock wave generated can be estimated from the one-dimensional shock tube relation[51]

$$\frac{p_4}{p_1} = \left(\frac{\gamma-1}{\gamma+1}\right)\left(\frac{2\gamma}{\gamma-1} M_s^2 - 1\right)\left[1 - \frac{(\gamma-1)(M_s^2-1)}{(\gamma+1)(T_4/T_1)^{\frac{1}{2}} M_s}\right]^{-\frac{2\gamma}{\gamma-1}} \tag{5-16}$$

For $T_4/T_1 = p_4/p_1 = 1.2$ and $\gamma = 5/3$ (monatomic gas), this equation yields $M_s = 1.04$ for the shock Mach number.
The pressure ratio across a normal shock is then given by

$$\frac{p_2}{p_1} = \frac{2\gamma}{\gamma+1}\left(M_s^2 - \frac{\gamma-1}{2\gamma}\right) = 1.10 \tag{5-17}$$

The initial pressure rise of $(\Delta p/p)_{SHOCK} = 0.1$ is several hundred times above the premissible limit for an ordered disturbance (Section 5.1.2).

At a shock speed of 800 m/s and an [illegible] pulse period of 10 ms (100 Hz laser), the shock wave can, however, undergo many reflections from the turbulence grids and the duct walls, and can be attenuated in the heat exchanger structure. The proposed Helionetics laser, operating at a PRF of

100 Hz will therefore need only a limited amount of acoustic damping material to reduce the remaining disturbances to acceptable levels.

For lasers operating in the kilohertz regime, shock wave attenuation and acoustic damping become major issues. A separate study will be necessary to optimize the acoustic design for these high-power devices.*

For determining the strength of the cathode shock, the cathode fall potential V_c and the cathode sheath thickness d_c have to be known. Typical values are V_c = 180 V and d_c = 12 μm. The energy added per unit volume of cathode sheath is then given by

$$\frac{U_c}{v_c} = \frac{V_c}{d_c}\int i\,dt \quad , \qquad (5\text{-}18)$$

where i is the discharge current density, and the time integral is performed over the total pulse length. For i = 200A/cm^2 and a pulse duration of 100 ns, this yields an energy addition per unit volume of 3.0 J/cm^3. If 2/3 of this energy is immediately converted to heat, the temperature rise in the cathode sheath is approximately 2000^{0}K. The resulting shock Mach number is 1.84. The pressure ratio across the shock is 5. This is a very sizable disturbance and needs to be dissipated between laser pulses.

As before, this does not present a major problem for the 1 J, 100 Hz laser. At a speed of over 1 km/s, this shock will bounce back and forth from electrode to electrode approximately 200 times between pulses. Even if this shock is attenuated by only 10% at each reflection from the convex anode surface and the cathode screen, the pressure wave will attenuate by almost 200 dB in 10 ms and will be far below the permissible maximum value.

5.2 Gas Flow as a Function of Average Power

In Section 3 we have shown that the proposed laser configuration can in principle be scaled to high pulse energies in the kilojoule range. For certain projected DoD applications, average powers at megawatt levels are required. The minimum gas flow requirements for such high-average power lasers have been investigated here and are summarized in Figure 5-1.

*Problems associated with high-PRF operation of gas lasers are presently being investigated by other research laboratories, notably AVCO, AERL and Poseidon.

Figure 5-1. GAS FLOW REQUIREMENTS FOR 1kJ/PULSE HIGH-PRF LASER

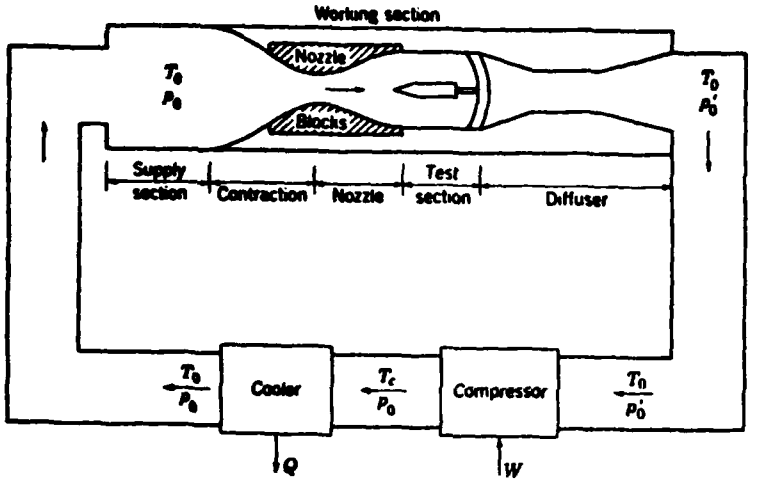

Assumptions: $\gamma = 1.67$

$p = 3$ atm

Flush factor = 1.5

Compressor power for closed-cycle flow:

$$P_C = p\frac{dV}{dt}\left(\frac{\gamma}{\gamma-1}\right)\left[\left(\frac{p_2}{p_1}\right)^{\frac{\gamma-1}{\gamma}} - 1\right] \quad \text{FOR} \quad M < 1$$

$$P_C = \rho\frac{dV}{dt}\left(\frac{\gamma}{\gamma-1}\right)RT_0\left[\left(\frac{p_0}{p_0'}\right)^{\frac{\gamma-1}{\gamma}} - 1\right] \quad \text{FOR} \quad M > 1$$

Opt. Power P_o (MW)	PRF (kHz)	Flow Velocity u (m/s)	Flow Mach No. M	Stagn. Pressure P_o (atm)	Volum. Gas Flow dV/dt (m^3/s)	El. Power into Discharge P_E (η_E=2%) (MW)	Compressor Power P_c (MW)	Overall System Efficiency η_o
1	1	500	0.6	4	300	50	20	1.4%
3	3	1670	1.8	19	900	150	104	1.2%
5	5	2500	3	96	1500	250	1850	0.24%
10	10	5000	6	1818	3000	500	50000	0.02%

A RGH laser with an output energy of 1 kJ has been assumed here. Note that the gas velocity in the optical cavity reaches Mach 1 at PRFs close to 2 kHz. Above pulse frequencies of 2 kHz, a supersonic gas flow is required. The compressor power required for a closed-cycle supersonic wind tunnel[51] is given by the expression for M>1 in Figure 5-1. The model assumes:

1. Adiabatic, reversible compression from (p_o' , T_o) to (p_o, T_c).
2. Isobaric cooling back to T_o in a suitable heat exchanger; p_o and T_o are the stagnation chamber pressure and temperature, respectively.
3. Isentropic expansion in a Laval nozzle to the "test section" (discharge section) Mach number M.
4. Adiabatic normal shock recovery to (p_o' , T_o).

Since no viscous pressure losses have been taken into account for the M>1 calculations, the compressor powers tabulated represent lower limits only. Shock reflectors, acoustic damping sections and viscous losses in the cooler may greatly increase these numbers.

In the formula for subsonic velocities (M<1) the pressure ratio p_2/p_1 represents the actual compression ratio required by the compressor to overcome the sum of all viscous pressure losses Δp is the flow loop. For the 1 MW laser a representative value of Δp = 1 atm has been assumed. All numbers listed in Figure 5-1 are based on a flush factor of 1.5, a laser cavity pressure of 3 atmospheres and a laser efficiency of 2 per cent.

It is evident from this analysis that up to 3 MW output power,the power requirements for the gas compressor are less than the electric power going into the laser discharge. With higher average output powers, this situation quickly reverses, so that the compressor input power becomes the dominant factor which determines the overall system efficiency.

5.3 Practical Scaling Limits

As demonstrated by the results presented in Figure 5-1, a 10 MW average-output-power would require a stagnation pressure of close to 2000 atm and a stagnation temperature of nearly 4000 ^oK to generate a room-temperature, M=6 flow through the discharge gap. Apart from the engineering difficulties

involved, the enormous compressor input power of 50 GW makes such a laser a very impractical system.

The tabulated numbers suggest that efficient, practical gas lasers can be developed with flow Mach numbers up to 2. This corresponds to RGH lasers with optical output powers around 3 MW (e.g., a 1 kJ laser operating at 3 kHz). High-energy lasers with PRFs above several kilohertz appear to be impractical. It is also of interest to note here that at these pulse frequencies the shock waves generated by the discharge pulse (Section 5.1.4) do not completely clear out of the discharge region between pulses. Under such conditions all acoustic damping techniques become ineffective, and the resulting optical beam quality would be greatly degraded.

6.0 CONCLUSIONS

In this report design considerations critical to the development of discharge-excited rare-gas halide excimer lasers of high pulse energy and high average power have been surveyed. As part of this study the requirements for maintaining uniform and stable electric discharges have been reviewed. Original calculations that dictate the positioning and the spacing of the spark array, required for uniform preionization by use of the ultraviolet light from sparks, have been presented. The need for use of X-ray preionization has been established for the higher pressure-density products required for the larger lasers.

Scaling of the electric and geometric design parameters for lasers of 100 to 1000 joule pulse energy were presented and it has been concluded that neither the high-voltage switching requirements nor the range of the preionizing X-ray radiation is a limitation, but that the increasing dielectric stress on the water of the Blumlein transmission line would limit the pulse energy of this class of excimer lasers to the kilojoule range for a single module. The gas flow requirements have been shown to limit the pulse repetition rate to several kilohertz. Even at these repetition rates, the gasdynamic losses dictate a significant reduction in the laser efficiency. At moderate pulse repetition rates ($\sim$1 kHz), however, there is good reason to expect operation with system efficiencies above 2 per cent.

Detailed calculations performed for the design of a 1 joule-per-pulse, 100 hertz RGH laser indicate that such a system can be built with presently existing technology based on the expertise and experience of the technical personnel associated with Helionetics (Appendix B). Analysis of the uniformity of uv-illumination that can be achieved with arrays of discrete spark sources has shown that uv-preionization is capable of providing the required uniformity and intensity of ionizing radiation throughout the discharge volume for this size of laser.

The development of a ruggedized, triggered, low-impedance, rail-type spark gap by Helionetics provides critical new technology, which makes the development of reliable high-average-power RGH lasers possible at this time. Expected operational lifetimes for such systems are well in excess of 10^{10} pulses.

The 100 to 200 watt laser, presently being developed by Helionetics will satisfy the minimum requirements for a space-borne device useful in the U.S. Navy's blue-green laser program.

With further development, but requiring no major technological breakthrough, it appears quite feasible to develop discharge-pumped RGH lasers with pulse energies of hundreds of joules and tens of kilowatt average powers. For these larger laser systems a repetitively pulsed X-ray generator would be employed for the preionization. If the electrical discharge duration and optical pulse can be increased to 300 ns (a 50% increase from that already demonstrated) then kilojoule and hence megawatt uv laser systems would become a realistic possibility.

When combined with efficient Raman conversion techniques, kilowatt-average-power uv lasers are of interest to the U. S. Navy for an advanced space-based communication system. Pulsed discharge-pumped lasers with megawatt average powers would also provide a more reliable alternative to the e-beam pumped machines presently being considered by DARPA for a possible ground-based blue-green laser communications network.

UV-lasers with kilowatt average powers would also be important for the large-scale production of VHSIC devices. Other potential applications exist in tactical warfare for air-to-air combat and optical countermeasures.

7.0 REFERENCES

1. G. Eden, R. Burnham, L. F. Champagne, T. Donahue and N. Djeu, "Visible and UV Lasers, Problems and Promises", IEEE Spectrum, 50 (April 1979)
2. G. Yaron and L. D. Hess, Appl. Phys. Lett. 36, 220 (1980)
3. J. J. Ewing and C. A. Brau, Appl. Phys. Lett. 27, 435 (1975)
4. M. L. Bhaumik, R. S. Bradford and E. K. Ault, Appl. Phys. Lett. 28, 23 (1976)
5. J. A. Mangano and J. H. Jacob, Appl. Phys. Lett. 27, 495 (1975)
6. R. Burnham and N. Djeu, Appl. Phys. Lett. 29, 707 (1976)
7. D. E. Rothe and R. A. Gibson, Opt. Commun. 22, 265 (1977)
8. W. J. Sarjeant, A. J. Alcock and K. E. Leopold, Appl. Lett. 30, 635
9. S. C. Lin and J. I. Levatter, Appl. Phys. Lett. 34, 505 (1979)
10. J. I. Levatter and S. C. Lin, J. Appl. Phys. 51, 210 (1980)
11. C. P. Wang, Appl. Phys. Lett. 32, 360 (1978)
12. J. L. Miller, J. Dickie, J. Davin, J. Swingle and T. Kan, Appl. Phys. Lett. 35, 912 (1979)
13. G. L. Rogoff, Phys. Fluids 15, 1931 (1972)
14. S. Friedman, S. Goldberg, J. Hamilton, S. Merz, R. Plante and D. Turnquist, "Multi-Gigawatt Hydrogen Thyratrons with Nanosecond Risetimes," 13th Pulse Power Modulator Symposium (1978)
15. J. C. Martin, Switching Notes, No. 10, AWRE, unpublished (1970)
16. J. C. Martin, Multi-Channel-Gaps, AWRE, SSWA/JCM/703/27 (1970)
17. J. I. Levatter and R. S. Bradford, Jr., Appl. Phys. Lett. 33, 742 (1978)
18. T. S. Fahlen, J. Appl. Phys. 49, 455 (1979)
19. R. Fujimoto and N. Toshima, Trans. Inst. Eng. Japan 98-C, 133 (1978)
20. S. Sumida, M. Obara and T. Fujioka, Appl. Phys. Lett. 33, 413 (1978)
21. G. R. White, "X-Ray Attenuation Coefficient from 10 keV to 100 MeV," NBS Report No. 1003 (U.S. GPO, Washington, D. C., 1952)
22. D. E. Rothe, "Parametric and Scaling Studies of Spark-Preionized Discharge-Excited Rare-Gas Halide Lasers," Paper CA-7, 30th Annual Gaseous Electronics Conference, Palo Alto, California (18-21 Oct 1977)

    also

    M. L. Bhaumik and D. E. Rothe, "Self-Sustained Visible and Ultraviolet Lasers," Northrop IR&D Report 79-R-533 (1979)
23. J. I. Levatter, "A Review of Engineering Considerations and Recent Experimentation Regarding an X-Ray Preionized Avalanche Discharge Excimer Laser," Electro-Optics/Laser 80 Conference, Boston, Mass. (Nov. 19-21, 1980)
24. R. Burnham and N. Djeu, Opt. Lett. 3, 215 (1978)
25. D. Cotter and W. Zapka, Opt. Commun, 26, 251 (1978)

26. H. Komine and E. A. Stappaerts, Opt. Lett. 4, 398 (1979)

27. C. K. Rhodes, Dept. Phys., Univ. of Illinois, Chicago, Ill. (1980),private communication

28. "Strategic Laser Communications Program", NOSC Tech. Doc. 352, Vol. 1, Naval Oceans Systems Center, San Diego, Calif. (31 July 1980)

29. R. T. Hawkins, H. Egger, J. Baker and C. K. Rhodes, Appl. Phys. Lett. 36, 391 (1980)

30. M. Maeda, T. Mizunami, A. Sato, O. Uchino and Y. Miyazoe, Appl. Phys. Lett. 36, 636 (1980)

31. G. Wakulopulos, "High Peak Power Pulsed WIP Electron Gun," Lawrence Livermore Radiation Laboratory Report, Livermore, California (1978)

32. S. C. Lin, University of California, San Diego, private communication (1980)

33. F. E. Gruber and R. Suess, "Investigation of the Erosive Phenomena in High-Pressure Gas Discharges," Institut für Plasmaphysik, Garching, Germany (1969) (Unpublished)

34. J. W. Keto, T. D. Raymond and S. T. Walsh, Rev. Sci. Instrum. 51, 42 (1980)

35. M. A. Akerman and R. A. Tenant, "Discharge-Pumped RGH Laser Materials and Gas Clean-Up Studies," IEEE/OSA Topical Meeting of Excimer Lasers (1979)

36. R. A. Olsen, P. Bletzinger and A. Gascadden, "High-Repetition-Rate Closed-Cycle Atomic Rare-Gas Lasers," International Conference on Lasers '79, Orlando, Florida (Dec. 17-21, 1979)

also IEEE J. Quant, Electron. QE-12, 316 (1976)

37. D. E. Rothe, "Excimer Laser Technology: High-PRF, Closed-Cycle Mercury-Halide Laser Development," Report No. AFWAL-TR-80-1169, Air Force Avionics Laboratory, Wright-Patterson AFB, Ohio (Jan. 1981)

38. A. E. Siegman, IEEE J. Quant. Electron. QE-12, 35 (1976)

39. D. E. Rothe, Experiments performed with a continuously-coupled unstable resonator on a high-gain HF/DF laser (Northrop RTC, 1979)

40. H. Komine, Northrop Research and Technology Center, private communication (1980)

41. A. E. Siegman, "Stabilizing Output with Unstable Resonators," Laser Focus, 42 (May 1971)

42. H. E. Bennett et al., "UV Components for High Energy Applications," Naval Weapons Center Tech. Paper NXC-TP-6015 (1978)

43. A. J. Palmer, Appl. Phys. Lett. 25, 138 (1974)

44. L. E. Kline and L. J. Denes, J. Appl. Phys. 46, 1567 (1975)

45. N. W. Harris, F. O'Neill and W. T. Whitney, Appl. Phys. Lett.25, 146 (1974)
R. E. Carter, IEEE J. Quantum Electron. QE-10, 208 (1974)
J. A. Mangano, J. H. Jacob and J. B. Dodge, Appl. Phys. Lett. 29, 426 (1976)

46. R. C. Sze and P. B. Scott, Rev. Sci. Inst. 49, 772 (1978)

47. C. R. Tallman, presented at the Topical Meeting on Excimer Lasers, Charleston, S.C. (1979), paper WB4-1

48. L. J. Denes, et al., "Research Program on UV-Initiated Rare Gas Halide Excimer Lasers," Westinghouse Technical Report (1978)

49. G. W. Sutton, AIAA J. 7, 1737 (1969)

50. W. H. Long, Northrop Research and Technology Center, private communication (1977)

51. H. W. Liepmann and A. Roshko, "Elements of Gasdynamics," John Wiley & Sons, N.Y. (1957)

APPENDIX A
DESCRIPTION OF CALCULATION OF PREIONIZATION DISTRIBUTION

As is noted in the text, unless the preionization is uniform over the discharge space between the electrodes, the glow discharge seeks the regions of intense preionization and a non-uniform discharge results. We have investigated the uniformity of the preionization by numerically modeling the geometry of the spark preionization region and incorporating the absorption of the ultraviolet light by the laser gas.

The geometry of a typical spark array is shown in Figure A-1. The sparks are represented by asterisks at the bottom; the radius R_i is the distance from the ith spark source at x_i, y_i, z_i to the observation point at x_o, y_o, z_o. The light intensity at x_o, y_o, z_o is proportional to

$$I \sim \sum_{i=1}^{n} \frac{T(\theta_i)}{R_i^2} e^{-\alpha R_i} \qquad \text{(A-1)}$$

where $R_i = \left[(x_o-x_i)^2+(y_o-y_i)^2+(z_o-z_i)^2\right]^{\frac{1}{2}}$,

$T(\theta_i)$ = screen transmissivity as a function of viewing angle θ_i,

α = gas absorption coefficient (cm^{-1}).

The sums are taken over all n radius vectors which are transmitted by the screen.

The screen is made of perforated nickel sheet. Typically, the holes are one half millimeter in diameter in a ¼ millimeter thick sheet. These holes act to direct the ultraviolet radiation normal to the screen by blocking these rays which are tangential to the screen.

To calculate the screen transmissivity, we note that when viewed at an angle θ from the normal to the screen, the holes appear as ellipses and the finite thickness of the screen narrows the viewed opening to two segments of an ellipse. Consider these holes in a pattern array such that the normally viewed transparency is $T_o = \pi r^2/A_g$, where πr^2 is the hole area and A_g is the area of that portion of the grid structure attributable to that hole (i.e., for hexagonal array, the hexagonal cell centered on the hole).

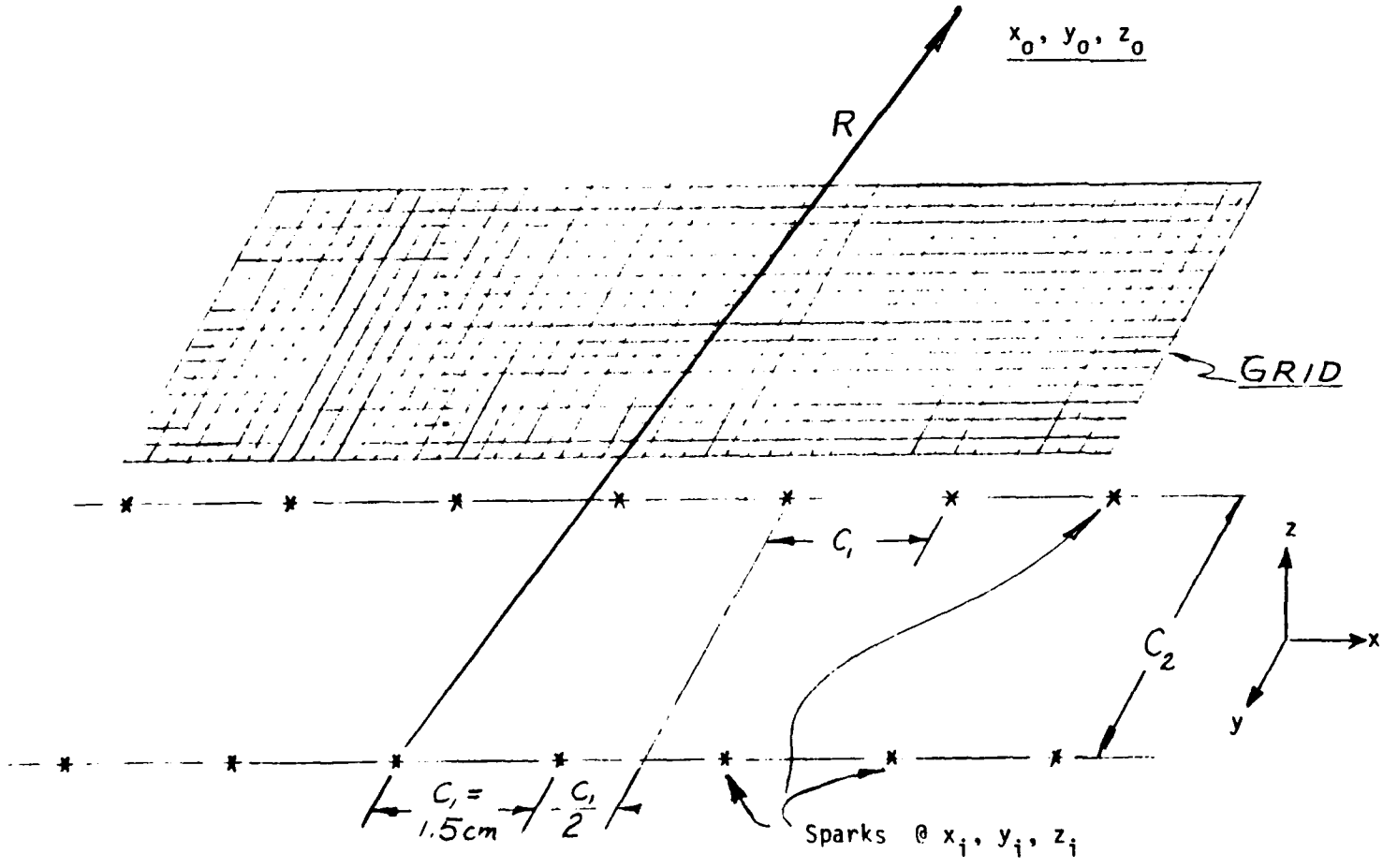

Figure A-1. The preionization at the point x_0, y_0, z_0 is the cumulative effect of sparks at x_i, y_i, z_i acting at the distance R and attenuated by the screen (here represented as a grid) which has transmissivity T, and a ratio or thickness to hole diameter t/D.

The transparency when viewed at the angle $\Theta = \cos^{-1}\left(\frac{z_o - z_i}{R}\right)$ is the sum of two circle segments over A_g:

$$\frac{T(\Theta_i)}{T_o} = \frac{2}{\pi}\cos^{-1}\left(\frac{\delta}{r}\right) - \frac{\delta}{r}\left[1-\left(\frac{\delta}{r}\right)^2\right]^{\frac{1}{2}} \qquad \text{(A-2)}$$

where $\delta = \frac{t}{2}\tan\Theta_i$ is that width of the center circle segment blocked out while viewing through a hole punched through material of thickness t.

The sum of the rays R from all spark sources with reduced transmission $T(\Theta)$ was taken with the aid of small computer programed to give plots of the preionization intensity throughout the discharge volume. Typical results of these calculations are presented in Section 4.

APPENDIX B

PERSONNEL

The Laser Division of Helionetics was founded in the Spring of 1980 for the purpose of developing high-PRF, ultraviolet excimer laser systems for semiconductor processing and DoD applications. The Laser Division is under the direction of Dr. J. I. Levatter and is managed by Dr. D. E. Rothe. Resumes of some of the key technical staff members associated with the laser group are included in this section.

At present the laser group consists of the following personnel:

Dr. J. I. Levatter	Director, Laser Division
Dr. D. E. Rothe	Manager, Laser Division
Dr. R. L. Sandstrom	Research Scientist
Mr. R. Akins	Mechanical Engineer
Mr. D. Floyd	Associate Engineer
Mr. R. A. Donaldson	Machinist
Mr. M. W. Grey	Designer
Dr. S. C. Lin	Scientific Consultant
Dr. C. K. Rhodes	Scientific Consultant
Dr. R. N. Keeler	Scientific Consultant
Dr. P. B. Scott	Technical Consultant

To augment the Research and Engineering Staff associated with the Laser Division, additional personnel from the Engineering and Design Staff of the DECC Division can be made available.

JEFFREY I. LEVATTER

Director, Helionetics, Laser Division

Experience - Laser Physics and High Voltage Pulse Electronics

Research and Engineering Interests

For the past ten years Dr. Levatter has been actively engaged in studying the physics and engineering of gas lasers. During this period his research has involved almost all of the presently important gas laser systems and some of the more common solid state lasers (Ar^+, Ar^{++}, BCl_3, pulsed and CW CO_2, F-, H_2, HCl, I_2, Kr^+, N_2, N_2^+, ruby, Yag, XeF, XeCl, KrF, KrCl, Ar^F, etc.) Dr. Levatter's early investigations concentrated on the quantitative measurement of Raman scattering cross-sections and applications to remote air pollution monitoring using Lidar techniques. During this time he developed new photon counting statistics and a new ultrahigh power pulsed N_2 laser. While continuing research in the area of high power pulsed lasers, a unique knowledge of discharge plasma-physics and high voltage pulse power technology has been acquired. Applying this expertise, Dr. Levatter has developed many specialized pulse power gaps, multi-arc-channel spark gaps, an ultra-fast electro-optic driver, and several laser pulse power systems. He has also been investigating the plasmaphysics underlying the basic mechanism of the glow-to-arc transition associated with high E/N laser discharges. Dr. Levatter has applied this research, and has successfully designed and constructed the largest, highest energy "fast discharge" excimer laser (2.5 liter, 5 joules using XeCl) presently in operation. Dr. Levatter's current research is focused on the extension of the electrical and optical pulse duration of the excimer into the microsecond pulse regime.

In addition to his extensive research programs, Dr. Levatter has also been actively engaged in industrial program management. His activities in this area have involved the research and product development of several lasers and electro-optic systems, and the construction of numerous funding proposals. At present he is consulting exclusively for Helionetics as the Director of the Laser Division.

Education

1974 B.A. Physics, University of California, San Diego, La Jolla, California
1976 M.S. Applied Physics, Stanford University, Stanford, California
1979 Ph.D. Engineering Physics, University of California, San Diego

Research and Professional Experience

Since 1970 Dr. Levatter has completed numerous research and engineering projects. The list which follows serves to highlight several of those projects which he designed and constructed.

1970 CW CO_2 laser

1971 100 kW pulsed N_2 laser, ½ watt average power

1972 a. High speed, gated photon counting system
b. Laboratory measurement of Raman cross-section using fast pulse laser scattering

Dr. Jeffrey I. Levatter

1973
a. Theoretical feasibility study of remote monitoring of atmospheric pollutants using Raman Lidar techniques.
b. 150 watt cw Ar^{++} laser (assisted C.P. Wang)
c. 1 kW CO_2 laser amplifier (assisted J. M. Morris)

1974
a. Raman spectroscopy of organic molecules
b. High power, parallel-plates driven N_2 laser-2.5 MW and 20 mj.

1975
a. Low inductance, flow through electrode, pulsed gas laser (Xonics).
b. Subanosecond electro-optic shutter for mode locked pulse selection.
c. Sapphire to tantalum, eutectic seal.
d. Optically pumped Na_2 laser.
e. Coaxial cable, Blumlein driven N_2 laser--1 MW, 100 pps @ n ≈0.2%.
f. Coaxial flow, spark gap (Xonics)

1976
a. Discharge pumped Na_2 laser
b. Discharge pumped XeF laser
c. Theoretical analysis of X-ray ionized high pressure gas lasers.
d. H_2O dielectric Blumlein, fast discharge laser (Xonics).
e. Production of electro-optic driver--"Laser Pulse Selector" (Xonics)
f. Multi-arc-channel rail spark gap (Xonics)

1977
a. 250 kV, 5 kj Marx bank
b. High vacuum system ($<10^{-8}$ torr)
c. Hot cathode e-beam
d. Cold cathode e-beam (10 cm x 110 cm)
e. F_2 gas handling system
f. 300 joule e-beam controlled CO_2 laser
g. XeF direct pumped e-beam laser
h. XeCl e-beam controlled-mode discharge laser
i. Commerical excimer laser--¼ joule, 20-25 watt (Xonics)

1978
a. Large volume, low inductance, self-sustained (avalanche) discharge excimer laser
b. X-ray preionized CO_2, XeCl, and KrF laser
c. Theoretical investigation of discharge instabilities
d. Triggered multi-arc-channel rail spark gap (Xonics)
e. 35 kV, 1 kc, saturable reactor power supply
f. 35 kV, 100 Hz, inductive charging supply (Xonics)

1979
a. Established theoretical criteria for the homogeneous volume initiation of high pressure avalanche discharges
b. High energy ultraviolet lasing from discharge XeCl laser (5 joules)
c. Raman frequency down conversion in lead vapor
d. Hybrid-unstable laser oscillator for XeCl laser

1980
a. Low energy pulsed-X-ray source for laser preionization
b. Excimer laser avalanche discharge pulse time duration extension.

Teaching Experience

Guest lecturer at University of California, San Diego for the following courses:

"Environmental Pollution"
"Gas Lasers Kinetics"
"Laser and Gasdynamics Research Seminar"

Dr. Jeffrey I. Levatter

Publications

1. "Lead Vapor Downconversion of an X-Ray Preionized XeCl Laser," presented at NOSC Strategic Blue-Green Optical Communications Technical Interchange Meeting (TIM IV), San Diego, CA, Mar. 1980

2. "Annealing of Arsenic Implanted Silicon Using a 2-J uv Excimer Laser," with R. J. Presseley, T. T. Bardin and T. K. McNab, presented at CLEOS, San Diego, CA, Feb. 1980.

3. "Necessary Conditions for the Homogeneous Formation of Poked Avalanche Discharges at High Gas Pressures, J. Appl. Phys. S1, 210(1980)

4. "X-Ray Preionization for Electric Discharge Lasers," with S. D. Lin, Appl. Phys. Lett. 34, 505(1979).

5. "Criteria for Maintenance of Spatial Homogeneity During the Formative Phase of a Pulsed Avalanche Discharge," with S. C. Lin, presented at the 31st GEC, Buffalo, N.Y., Oct. 1978.

6. "Water Dielectric Blumlein-Driven-Fast Electric-Discharge KrF Laser," with R. S. Bradford, Appl. Phys. Lett. 33 742(1978)

7. "E-beam Controlled-Mode-Discharge XeCl Laser," with J. Morris and S. C. Lin, Appl. Phys. Lett. 32 630(1978)

8. "High Power Generation from a Parallel-Plates Driven Pulsed Nitrogen Laser," with S. C. Lin, Appl. Phys. Lett. 25 703(1974)

9. "Raman Cross Sections Measured by Short Pulse Laser Scattering and Photon Counting," with R. L. Sandstrom and S. C. Lin, J. Appl. Phys. 44 3273-3276 (1973)

10. "Remote Monitoring of Atmospheric Pollutants Using Raman Lidar Techniques," with R. L. Sandstrom and S. C. Lin, Project Clean Air, University of California, San Diego(1972)

Patents

1. J. I. Levatter, "High Repetition Rate, Uniform Volume, Transverse Electric Discharge Laser with Pulse Triggered Multi-Arc Channel Switching," patent applied for Dec. 1979

2. J. I. Levatter and R. S. Bradford, "Triggered Multi-ARc-Channel, High Repetition Rate Spark Gap Switch," patent applied for July 1978

3. J. I. Levatter, R. S. Bradford and L. B. Braverman, "Pulsed Electric Discharge Laser Utilizing Water Dielectric Blumlein Transmission Line," patent applied for Feb. 1978

4. J. I. Levatter, S. C. Lin and P. B. Scott, "Coaxial Flow-Spark Gap Switch," #3, 983, 438 (1976)

5. J. I. Levatter and S. C. Lin, "Pulsed Gas Laser with Low-Inductance Flow-Through Electrodes," #4, 005, 374(1974)

Dietmar E. Rothe, Ph. D.

Dr. Dietmar E. Rothe, Manager, Helionetics Laser Division, has more than 15 years of on-hands experience in research and engineering in the areas of plasmaphysics and pulsed gas laser research. As the senior research scientist with Lumonics Research Ltd., Canada (1971 to 1976), Dr. Rothe contributed heavily towards the development of the first line of commercially available high-energy CO_2 TEA-Lasers (10 J to 200 J). In addition he was in charge of all chemical HF/DF laser contracts and all internally funded research. All of these projects were outstandingtly successful, and the laser systems met and/or exceeded their predicted technical specifications and were delivered on time. Among these projects were:

1. Line-tunable HF/DF laser with better than 0.2 mR beam divergence (delivered to Rome Air Development Center, New York for atmospheric propagation studies).

2. Two to 10 pps HF/DF laser with 1 J output energy (systems delivered to Air Force Avionics Lab, WPAFB, Ohio, and to Kirtland AFB, New Mexico for propagation and optical countermeasures work).

3. High-energy single-mode HF/DF laser with 10 cm aperture and 10 J multiline output. Line selectable to provide single-line peak powers in excess of 1 MW (delivered to U.S. Army Harry Diamond Labs, D.C. for Raman Conversion Studies).

4. A 200 pps closed-cycle HF/DF laser with 20 W average power output (delivered to Canadian Defense Research Establishment, Valcartier, Quebec for optical radar).

5. A 500 W closed-cycle CO_2 TEA-laser (internal research).

6. Fast transmission-line driven short wavelength laser (N_2(C-B), He-N_2^+ charge transfer, He-Ar and Ar-Xe energy transfer) emitting between 1 and 20 mJ pulses in the uv, blue and near-IR (internal research).

For a period of two years he was project leader on high-pulse-repetition-frequency (PRF) lasers. Whereas this work was directed towards the development of high-average-power CO_2 and HF lasers, much of this experience is directly applicable to high-PRF rare-gas halide lasers.

As a research scientist with the Northrop Corporation, Northrop Research and Technology Center, California (1976 to 1980), Dr. Rothe was project leader for several government contracts (ONR, AFAL) including the development and evaluation of a novel double-discharge longitudinal rare-gas halide laser and the development of a high-PRF 5 W mercury halide laser. He also directed all self-sustained discharge-excited rare-gas halide laser work (KrF, XeF and XeCl), advancing the state-of-the-art of these devices. Another of his projects dealt with the efficient e-beam-sustained discharge excitation of XeCl. For the successful completion of many of these projects it was necessary for Dr. Rothe and his team to design and develop uv-preionization arrays, multichannel spark gaps and other high-voltage technology. All of this very recent experience will be of direct benefit to the high-power uv-laser program.

Dr. Dietmar E. Rothe

Before becoming involved in laser research on a full-time basis, Dr. Rothe made significant contributions in the fields of plasmaphysics and gasdynamics. As a Research Scientist with Cornell Aeronautical Laboratory, Inc., between 1966 and 1971, he performed research work in the fields of shock tube spectroscopy, radiative recombination of ions and electrons, electron attachment to halogen atoms and SF_6, spectra of electron-beam excited gases, viscous nozzle flows and nozzle plumes, and gasdynamic lasers.

He received his B. Eng. (Honours, 1961) degree in Engineering Physics from McMaster University (Hamilton, Canada) and his M.A.Sc. (1962) and Ph.D. (1966) in Aerospace Engineering Science from the University of Toronto, majoring in plasmaphysics. His postgraduate work included studies of free molecular pressure probes, flow visualization in low density wind tunnels, electron-beam excitation of gases, and diffusion of gas components in supersonic free jets and shock waves.

He is a member of Sigma Xi and the Association of Professional Engineers of the Province of Ontario. He is a biographee of Who's Who in the West.

Dr. Dietmar E. Rothe
Publications

"The Free Molecule Impact Pressure Probe of Arbitrary Length," with J. H. deLeeuw, AIAA Journal 1, 220(1963).

"Flow Visualization Using a Traversing Electron Beam," AIAA Journal 3, 1945 (1965)

"Electron Beam Studies of the Diffusive Separation of Helium-Argon Mixtures," Phys. Fluids 9, 1643 (1966).

"Radiative Ion-Electron Recombination in a Sodium-Seeded Plasma," JQSRT 9, 49(1969)

"A Study of Energy Transfer Processes in Ionized Gases," with W. H. Wurster, CAL Report No. RM-2295-A-1, Cornell Aeronautical Laboratory, Buffalo, N.Y., June 1968

"Radiative Capture of Electrons by Chlorine, Bromine, and Iodine Atoms," Phys. Rev. 177, 93 (1969)

"Emission Spectra of Atmospheric Gases Excited by an Electron Beam," with D. J. McCaa, AIAA Journal 7, 1948 (1969)

"Radiative Electron Recombination into the First Excited State of Lithium, JQSRT 11, 355 (1971)

"Electron Beam Studies of Viscous Flow in Supersonic Nozzles," AIAA Journal 9, 809 (1971)

"Development and Construction of a Line-Tunable Fundamental-Mode Pulsed HF/DF Laser," RADC-TR-73-173, Rome Air Development Center, Air Force Systems Command, Griffiss Air Force Base, N.Y., April 1973

"Spectral Tuning and Single-Mode Operation of a Superradiant HF/DF Laser," IEEE/IEDM Technical Digest, 453 (1973)

"Blue N_2^+ Laser Pumped by Charge Transfer in a High-Pressure Pulsed Glow Discharge," with K.O. Tan, Appl. Phys. Lett. 30, 152 (1977)

"Parametric and Scaling Studies of Self-Sustained Discharge-Excited Rare-Gas Halide Lasers," with R. A. Gibson, Proc. Army Symposium on New Concepts in High Energy Lasers, Special Report H-77-3, U.S. Army Missile Research and Development Command, Redstone Arsenal, Alabama (July 1977), p. 190

"A 10 W Repetitively Pulsed, Closed-Cycle HF/DF Laser," with K. O. Tan, J. A. Nilson, and D. J. James, presented at IEEE Conference on Laser Engineering and Application (CLEA), Washington, D.C., 1-3 June 1977

"Analysis of a Spark-Preionized Large-Volume XeF and KrF Discharge Laser," with R. A. Gibson, Opt. Commun. 22. 265 (1977)

Dr. Dietmar E. Rothe, Publications (Continued)

"Parametric and Scaling Studies of Spark-Preionized Discharge-Excited Rare-gas Halide Lasers," Paper CA-7 presented at the 30th Annual Gaseous Electronics Conference, Palo Alto, California, 18-21 October 1977

"Efficient E-Beam Excitation of XeCl," with J. B. West, and M. L. Bhaumik, Special issue on excimer laser, IEEE J. Quant. Electron. QE-15, 314 (May 1979)

"Device Development Program for Efficient Excitation of a Blue-Green Laser," with W. H. Long, Northrop Research and Technology Center, Final Report No. NRTC 80-10R (July 1980), prepared for ONR, Arlington, Va.

"Excimer Laser Technology;High-PRF, Closed-Cycle Mercury-Halide Laser Development," Report No. AFWAL-TR-80-1169 Air Force Avionics Laboratory, Wright-Patterson AFB, Ohio (Jan. 1981)

Patents

"Transverse-Longitudinal Sequential Discharge Excitation of High-Pressure Laser," U.S. Patent No. 4240043 (Dec. 1980)

RICHARD L. SANDSTROM

Education

1972	B. A. Physics	University of California, San Diego
1979	Ph.D. Engineering Physics	University of California, San Diego

Academic Research Experience

1972 - 1980 During his graduate career, Dr. Sandstrom investigated the degrading effects of heated-air turbulence on the propagation of laser beams. In particular, one- and two-point statistics of the perturbations in the optical phase were measured. He designed and built a dual-beam laser heterodyne interferometer for these measurements.

In addition to his thesis program, Dr. Sandstrom was extensively involved in the design of several high-power laser systems, including a 150 W CW argon-ion laser with a folded three-mirror cavity, a 100 KW peak power 500Hz N_2 laser, a 2MW peak power Blumlein-drive N_2 laser, and an E-beam preionized fast discharge excimer laser. While working with these laser systems, Dr. Sandstrom acquired considerable experience in the design of high-power, fast discharge circuitry, and associated diagnostic techniques. He is also familiar with E-beam and ultra-high vacuum technology. Other projects during this period included the measurement of relative Raman cross-sections for several molecular species relevant to remote pollution monitoring, and the construction of a UV absorption fluorine concentration monitor.

Upon receiving his Ph.D., Dr. Sandstorm accepted a one-year post-doctoral appointment in the field of coherent optical processing. He designed and built a computer-controlled laser scanning system for encoding images for non-linear optical processing, and for generating complex coordinate transform filters for image modification experiments.

Professional Experience

1978 - 1980 For two years Dr. Sandstrom was a consultant for the Aerospace Corporation in El Segundo, California, bringing an extensive knowledge of digital and analog electronics, servo-control systems, and heterodyne interferometers. He assisted in the measurement of the wavefront profiles of HF and CO_2 lasers, and was involved in several actively stabilized cavity projects.

1980 - Present Since joining Helionetics in July, 1980, Dr. Sandstrom has been Senior Research Scientist for the Helionetics excimer laser project. His duties included the design and fabrication of various laser subsystems, and he is actively involved in every phase of the project.

Dr. Richard L. Sandstrom

Publications

"Raman cross-sections measured by short pulse laser scattering and photon counting", Journal of Applied Physics, 44, 3273(1973) with J. Levatter and S.C. Lin.

"Three mirror stable resonator for high power and single mode lasers", Applied Optics 14, 1285(1975), with C. P. Wang.

"Scanning interferometric pattern system for encoding theta-modulated images", to be submitted to Applied Optics, with S. H. Lee.

AD-A102 337 HELIONETICS INC SAN DIEGO CA LASER DIV F/G 20/5
SCALING AND DESIGN OF DISCHARGE-EXCITED RARE-GAS HALIDE LASERS.(U)
JAN 81 D E ROTHE, J I LEVATTER, R L SANDSTROM N00014-81-C-0044
UNCLASSIFIED HLD-81-1R NL

NAME:	Shao-Chi Lin, Ph.D.
EDUCATION:	B.Sc., National Central University, Chungking, China,1946 Air Force Technical School, Chengtu, China, 1946-47 Ph.D., Cornell University, Ithaca, New York, 1952
EMPLOYMENT:	
1947-1948	Research Engineer, Bureau of Aircraft Industry, Nanching, China
1948-1952	Research Assistant, Cornell University, Ithaca, NY
1952	Instructor (Part Time), Cornell University, Ithaca, NY
1952-1955	Research Associate, Cornell University, Ithaca, NY
1954	Assistant Professor (Part Time), Cornell University, Ithaca, NY
1955-1964	Principal Research Scientist, AVCO Everett Research Laboratory, Everett, Massachusetts
1963	Visiting Lecturer, Massachusetts Institute of Technology Cambridge, Mass.
1964	Professor Engineering Physics, University of California, San Diego, La Jolla, California
PROFESSIONAL ACTIVITIES:	
1961	Consultant to governmental and industrial ogranizations
1965-1969	U.S. National Academy of Sciences/National Research Council, Advisory Committee to the Air Force Systems Command - Re-entry Physics Panel Member
1963	American Institute of Aeronautics and Astronautics - Member of various Technical Committees, conference organizing committees, session chairman, and AIAA Journal Reviewer
1955	American Institute of Physics - Reviewer for various journal papers
1955	National Science Foundation - Reviewer for research proposals

1970	Xonics, Inc. - Founder and Member of the Board of Directors

SOCIETY AFFILIATION :

American Institute of Aeronautics and Astronautics (Fellow since 1974)

American Physical Society

American Geophysical Union

American Association for the Advancement of Sciences

Society of Sigma Xi,

New York Academy of Science (Life Member

HONORS & AWARDS:

1945	National Central University - Top 10 Student Award
1950	Society of Sigma Xi, Cornell Chapter - Scholarship Award
1955	American Men of Science (9th Edition, Vol. I, The Science Press and R.R. Bowker Company) - Biographee
1964	Who's Who in the East (9th Edition Marquis) - Biographee
1966	American Institute of Aeronautics and Astronautics - Research Award
1968	World Who's Who in Science (1st Edition, Marquis) - Biographee

Selected Publications
Shao-Chi Lin, Ph.D.

Dr. Lin has published about 60 scientific papers and is the holder of one of the earliest patents issued by the U.S. Patent Office on gas lasers and their methods of operation. This patent, which was filed on April 30, 1963, and subsequently granted as No. 3,302,127 and assigned to the AVCO Corporation on January 31, 1967, covered a number of advanced and important gas laser concepts, including the use of flow system, gas mixing, and excitation transfer for the achievement of high power and efficiency. A representative set of Dr. Lin's publication follows (a detailed list also appended).

1. "The Production of High Temperature Gases in Shock Tubes," co-authored with E. L. Resler and A. R. Kantrowitz, Journal of Applied Physics, 23, pp. 1390-1399 (1952).

2. "Cylindrical Shock Waves Produced by Instantaneous Energy Release," Journal of Applied Physics, 25, pp. 54-57 (1954).

3. "Electrical Conductivity of Highly Ionized Argon Produced by Shock Waves," co-authored with E.L. Resler and A.R. Kantrowitz, Journal of Applied Physics, 25, pp. 95-109 (1955).

4. "Electrical Conductivity of Thermally Ionized Air Produced in a Shock Tube," co-authored with L. Lamb, Journal of Applied Physics, 28, pp. 754-759 (1957).

5. "Radio Echoes from a Manned Satellite During Re-Entry," Journal of Geophysical Research, 67, pp. 3851-3870 (1962).

6. "Rate of Ionization Behind Shock Waves in Air. I. Experimental Results," co-authored with R.A. Neal and W.I. Fyfe, Physics of Fluids, 5, 1633-1648 (1962).

7. "Rate of Ionization Behind Shock Waves in Air. II. Theoretical Interpretation," co-authored with J.D. Teare, Physics of Fluids, 6, pp. 355-375 (1963).

8. "Experimental Study of Argon Ion Laser Discharge at High Current," co-authored with C. P. Wang, Journal of Applied Physics, 43, pp. 5068-5073 (1972).

9. "Temperature Field Structure in Strongly Heated Buoyant Thermals," co-authored with Leslie Tsang and C. P. Wang, Physics of Fluids, 15, pp. 2118-2128 (1972).

10. "Raman Cross-Section Measured by Short-Pulse Laser Scattering and Photon Counting," with J. I. Levatter and R. L. Sandstrom, Journal of Applied Physics, 44, pp. 3273-3276 (1973).

Publications

1. "Analysis of Pressure Waves in the Inlet Piping of the High Altitude Test Facility Due to Explosion in the Test Chamber, "co-authored with A.R. Kantrowitz, and E. E. McDonald, Cornell University, Graduate School of Aeronautical Engineering Report, A.E.D.C. Contract W33-038-ac015497 (1949).

2. "Design of a Shock Tube to Provide a Pulse for Starting Flow in Supersonic Wind Tunnels," co-authored with A. R. Kantrowitz and H. Petschek, Cornell University, Graduate School of Aeronautical Engineering Report, A.E.D.C. Contract W33-038-ac015497 (1950).

3. "Wind Tunnels for Aerodynamic Development at Very High Mach Numbers," co-authored with H. Petschek and A. R. Kantrowitz, Cornell University Graduate School of Aeronautical Engineering Report, A.E.D.C. Contract W33-038-ac015497 (1951).

4. "The Production of High Temperature Gases in Shock Tubes," co-authored with E. L. Resler and A. R. Kantrowitz, Journal of Applied Physics, 23, 1390 (1952).

5. "Estimate of Radiation from High Temperature Air," co-authored with H. Petschek and A. R. Kantrowitz, Graduate School of Aeronautical Engineering Report (1953).

6. "Cylindrical Shock Waves Produced by Instantaneous Energy Release," Journal of Applied Physics, 25, 54 (1954).

7. "Electrical Conductivity of Highly Ionized Argon Produced by Shock Waves," co-authored with E. L. Resler and A. R. Kantrowitz, Journal of Applied Physics, 25, 95 (1955).

8. "A Rough Estimate of the Attenuation of Telemetering Signals through the Ionized Gas Envelope Around a Typical Reentry Missile, " Avco-Everett Research Laboratory, Research Report 74 (1956).

9. "Electrical Conductivity of Thermally Ionized Air Produced in a Shock Tube," co-authored with L. Lamb, Journal of Applied Physics, 28, 754 (1957).

10. "Ionization Phenomenon of Shock Waves in Oxygen-Nitrogen Mixtures," Avco-Everett Research Laboratory, Research Report 33 (1958); also Report on the 18th Annual Conference on Physical Electronics, Mass. Inst. of Technology, Cambridge (1958).

11. "Shock Wave Studies of Transport Properties in High Temperature Gases," Transport Properties in Gases, A.B. Gambel and J. B. Fenn, eds., Northwestern University Press (1958).

12. "Slow Electron Scattering by Atomic Oxygen," co-authored with B. Kivel, Physical Review, 114, 1026 (1959).

13. "Ionized Wakes of Hypersonic Objects," Avco-Everett Research Laboratory, Research Report 151, June 1959.

14. "Encyclopedia of Science and Technology," S.C. Lin, contributing author, McGraw-Hill, New York (1960).

15. "Low-Density Shock Tube for Chemical Kinetic Studies, "co-authored with W.I. Fyfe, Physics of Fluids, 4, 238 (1961).

16. "Limiting Velocity for a Rotating Plasma, "Physics of Fluids, 4, 1277 (1961).

17. "A Streamtube Approximation for Calculation of Reaction Rates in the Inviscid Flow Field of Hypersonic Objects," co-authored with J. D. Teare, Proc. 6th Symposium on Ballistic Missile and Aerospace Technology, Vol. IV, C. T. Morrow, L. D. Ely, and M. R. Smith, eds., Academic Press, New York(1961).

18. "Survey of Shock Tube Research Related to the Aerophysics Problem of Hypersonic Flight," Progress in Astronautics and Rocketry, 7, F. R. Riddell, ed., Academic Press, New York (1962).

19. "Radio Echoes from a Manned Satellite During Re-Entry," Journal of Geophysical Research, 67, 3851 (1962).

20. "Rate of Ionization Behind Shock Waves in Air. I. Experimental Results," co-authored with R. A. Neal and W. I. Fyfe, Phys. Fluids, 5, 1633 (1962).

21. "Hydrodynamic Effects Produced by Pulse Microwave Discharges," co-authored with G. P. Theofilos, Avco-Everett Research Laboratory, Research Report 138, October 1962; Phys. of Fluids, 6, 1369 (1963).

22. "Rate of Ionization Behind Shock Waves in Air. II. Theoretical Interpretation," co-authored with J. D. Teare, Physc. of Fluids, 6, 335 (1963).

23. "A Quasi-One-Dimensional Model for Chemically Reacting Turbulent Wakes of Hypersonic Objects," co-authored with J. E. Hayes, Avco-Everett Research Laboratory, Research Report 157, July 1963; AIAA Journal 2, 1214 (1964).

24. "A Partial-Dissipation Approximation for Chemical Reactions in Heterogeneous Turbulent Flows," Avco-Everett Research Laboratory, Research Report 180, April 1964.

25. "Detection of, and Communication with Space Vehicles During Atmospheric Entry; Problems in Simulation," Proceedings of the Conference on the Role of Simulation in Space Technology, Virginia Polytechnic Institute, Engineering Extension Series Circular No. 4, Part B-IX, August 1964.

26. "A Bimodal Approximation for Reacting Turbulent Flows. I. Description of the Model, "AIAA Journal 4, 202-209 (1966).

27. "A Bimodal Approximation for Reacting Turbulent Flows. II. Example of Quasi-One-Dimensional Wake Flow," AIAA Journal 4, 210-216 (1966).

28. "On Cometary Impact and the Origin of Tektites," J. Geophys. Research 71, 2427-37 (1966).

29. "On the Propagation of an Intense Optical Beam in an Absorbing Atmosphere," AVCO-Everett Research Laboratory, Research Note 658, September 1966, published in J.M.D.R. 1967.

30. "Temperature Relaxation and Heat Conduction for Two Rarefied Fully-Ionized Gases in Sudden Thermal Contact," co-authored with H. Y. Wei, Presented at the American Physical Society, Fluid Dynamics Divisional Meeting, Stanford, November 1966, Bull. Am. Phys. Soc. 12, 830 (1967).

31. "Measurements of Turbulent Velocity and Temperature Fluctuations in the Wake of a Sphere," co-authors, C. H. Gibson and C. C. Chen, presented at the AIAA Fifth Aerospace Sciences Meeting, New York, January, 1967. AIAA Preprint No. 67-20, AIAA Journal 6, 642-649 (1968).

32. "Reply to Critique by Chapman and Gault on 'Cometary Impact and the Origin of Tektites'," Journal of Geophysical Research 72, 2700-2703 (1967).

33. "Effect of Charge-Exchange Collisions on Plasma Rotation," (Reply to the Comments by J. A. Fay and P. Sockol), Physics of Fluids 11, 695-697 (1968).

34. "The Rayleigh Problem of a Hot Plasma in Sudden Contact with a Cold Wall," Northwestern University Gas Dynamics Colloquium, October 31, 1967.

35. "Hypersonic Flow Fields and Wakes," IDA Jason Summer Study Report (1967).

36. "Some Outstanding Problems in Reentry Plasma Turbulence," comments partially given at the Plasma Turbulence Meeting, IDA, Arlington, VA., November 29-30, 1966, IPAPS Report No. 67-113, January 1967.

37. "Transient Heat Conduction in Ionized Gases," lecture given at University of California, Los Angeles, Short Course on Modern Developments in Fluid Mechanics and Heat Transfer," March 4-15, 1968. IPAPS 68/69-233.

38. "Temperature Relaxation Near the Interface of Two Semi-Infinite Plasmas," co-author, H. Y. Wei, Physics of Fluids, 12, 172-182 (1968).

39. "Effect of Negative Ion Formation of Dielectric Constant Fluctuation in a Weakly-Ionized Plasma," presented at the 21st Annual Meeting of the Division of Fluid Dynamics, American Physical Society, Seattle, Wash., November 25-27, 1968, Bull, Am. Phys. Soc., Series II, 13, 1586 (1968).

40. "Temperature Relaxation of a Hot Plasma in Sudden Contact with a Cold Wall," co-author, H. Y. Wei, presented at the 21st Annual Meeting of the Division of Fluid Dynamics, American Physical Society, Seattle, Wash., November 25-27, 1968, Bull.Am. Phys. Soc., Series II, 13, 1586 (1968).

41. "Small-Scale Structure and Viscous Cutoff in the Scalar Spectrum of Hypersonic Wake Turbulance," Proceedings, ARPA Workshop on Radar Scattering from Random Media, La Jolla, California, August 5-16, 1968.

42. "Ionization Kinetics and Energy Balance in Noble Gas Ion Lasers," co-author, C. C. Chen, Bull. Am. Phys. Soc., Series II, 14, 839 (1969).

43. "Excitation Mechanisms and Rate-Limited Power in CW Argon Ion Lasers," co-author, C. C. Chen, Bull. Am. Phys. Soc., Series II, 14, 839 (1969).

44. "Thermal Interaction of a Laser Beam with an Absorbing Gas," co-author, R. A. Chodzko, Bull. Am. Phys. Soc., Series II, 14, 839 (1969).

45. "Spectral Characterization of Dielectric Constant Fluctuation in Hypersonic Wake Plasmas," AIAA Journal, 7, 1853-1861 (1969).

46. "Kinetic Processes in Noble Gas Ion Lasers, A Review," co-author, C. C. Chen, Presented at the AIAA 8th Aerospace Sciences Meeting, January 19-21, 1970, AIAA Paper No. 70-82 (1970): AIAA Journal 9, 4-11 (1971).

47. "Transition from Laminar to Turbulent Flow in a Laser-Induced Convection Column," co-author, Richard A. Chodzko, Appl. Physics Letters, 16, 434 (1970).

48. "A Study of Strong Thermal Interactions between a Laser Beam and an Absorbing Gas," AIAA Journal, 9, pp. 1105-1112 (1971).

49. "Experimental Study of Argon Ion Laser Discharge at High Current," co-authored with C. P. Wang, Journal of Applied Physics, 43, pp. 5068-5073 (1972).

50. "Temperature Field Structure in Strongly Heated Buoyant Thermals," co-authored with Leslie Tsang and C. P. Wang, Physics of Fluids, 15, pp. 2118-2128 (1972).

51. "Raman Cross-Sections Measured by Short-Pulse Laser Scattering and Photon Counting," with J. I. Levatter and R. L. Sandstrom, Journal of Applied Physics, 44, pp. 3273-3276 (1973).

52. "A Study of Strong Temperature Mixing in Subsonic Grid Turbulence," co-authored with Shih-Chin Lin, Physics of Fluids, 16, pp. 1587-1598 (1973).

53. "Performance of a Large-Bore High-Power Argon Ion Lasers," co-authored with C. P. Wang, Journal of Applied Physics, 44, pp. 4681-4682 (1973).

54. "Mode Structure and Beam Divergence of a Large-Bore High-Power Argon Ion Laser," co-authored with C. P. Wang, Journal of Applied Physics, 45, pp. 450-456 (1974).

55. "High-Power Generation from a Parallel-Plates-Driven Pulsed Nitrogen Laser," co-authored with Jeffrey I. Levatter, Applied Physics Letters, 25, pp. 703-705 (1974).

56. "Time Behavior of Second-Positive Emissions from a Fast-Discharge N_2 + SF_6 Laser," co-authored with R. P. Akins, Applied Physics Letters, 28, 221 (1976).

57. "Space-Time Variations of Aberrated Optical Images through Nearly Homogeneous Isotropic Turbulence," co-authored with Shih-Chun Lin, Physics of Fluids, 19, 1099 (1976).

58. "High CW Power Ultraviolet Generation from Wall-Confined Noble Gas Ion Lasers," Applied Physics Letters, 29, 795 (1976).

59. "Effects of Field Broadening and Pump Line Selection on Multi-Level Absorption in Molecular Systems," co-authored with J. H. Morris, Journal of Quantitative Spectroscopy and Radiative Transfer (in press, 1977).

60. "Optimizing and Power Enhancement Observed in a Double-Pulse Fast-Discharge-Drive XeF Laser," co-authored with R. P. Akins and G. Innis, J. Appl. Phys. 49, 2262 (1978).

61. "Electron-Beam-Controlled Discharge XeCl Excimer Laser," co-authored with J. I. Levatter and J. H. Morris, Appl. Phys. Lett. 32, 630 (1978).

62. "Pulsating Ion Laser Action Observed in a Magnetically Confined Plasma," co-authored with D. W. Lischer, J. Appl. Phys. 49, 4270-4272 (1978).

63. "X-ray Preionization for Electric Discharge Lasers," co-authored with Jeffrey I. Levatter, App. Phys. Lett. 34, 505-508 (1979).

PAUL B. SCOTT, Sc.D.

Synopsis of Capabilities and Experience: Dr. Scott was educated at the Massachusetts Institute of Technology in the School of Engineering Department of Aeronautics and Astronautics. His area of concentration was fluid mechanics with minor programs in Physics and Economics. While at MIT he was an employee of the Wright Brothers Wind Tunnel and of the Naval Supersonic Laboratory. There he contributed to the theory of cooling of a re-entry body by mass injection into the boundary layer, finally applying finite difference methods to the calculation of the heat transfer as a function of position on the body.

In 1959 he joined the staff of Space Technology Laboratories where he assisted in the preliminary design for launch and re-entry vehicles.

In the period 1961-65 Dr. Scott was at MIT and helped build a group which measured the interaction of beams of molecules with a solid surface to provide basic information from which the drag and heating of a low altitude satellite could be estimated. In this effort, he designed and constructed special electronic equipment (now--but not then--commercially available) for enhancement of the signal-to-noise ratio of the waveform of the experimental signal. Using the apparatus he developed, he made the first measurements of the change of velocity distribution of gas molecules scattered from a surface.

In the Spring of 1965 he was a guest research associate of the University of California at Berkeley for the purpose of reproducing the equipment developed at MIT for the Berkeley laboratory.

He returned to MIT to accept an Assistant Professorship, which he held for two years while continuing his molecular beam research.

In 1967 he joined the staff of the Aerospace Engineering Department of the University of Southern California. At USC he developed new apparatus for molecular beam research, and directed the implementation of an Experimental Projects Laboratory for undergraduate education. The molecular beam effort culminated in a series of measurements of the shape of the potential energy field between molecules which were published in 1970-1972.

In 1969 Dr. Scott and co-workers started research regarding novel means of X-ray imaging, culminating in a patent on the method, and the formation of Xonics, Inc. He left the University in 1972 to work with Xonics fulltime, where he directed experiments related to submarine wake detection and chemical lasers, as well as contributing to the X-ray imaging development at Xonics. For limited periods at Xonics he was engaged in the development of high altitude environmental sensing and directed the initial program of manufacture of the Xonics (X-ray) mammography equipment.

Since leaving Xonics in 1978 he has acted as a consultant in the areas of environmental sensing instruments, photographic imaging and laser equipment, and is president of University Consultants, Inc.

Dr. Paul B. Scott

Patents

1. Radiographic System with Xerographic Printing, by E. P. Muntz, A. Proudian and P. B. Scott, granted 1973.

2. Imaging Gas for Improved Resolution in Imaging Chamber of Electron Radiography System, by A. Proudian and P. B. Scott, granted 1974.

3. Electron Radiographic System with Liquid Absorber, by F. V. Allan, etal., granted 1975.

4. Electrode for Electron Radiography Imaging Chamber, with T. Azzarelli and E. P. Muntz, granted 1975.

5. Spark Gap Switch, with J. I. Levatter and S. C. Lin, granted 1975.

6. Solar Heater with Automatic Venting, granted 1977.

7. Jet Membrane Gas Separator and Method, B. Hamel, E. P. Muntz and P. B. Scott, granted 1978.

Publications

1. "Heat andMass Transfer for Flow Past an Arbitrary Cylinder", MIT Naval Supersonic Laboratory, TR No. 383, September 1959.

2. "The Laminar Diffusion Boundary Layer with External Flow Field Pressure Gradients", with J. R. Baron, MIT Naval Supersonic Laboratory, TR No. 419, December 1959.

3. "Some Mass-Transfer Results with External Flow Pressure Gradients", with J. P. Moran, J. of the Aerospace Sciences 27, No. 8, August 1960.

4. "Mass-Transfer Results with External Flow Pressure Gradients", with J. P. Moran, J. of the Aerospace Sciences 28, No. 9, September 1961.

5. "A Preliminary Consideration of the Powered Flight Dynamics of an Unguided Rolling Missile", with D. H. Mitchell, STL/Technical Memo. 60-0000-19104.

6. "On Accommodation Coefficients", with L. Trilling and H. Y. Wachman, Archiwum Mechaniki Stosowanej 16, 1964.

7. "Molecular Beam Velocity Distribution Measurements", MIT Fluid Dynamics Laboratory Report No. 65-1, February 1965.

8. "Preliminary Measurements of the Velocity Distributions of Argon Scattered by Hot Platinum and Nickel Surfaces for the Case of a Near Monoenergetic Incident Beam", Symp. on Fundamentals of Gas-Surface Interaction, December 1966.

Dr. Paul B. Scott
Publications (continued)

9. "Molecular Beam Velocity Distribution Measurements by a Sensitive Time of Flight Method", Proc. 5th Intern. Symp. on Rarefied Gas Dynamics 11, Academic Press, 1967.

10. "Measurements of the Rotational State Distribution of a Molecular Beam", with T. Mincer, Entropie, November-December 1969; also presented at 2nd International Symposium on High and Middle Energy Molecular Beams, Cannes, Frances, July 1969.

11. "Molecular Beam Rotational Temperature Measurement", with T. Mincer, 7th Symposium on Rarefied Gas Dynamics, 1970.

12. "Measurements of the Hypersonic Flow Field of a Disk", with S. Berlin, USCAE Report 115, Department of Aerospace Engineering, University of Southern California, 1970.

13. "Measurements of the Hypersonic Rarefied Flow Field of a Disk", with S. Berlin, Phys. Fluids 14, p. 773(1971).

14. "Rotational Transitions by Nitrogen Rare-Gas Collisions", with T. Mincer, Entropie No. 42, p. 155, November-December 1971.

15. "A Study of Background Gas Penetration into Underexpanded Jets and the Resulting Separation of Gas Mixtures", with E. P. Muntz and B. Hamel, Entropie No. 42, p. 28, November-December 1971.

16. "Observations of the Exponentially Large Separation when a Background Gas Penetrates an Underexpanded Jet", with E. P. Muntz and B. Hamel, APS Bulletin, 1307, November 1971.

17. "Below 10^{o}K Nitrogen in a Free Jet", with E. P. Muntz, APS Bulletin, 1307, November 1971.

18. "Intermolecular Potential Shape from Inelastic Molecular Scattering", with T. R. Mincer, Proceedings of the 8th International Symposium on Rarefied Gas Dynamics, Stanford University, July 10-14, 1972.

19. "Orientational Averaging of Rotational Transition Probabilities Computed Using the Sudden Approximation", J. Chem. Phys., 58, p. 644(1973).

20. "Nitrogen Rotational Excitations by Collision with Argon-Observations and Comparison with Theory:, with T. R. Mincer and E. P. Muntz, Chem. Phys. Letters, 22, 71(1973).

21. "The Electron Beam Fluorescence Method for Molecular Scattering Experiments", with T. R. Mincer and E. P. Muntz, Rev. Sci. Inst. 45, 207(1974).

22. "Visible Chemiluminescence from Supersonic Mixing Metal-Oxidant Flames", with S. E. Johnson and G. W. Watson, J. of Chem. Phys., 61, p. 2834(1974).

Dr. Paul B. Scott
Publications (continued)

23. "Electron Radiography Using Liquid Absorbers", with S. E. Johnson and G. W. Watson, J. App. Phys., June 1975.

24. "Boron Fluoride and Aluminum Fluoride Infrared Lasers with Quasicontinuous Supersonic Mixing Flames", with S. E. Johnson, W. W. Rice, W. H. Beattie, and R. C. Oldenborg, Ap. Phys. Letters, Vol. 28, No. 8, pp. 444-446(1976).

25. "Preliminary Clinical Mammography Studies using Xonics Electron Radiography", with E. Wilkinson, E. Kaegi, J. H. Lewis, A. L. Morsell, E. P. Muntz, and M. S. Welkowski, presented at the 3rd International Symposium on Detection and Prevention of Cancer, New York(1976).

26. "Neutron Radiographs using the Ionographic Process", with S. E. Johnson, G. W. Watson, and H. Berger, J. Appl. Phys. 49, 5078(1978).

ROBERT P. AKINS

Education

1975	B. A. Physics	University of California, San Diego
1977	M. A. Engineering Physics	University of California, San Diego
1977 - Present	Doctoral Program	Electrical Engineering Dept. University of California, San Diego

Academic Research Experience

1975 - Present Throughout his graduate studies, Robert Akins has been engaged in the development of a variety of laser systems. While completing his master's degree in engineering physics, he performed time resolved spectroscopic studies on a fast-discharge Blumlein driven N_2+SF_6 laser, measured several new lasing lines in atomic fluorine and participated in the development of a hot-cathode e-beam preionizer. After designing a gas control system for the mixing and recycling of F_2 and Cl mixtures, he developed a fast discharge excimer laser capable of operating with noble gas halogen such as XeF and KLF and performed time variable preionization studies.

Presently Mr. Akins is completing his doctoral work in the Electrical Engineering Department at the University of California at San Diego where he has designed and built several dye laser/amplifiers and has recently developed an injection-locked dye ring laser for coherent image amplification. He is also currently involved with the optic design for a 15 watt Ar+ annealing system for the University of California at San Diego.

In addition, while persuing these goals, Mr. Akins has acquired considerable experience in the fields of: high voltage fast-discharge devices, electro-optic switching, caustic gas handling and materials compatability, Fourier optics, and optical image processing.

Professional Experience

1976 Robert Akins worked on a consulting basis for Xonics, Inc. to design and test an F_2 gas control system for their excimer laser program.

1977 Design and testing of the laser optics for an industrial laser grading system for Dimako, Inc.

Robert P. Akins

Publications

"Time behavior of second-positive emissions from a fast-discharge N_2+SF_6 laser." Robert P. Akins and Shao-Chi Lin, Applied Physics Letters 28, 221 (1976).

"Optimal timing and power enhancement observed in a double-pulse fast-discharge-driven XeF laser." Robert P. Akins, George Innis and Shao-Chi Lin, Journal of Applied Physics 49 (4), 2262 (1978).

"Progress on incorporating gain into a coherent optical feedback system." Robert P. Akins and Sing H.Lee. Presented at the Optical Society of America's annual conference, San Francisco, Oct., 1978. Also published Journal of Optical Society of America 68, 1361A (1978).

"Coherent optical image amplification by an injection-locked dye amplifier at 632.8nm. Robert P. Akins and Sing H. Lee, Applied Physics Letters 35(9), 660 (1979).

"Feedback in analog and digital optical image processing." R. P. Akins and R. A. Athale and S. H. Lee. Presented at the SPIE seminar on Optical Pattern Recognition, San Diego, Aug., 1979.

"A Review: Feedback in analog and digital optical image process." R. P. Akins and S. H. Lee, Optical Engineering 19, 347 (1980)

DISTRIBUTION LIST

ADDRESSES	DODAAD CODE	NUMBER OF COPIES
Scientific Officer	N00014	1
Administrative Contracting Officer	S0513A	1
Director, Naval Research Laboratory Attn: Code 2627, Washington, D.C. 20375	N00173	6
Defense Technical Information Center Building 5, Cameron Station Alexandria, Virginia 22314	S47031	12
Office of Naval Research Western Regional Office 1030 E. Green St., Pasadena, CA 91106	N62887	1
Defense Contract Administrative Services 34 Civic Center Plaza P.O. BOX C-12700, Santa Ana, CA 92712		1